FLOW BIREFRINGENCE AND THE STRUCTURE OF MACROMOLECULES

V. N. TSVETKOV

Usp. Fiz. Nauk 80, 51-118 (September, 1963)

CONTENTS

THE study of the birefringence which arises in a gaseous or liquid medium under the action of an external potential field (electric or magnetic) is one of the well-known methods of studying the structure of the molecules of a substance being investigated.[2,5,74]

However, when applied to solutions of flexible chain macromolecules, this method proves not to be very productive. In fact, every chain molecule can be divided into statistical segments whose spatial orientations are mutually independent. If a segment is anisotropic in its optical (electric) or magnetic polarizability, then it will rotate in an external field (electric or magnetic) and orient itself with its axis of greatest polarizability in the direction of the field. However, owing to the lack of correlation of the orientations of the different segments, the macroscopic anisotropy of the solution that arises here is simply proportional to the total number of segments, independently of whether they form part of longer or shorter chains. Hence the electric (Kerr electrooptic effect) and magnetic (Cotton-Mouton magnetooptic effect) birefringence of the polymer solution is proportional to the weight concentration of the solute, is practically independent of its molecular weight, and usually differs little from the effect observed in a solution of the monomer of equal concentration.*

The situation changes radically when the optical anisotropy of the solution is produced by mechanical forces, e.g., shear forces in laminar flow (the dynamooptic Maxwell effect). The birefringence of the solution that arises here, just as in the case of the potential fields, ultimately results from the orientation of segments. However, these orientations are mutually correlated over the volume of the macromolecule, since the mechanical forces of flow give rise to translational and rotational motion, as well as to deformation of the macromolecule as a whole.

Hence, the Maxwell effect in a polymer solution is determined by the geometric, mechanical, and optical properties of the solute macromolecules, and by studying it we can get some very direct information on their dimensions and configuration.

In this review we shall not attempt any thorough presentation of the theory and experimental studies on the Maxwell phenomenon. The pertinent material can be found in other reviews.[1-10] We shall throw some light briefly here only on some current experimental and theoretical results that can be used to characterize the dimensions, shapes, and structures of macromolecules in solution.

I. APPARATUS

1. Mechanical Part

In observing flow birefringence the best form of instrument is a cylindrical apparatus. In this apparatus, the liquid being studied is placed in the gap between two coaxial cylinders, one of which is stationary, while the other rotates uniformly. The liquid is examined in the direction of the elements of the cylinder (the z axis in Fig. 1). Here, in the small region included in the observer's field of view (Fig. 1), the laminar flow arising in the gap can be considered to be practically uniform. It will have a constant velocity gradient $g = du/dx = du/dR$ in the direction of the radius R, equal to

$$g = \frac{2\pi R\nu}{\Delta R}, \qquad (1)$$

where ν is the number of rotations per second of the cylinder, and $R = \frac{1}{2}(R_a + R_i)$ is the mean radius, and $\Delta R = R_a - R_i$ is the width of the gap.

*This is not true of chain molecules having a marked secondary structure giving rise to rigidity of the chain and a high degree of mutual orientation of its elements (e.g., rigid helical structures of polypeptide chains).

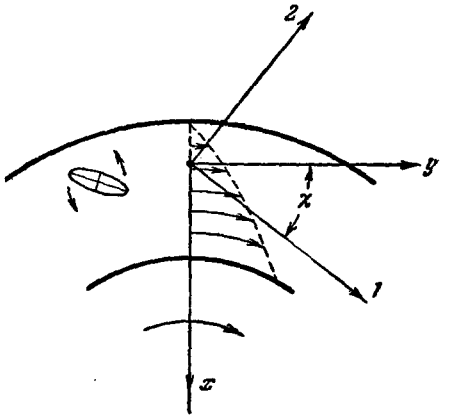

FIG. 1. Velocity-gradient distribution in a cylindrical apparatus having an inner rotor.[7] y – flow direction, 1 and 2 – principal optical directions corresponding to the refractive indices n_1 and n_2.

The liquid becomes optically anisotropic under the action of the shear stresses in the flow. Here, when the light beam is normal to the direction of the gradient g or the flow velocity u (i.e., parallel to the axis of the cylinder), the properties of the anisotropic layer resemble the optical properties of a crystal plate having a principal section forming an angle χ with the flow direction y. This angle is called the orientation angle or the "extinction" angle.

The orientation angle is the first of the two fundamental quantities to be determined experimentally by studying the Maxwell effect.

The second fundamental quantity to be determined is the difference between the two principal refractive indices $\Delta n = n_1 - n_2$ of the liquid. Of these, the former (n_1) corresponds to a ray whose electric vector is parallel to the principal section (in the plane of the drawing—axis 1) of the anisotropic layer, and the latter (n_2) is perpendicular to the principal section (axis 1) of the layer. Δn characterizes the magnitude of the birefringence, and can be either positive or negative.

The literature gives descriptions of a large number of possible designs of cylindrical apparatus and optical systems used by various investigators.[1-39]

In the quantitative study of the Maxwell effect, the fundamental experimental prerequisite is to maintain laminar flow.

The study of the conditions for laminarity when cylindrical apparatus is used[11,12] has shown that these conditions are essentially different, depending on whether the rotor of the apparatus is the outer or the inner cylinder.

For an apparatus with an inner rotor, the value of the critical velocity gradient g_c (the maximum gradient at which the flow remains laminar) is

$$g_c = \frac{\pi^2}{\sqrt{A}} \frac{\eta}{\varrho} \frac{\sqrt{R}}{(\Delta R)^{5/2}}, \qquad (2)$$

where η is the viscosity, and ρ is the density of the liquid. The constant A depends on $\Delta R/R$, and for all apparatus used in practice, it can be taken to be 0.0571.

In an apparatus having an outer rotor, turbulence of flow sets in at a considerably higher number of revolutions per second than in one having an inner rotor. Thus, for example, when $R/\Delta R = 60$, the critical gradient is six times as great for the outer-rotor case, while for $R/\Delta R = 10$, it is fifty times as great as for an inner rotor of the same dimensions.

Hence, in principle, the use of apparatus having outer rotors is greatly preferable, especially in studying dilute solutions in solvents of low viscosity using gaps that are not too narrow (e.g., as is necessary in measuring orientation angles).

However, many of the instruments in use having an outer rotor show a very essential defect, that of rotating glass windows. At high rates of revolution, centrifugal stresses appear in the glass and produce an appreciable birefringence. Besides, the rotating glass practically always introduces a time-dependent birefringence that reduces the accuracy of measurement of the fundamental effect.

These phenomena have given rise to erroneous conclusions in certain studies.[22,40]

This defect is eliminated in an apparatus having a perforated outer rotor[42-44] (dynamooptimeter), in which the glass of the windows is fixed rigidly to the stator.

A diagram of this instrument is shown in Fig. 2. Observations can be performed either under outer-rotor (with gap ΔR_1) or inner-rotor conditions (with gap ΔR_2). The inner thermostatic system A and the outer system B minimize the temperature gradients and their concomitant optical distortions.[45]

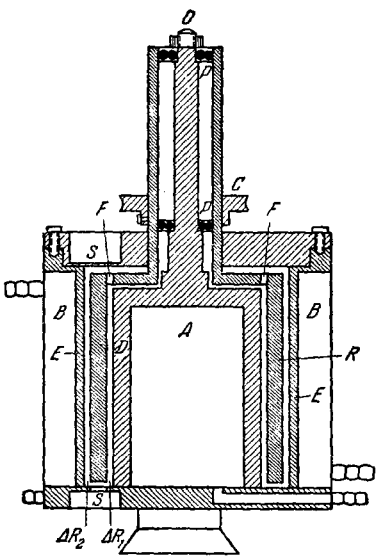

FIG. 2. Diagram of a cylindrical apparatus.[42-44] R – rotor; P – bearing; O – axle; D and E – stator; ΔR_1 and ΔR_2 – viewing gaps; S – viewing windows; F – perforation in the rotor for observation; C – pulley; A and B – thermostatic jacket.

Similar variants of analogous instruments have also been described in other papers.[5,46,47]

Experiment has shown that instruments of this type are most suitable for studying the weak birefringence of dilute solutions.

2. Optical Part

In the overwhelming majority of the existing studies, visual-observation systems have been used in the optical part of the apparatus.

Here one can use one of the known standard systems [48,69] for measuring optical phase differences and directions of the principal section (orientation angles). The compensator is selected in accordance with the magnitude of the birefringence to be measured.

To study the weak effects observed in dilute polymer solutions, the system shown in Fig. 3 can be recommended.[42,44]

Here the very sensitive system of Brace [49,48] is used as the compensator. It consists of a thin mica compensating plate K (several hundredths of a wavelength λ) fastened to the graduated circle B_2, and a very thin half-shadow plate N (several thousandths of λ) covering half the field of view.

An essential part of the apparatus is the thin lens L (of strain-free glass with a small aperture) projecting an image of the half-shadow plate into the gap in the cylindrical apparatus D, on which the telescope T is focused. Such an arrangement[42] facilitates the diminution of errors due to stray light reflected by the glass walls of the gap,[50] temperature gradients in the solution,[45] and the presence of dust.

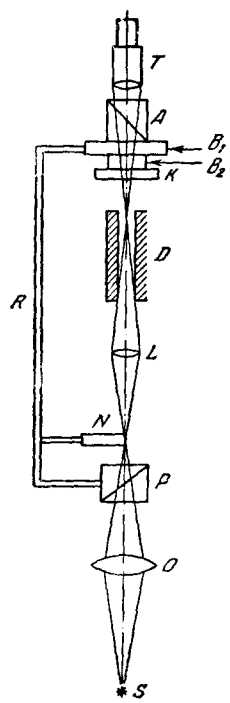

FIG. 3. Diagram of the optical part of the visual apparatus. P and A – polarizer and analyzer, linked by the arm R; S – monochromator slit, projected by lens O on the half-shadow plate.

The phase difference δ caused by the solution is measured by setting the compensator K (by rotating the circle B_2) to the position of equal illumination of both halves of the field of view (the half-shadow azimuth). Here

$$\delta = (\sin 2\alpha - \sin 2\alpha_0)\sin\delta_0, \qquad (3)$$

where α and α_0 are the half-shadow azimuths of the compensator, as measured from the plane of polarization of the polarizer in the presence and absence, respectively, of a velocity gradient in the liquid; δ_0 is the phase difference due to the compensator.

The principal optical directions of the anisotropic layer (1 or 2 in Fig. 1) are found by setting at the half-shadow positions by rotation of the entire optical system (circle B_1). The orientation angle χ is defined as half the angle between two half-shadow positions, one of which corresponds to clockwise rotation of the rotor, and the other, counterclockwise.

With a rotor length $\approx$ 10 cm, this system ensures reliable measurements of $\Delta n \approx 10^{-9}$ and of rotation angles with an accuracy of 0.5° when $\Delta n \approx 10^{-8}$.

For measurements of small values of Δn, one can also use the compensator of Szivessy,[51,37] and for determining χ, the Bravais plate.[52]

A highly sensitive apparatus for measuring birefringence [53-55] by a photoelectric method has been recently proposed. A diagram of one such instrument [55] is shown in Fig. 4. In the optical instrumentation (Fig. 3), instead of the half-shadow plate

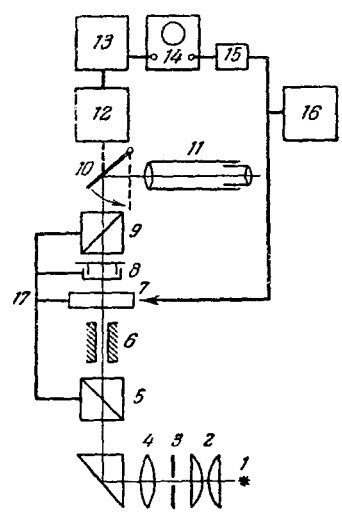

FIG. 4. Diagram of an apparatus for photoelectric recording[55] of Δn and χ. 1 – SVDSh-250 lamp; 2 – condenser lens; 3 – screen with aperture; 5 and 9 – crossed polarizer and analyzer; 6 – dynamooptimeter gap; 7 – elliptical modulator; 8 – mica compensator; 10 – movable mirror; 11 – viewing tube; 12 – photomultiplier; 13 – resonance amplifier; 14 – oscillograph; 15 – phase shifter; 16 – audio generator; 17 – rotation arm.

N, an elliptic light modulator 7 (Fig. 4) is introduced, with a system 12–16 for photoelectric recording of the light signal.

The basis of the modulator, which is firmly fastened to the rotation arm 17, is a small electrodynamic seismoreceiver having a coil supplied with current from the audio generator 16. The mechanical part of the seismoreceiver generates in a glass plate (by the photoelastic effect) a harmonically-varying optical anisotropy $\delta_1 = \delta_{10} \sin \omega t$, with an axis at an azimuth angle of 45° from the principal sections of the polarizer 5 and the analyzer 9.

Now, let a light ray incident on the photomultiplier 12 pass through an anisotropic layer 6 of the liquid being studied (of azimuth angle α and anisotropy δ) and the mica compensator 8 (of azimuth angle α_0 and anisotropy δ_0), as well as the modulator 7. Then at the output of the amplifier 13 (under the condition that δ_0 (and δ) $\ll 1$) one can measure a voltage

$$V = A(\sin 2\alpha \cdot \sin \delta - \sin 2\alpha_0 \cdot \sin \delta_0)\,\delta_{10} \sin \omega t, \qquad (4)$$

where A is a constant proportional to the light flux incident on the polarizer 5, to the amplification coefficient of the amplifier 13, and to the current sensitivity of the photomultiplier 12.

Thus the amplitude of the harmonic signal applied to one pair of plates of the oscillograph 14 (from the amplifier 13) depends linearly on δ. This fact makes the photoelectric method more sensitive than the visual method (in which the light flux acting on the eye is proportional to δ^2).

The amplitude of the signal becomes zero (as determined by the pattern on the oscillograph screen) either when the birefringence of the liquid is compensated by the compensator ($\sin 2\alpha \cdot \sin \delta = 2\alpha_0 \cdot \sin \delta_0$), or when the entire system is rotated (by arm 17) to the extinction position ($\alpha = 0$) with the compensator left out ($\alpha_0 = 0$). Thus, the orientation angle χ and the anisotropy δ are determined by the same methods as in visual optics.

The viewing tube 11 and the movable mirror 10 are for visual measurements and checks.

An analogous principle has been used in [54], where a rotating crystal plate was used as the elliptical modulator.

The sensitivity of the photoelectric method of measurement is at least an order of magnitude greater than that of a visual method using an analogous optical system.

In studying dilute solutions, we must take into account the effect of the solvent in the total birefringence of the solution in finding the values of Δn and the orientation angle χ of the birefringence of the solute polymer. This can be done by using Eqs. (18) and (19) of Sadron for a polydisperse system.[56-59]

II. THEORETICAL PREMISES OF THE MAXWELL EFFECT

A. Suspensions and Solutions of Rigid Particles and Macromolecules

The theory of the flow birefringence of solutions of absolutely rigid non-interacting particles has been developed by a number of investigators, who have used various molecular models (rigid rods, dumbbells, rigid strings of beads, ellipsoids).[60-65] These studies are treated in one of the cited reviews.[9] Peterlin and Stuart [65] have worked out the theory in a very complete and finished form.

The fundamental condition for the existence of a Maxwell effect in such systems is asymmetry of shape of the particles. Solutions of rigid spherical particles do not exhibit flow birefringence.

1. Hydrodynamic properties. Rigid particles in a laminar flow are subjected to viscous forces setting them into rotational motion (see Fig. 1). For particles having asymmetric shapes, this rotation is nonuniform and has a minimum velocity at the angular position of the particle where its long axis is parallel to the flow (in the y direction in Fig. 1). This produces a preferential kinematic orientation of the long axes of the particles in the flow direction.

However, the rotational Brownian movement interferes with this orientation and decreases the asymmetry of the angular distribution function of the axes of the particles. Besides, the rotational Brownian movement changes the direction of the maximum of the distribution function away from the flow direction y toward a direction rotated by 45° from the flow.

If the particles of the suspension are optically anisotropic, their preferential orientation will give rise to a macroscopic anisotropy of the solution. Here, for a monodisperse system, one of the two principal optical directions (1 in Fig. 1) will coincide with the direction of preferential orientation of the particles, forming the angle χ (the orientation angle) with the flow direction.

For a suspension of particles having the geometric and optical properties of ellipsoids of revolution, the theory gives [65]

$$\Delta n = \frac{2\pi N}{n}(\gamma_1 - \gamma_2) f(\sigma, p) = \frac{2\pi N}{n} v (g_1 - g_2) f(\sigma, p)$$
$$= \frac{2\pi C_v}{n}(g_1 - g_2) f(\sigma, p), \qquad (5)$$

$$\chi = \chi(\sigma, p). \qquad (6)$$

Here n is the refractive index of the solution, N is the number of particles per cm^3, $\gamma_1 - \gamma_2$ is the difference between the two principal polarizabilities of the particle, v is the volume of the particle, $C_v = Nv$ is the volume concentration of the solution,

$$g_1 - g_2 = \frac{\gamma_1 - \gamma_2}{v}$$

is the specific anisotropy of the substance in the particles; $f(\sigma, p)$ is a mechanical factor (the orientation function); $L/d = p$ is the ratio of the longitudinal (L) to the transverse (d) axis of the ellipsoids. The orientation parameter σ is equal to

$$\sigma = \frac{g}{D_r}, \qquad (7)$$

where D_r is the rotational diffusion coefficient of the particles. D_r depends on the viscosity η_0 of the solvent and the dimensions and shape of the particles. For ellipsoids of rotation,[66]

$$D_r = \frac{kT}{v_0 \eta_0 f_0(p)}, \qquad (8)$$

where

$$f_0(p) = 4\left(p^2 - \frac{1}{p^2}\right) \Big/ \left(\frac{2p^2-1}{2p\sqrt{p^2-1}} \ln \frac{p+\sqrt{p^2-1}}{p-\sqrt{p^2-1}} - 1\right). \qquad (9)$$

Here, v_0 is the "hydrodynamic" volume of the particle.

For highly extended ellipsoids ($p \gg 1$),

$$D_r = \left(\frac{3kT}{\pi\eta_0 L^3}\right)(\ln 2p - 0.5), \qquad (10)$$

and for highly extended cylinders (rods),[67]

$$D_r = \left(\frac{3kT}{\pi\eta_0 L^3}\right)(\ln 2p - 0.8). \qquad (10')$$

The orientation parameter σ can also be expressed in terms of the molecular weight M of the particles and the intrinsic viscosity $[\eta]$ of the solution:

$$\sigma = \frac{6\beta}{F(p)}, \qquad (11)$$

$$\beta = M[\eta]\eta_0 \frac{g}{RT}, \qquad (12)$$

where the function $F(p)$ varies from 2.5 (for $p = 1$) to 0.8 (for $p = \infty$). $F(p)$ has been tabulated by W. Kuhn[3] and by R. Simha.[72,6]

Thus, the magnitude of the birefringence Δn is determined by the product of two factors, the mechanical factor $f(\sigma, p)$ and the optical factor $N(\gamma_1 - \gamma_2)$. Since for rigid non-interacting particles, the optical factor does not vary with change in g, the relation of Δn to σ is determined only by the function $f(\sigma)$.

The orientation angle χ is also determined only by the mechanical factor, and is independent of the optical properties of the particles.

The functions $f(\sigma, p)$ and $\chi(\sigma, p)$ have been derived[65] in the form of power series in σ and

$$b_0 = \frac{p^2-1}{p^2+1}.$$

Sherага, Edsall, and Gadd[68] have carried out the numerical summation for various values of p, and have prepared tables of the functions f and χ.

The appropriate curves for two values of p are shown in Fig. 5.

The initial slopes of these curves give the intrinsic values of the birefringence $[n]$ and the orientation angle $[\varphi/g]$:

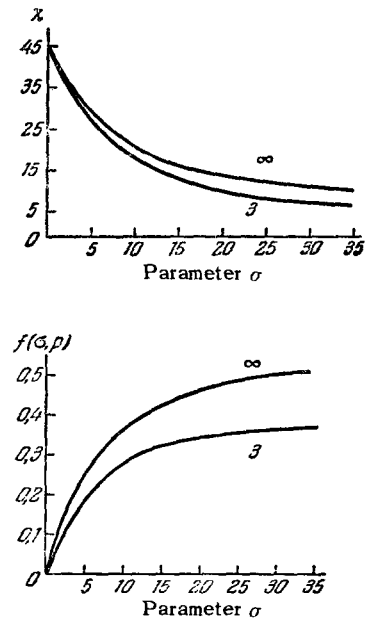

FIG. 5. The orientation angle χ and the orientation factor $f(\sigma, p)$ for the different axial ratios p indicated on the curves.

$$[n] = \lim_{\substack{C\to 0 \\ g\to 0}} \left(\frac{\Delta n}{g\eta_0 C}\right) = \frac{2\pi N_A b_0}{15nM\eta_0 D_r}(\gamma_1 - \gamma_2) = \frac{2\pi b_0 \bar{v}}{15n\eta_0 D_r}(g_1 - g_2), \qquad (13)$$

$$\left[\frac{\varphi}{g}\right] = \lim_{\substack{C\to 0 \\ g\to 0}} \left(\frac{\pi/4 - \chi}{g}\right) = -\left(\frac{d\chi}{dg}\right)_{\substack{C\to 0 \\ g\to 0}} = \frac{1}{12D_r}. \qquad (14)$$

Here $C = NM/N_A$ is the concentration of the solution in g/cm^3, N_A is Avogadro's number and $\bar{v} = vN_A/M$ is the partial specific volume of the solute.

By using Eqs. (7), (11), and (12), in place of (14), we can write

$$\left[\frac{\varphi}{g}\right] = \frac{M[\eta]\eta_0}{2RTF(p)}. \qquad (15)$$

Eq. (14) permits us to calculate D_r from the experimental values of $[\varphi/g]$, and by taking into account Eq. (8) or (10), to characterize the geometric properties of the particles.

By comparing the experimental values of $[\varphi/g]$, $[\eta]$, and $\bar{v}$, we can find the length and thickness of the ellipsoids.

By using D_r and the experimental value of $[n]$, we can determine from Eq. (13) the anisotropy $\gamma_1 - \gamma_2$ of the particle (if we know the molecular weight M) or the specific anisotropy $g_1 - g_2$ (if we know the partial specific volume $\bar{v}$). In some cases in determining $\gamma_1 - \gamma_2$, we can replace the measurements of $[\varphi/g]$ by measurements of the intrinsic viscosity $[\eta]$ of the solution. Thus, from Eqs. (11), (12), and (13), we can derive

$$\frac{[n]}{[\eta]} = \frac{4\pi}{5nkT}(\gamma_1 - \gamma_2)\frac{b_0}{F(p)}, \qquad (16)$$

which permits us to determine $\gamma_1 - \gamma_2$ from the ex-

perimental data for [n] and [η], if we have even a rough estimate of p.

We note that the quantity $g_1 - g_2$ which enters into (5) and (13) denotes the anisotropy per unit volume of the substance in the particles, and thus is insensitive to solvation and swelling, just as v is. In contrast, the hydrodynamic volume v_0 includes also the volume (Eq. (8)) of the solvent immobilized by the particle, and thus can vary greatly upon swelling.

2. Optical properties. The difference between the principal polarizabilities $\gamma_1 - \gamma_2$ of a rigid particle can in general be separated into two parts: the intrinsic anisotropy and the form anisotropy of the particles. The former arises from the anisotropy of the substance in the particle, which has differing refractive indices in different directions (n_1, n_2). Form anisotropy occurs in particles whose shapes are not spherical, and whose mean refractive index differs from the index n_S of the surrounding medium.

For ellipsoids having axial symmetry in their geometric and optical properties,

$$\gamma_1 - \gamma_2 = v(g_1 - g_2) = \frac{4\pi(n_1^2 - n_2^2) + \frac{(n_1^2 - n_3^2)(n_2^2 - n_3^2)}{n_s^2}(L_2 - L_1)}{\left(4\pi + \frac{n_1^2 - n_s^2}{n_s^2} L_1\right)\left(4\pi + \frac{n_2^2 - n_s^2}{n_s^2} L_2\right)} v, \quad (17)$$

where n_1 and n_2 are the refractive indices of the substance in the particle for rays polarized respectively in the directions of the longitudinal and transverse axes; L_2 and L_1 are functions depending only on p.

Here the first term gives the intrinsic anisotropy of the particle, and the second term gives the form anisotropy.

The intrinsic anisotropy can be either positive or negative, depending on the sign of $n_1^2 - n_2^2$, while the form anisotropy is always positive ($L_2 > L_1$).

The relation of the quantity $L_2 - L_1$ to p is shown in Fig. 6 (curve 1). The form anisotropy increases with increasing asymmetry of the particles; it practically attains its limiting value when $p \geq 10$, for which $L_2 - L_1 = 2\pi$. When n ($\approx n_1 \approx n_2$) $= n_S$, the form anisotropy is zero.

3. Concluding remarks. The brief treatment given of the basic conclusions of the orientation theory shows that from the experimentally-found values of [n] and [φ/g], together with the relations $\Delta n = f(g)$ and $\chi = \chi(g)$, we can calculate the basic geometric parameters (the dimensions and asymmetry of shape) and the optical anisotropy of rigid particles if we can apply the model of ellipsoids of revolution to them.

The geometric characteristics of a particle often reflect its internal structure, and thus can play an essential role (and sometimes even a deciding one) in establishing this structure.

The optical anisotropy may be of no lesser importance. Primarily, we must try to distinguish experimentally the effect of the intrinsic anisotropy

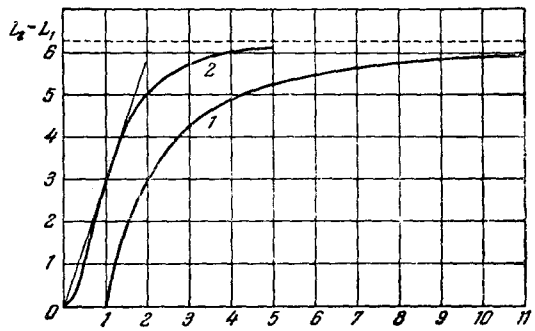

FIG. 6. The optical form factor $L_2 - L_1$ as a function of the asymmetry of the particle. 1: $L_2 - L_1 = f(p)$; 2: $L_2 - L_1 = f(x)$.

from the form anisotropy. The best way to do this is to study the birefringence Δn of the substance being studied in several solvents differing in their refractive indices n_S, and to extrapolate the Δn data to $n_S = n_k$ (the refractive index of the solute).

The magnitude and sign of the intrinsic anisotropy of the particle reflect the degree of order of its constituent parts (atomic groups or valence bonds). Thus they can serve as an essential characteristic its in-internal structure.

The experimentally-found value of the form anisotropy for particles with not too great asymmetry ($p < 10$) can be used (Eq. (17) and Fig. 6) to determine the axial ratio p.

If we measure the increment of the refractive index dn/dC and the partial specific volume $\bar{v}$ in the solute-solvent system, and use the equation [2]

$$\frac{dn}{dC} = \frac{2\pi\bar{v}}{n_s} \frac{g_1 + 2g_2}{3}, \quad (18)$$

we can determine $g_1 + 2g_2$.

By comparing this value with that of $g_1 - g_2$, we can calculate g_1 and g_2. When we use the formulas given above for Δn and χ, we must remember that they are all derived under the assumption that the system of particles being studied is absolutely monodisperse.

As Sadron [56] has shown, polydispersity can lead to a dependence of the quantity Δn and of the orientation angle χ of the birefringence on the velocity gradient that does not agree at all with the curves of Fig. 5.

According to Sadron, [56] for a polydisperse system,

$$\Delta n^2 = \left(\sum_i \Delta n_i \sin 2\chi_i\right)^2 + \left(\sum_i \Delta n_i \cos 2\chi_i\right)^2, \quad (19)$$

$$\operatorname{tg} 2\chi = \frac{\left(\sum_i \Delta n_i \sin 2\chi_i\right)}{\sum_i \Delta n_i \cos 2\chi_i}, \quad (20)^*$$

where the summation is made over all i types of particles in the mixture; each of these types, in the absence of the others, will give an anisotropy of the solution of Δn_i, characterized by an orientation angle χ_i, at the given velocity gradient.

*tg = tan

As has been shown, [70,71] data on flow birefringence, with application of Eqs. (19) and (20), can give information on the polydispersity of a dissolved sample.

B. Solutions of Chain Macromolecules

Chain macromolecules, which take the form of randomly wound coils in solution, are an example of particles that undergo not only orientation, but also deformation in a laminar flow.

Hence, the dynamic birefringence observed in these solutions is a complex orientation-deformation effect, in which the relative roles of orientation and deformation depend on the geometric, hydrodynamic, and mechanical properties of the molecular chains, i.e., ultimately, on their structure.

Here we must bear in mind the fact that, in comparison with the case discussed above of ideally rigid particles, solutions of flexible chain molecules are highly complex systems, both in their hydrodynamic and optical properties. At present, not nearly all of the experimentally-established laws and peculiarities of the Maxwell phenomenon in these systems have been completely and indisputably explained.

1. Optical properties of chain molecules. The conformational properties of true molecular chains in solutions can be described well theoretically in terms of a model of freely-linked linear segments [3,75] whose spatial orientations are mutually independent. Such a freely-linked chain takes the form of a randomly-wound Gaussian coil, in full accord with the shape of a real flexible chain molecule of sufficiently large molecular weight in the absence of volume effects (in an ideal solvent).

The theory shows [75-77] that the "external" shape of a random coil differs on the average from spherical, and can be described by a prolate spheroid whose mean length H is twice as great as its mean width Q. On the average, the molecular coil has the greatest geometrical extension in the direction of the vector h joining the ends of the chain molecule.

As Kuhn and Grün [78] have shown, the direction of h is also the direction of preferential orientation of the statistical segments comprising the molecular chain.

If the optical polarizability of the segment is anisotropic, the preferential orientation of the segments within the molecular coil will give rise to an optical anisotropy of the entire chain (intrinsic anisotropy).

For a chain molecule in a solvent of refractive index n_S, this anisotropy is [78]

$$(\gamma_1-\gamma_2)_i=\frac{3}{5}\left(\frac{n_s^2+2}{3}\right)^2(\alpha_1-\alpha_2)\frac{h^2}{\overline{h^2}}=\theta_i\frac{h^2}{\overline{h^2}}. \qquad (21)$$

Here γ_1 and γ_2 are the principal polarizabilities of the molecule in the direction of h and normal to h; α_1 and α_2 are the principal polarizabilities of the segment; $\overline{h^2}$ is the mean square of the quantity h for the undeformed molecule.

If the refractive index n_S of the solvent differs from the refractive index n_K of the solute polymer, an additional anisotropy of the molecule arises, due to the optical interaction of the individual parts of the chain with one another.

Here we must distinguish the interaction of elements sufficiently separated along the chain (optical long-range action) from the interaction of neighboring elements of the chain (optical short-range action).

Owing to the non-spherical distribution of mass in the coiled Gaussian chain, the optical long-range action in the chain molecule results in an anisotropy of the polarizing field within the molecular coil. This anisotropy is positive in sign and directly depends on the shape of the molecular coil (macroform anisotropy).

The difference between the principal polarizabilities of the macromolecule (in the h direction and normal to it) corresponding to the macroform effect is [79,80,43,81]

$$(\gamma_1-\gamma_2)_f=\left(\frac{n_s^2+2}{3}\right)^2\left(\frac{n_k^2-n_s^2}{4\pi n_s\varrho N_A}\right)^2\frac{M^2}{v}(L_2-L_1)=\theta_f(L_2-L_1), \qquad (22)$$

where ρ is the density of the polymer, and $v = 0.36\,(\overline{h^2})^{3/2}$ is the volume of the molecular coil in the solution (including the volume of solvent enclosed). $L_2 - L_1$ is the optical form factor, which is the function of the axial ratio p given by curve 1 in Fig. 6. It can also be expressed [82] as a function of the parameter $x = h/(\overline{h^2})^{1/2}$. The relation of $L_2 - L_1$ to x is given by curve 2 in Fig. 6. The graph shows that in the range $0.5 \le x \le 1.5$ (i.e., when the deformation of the molecule is small), $L_2 - L_1 \approx 3x$, and hence,*

$$(\gamma_1-\gamma_2)_{f,\,x<1.5}\approx 3\theta_f\frac{h}{(\overline{h^2})^{1/2}}. \qquad (23)$$

Neighboring elements (monomer units) of the chain are mutually arranged in a definite linear order. Hence the optical interaction cannot be spherically symmetrical. This asymmetric short-range action in the chain gives rise to local anisotropy of the polarizing field, similar to the way that the asymmetry of shape of the entire chain gives rise to the mean anisotropy of the field. The local anisotropy of the field depends on the microstructure of the molecular chain and increases with increase in its equilibrium rigidity (the dimensions of the segment and its asymmetry of shape). Consequently, the effect arises of an additional anisotropy in the polarizability of the macromolecule (microform anisotropy), which is also positive in sign.

The difference between the principal polarizabili-

*Eq. (23) coincides with the expression for the form anisotropy derived by Čopič.[83,84] Eq. (22) is more general in meaning, i.e., it can also be applied in the case of large deformations of the molecular coil.

ties of the macromolecules (along the vector h and normal to it) corresponding to the microform effect is [85,86]

$$(\gamma_1-\gamma_2)_{fs}=\frac{3}{5}\left(\frac{n_s^2+2}{3}\right)^2\left(\frac{n_k^2-n_s^2}{4\pi n_s}\right)^2\frac{M_0 s}{\varrho N_A}(L_2-L_1)_s\frac{h^2}{\bar{h}^2}$$

$$=\theta_{fs}\frac{h^2}{\bar{h}^2}. \qquad (24)$$

Here $(L_2 - L_1)_s$ is the function of the asymmetry of shape of the segment p_s given by curve 1 in Fig. 6, M_0 is the molecular weight of the monomer unit of the chain, and s is the number of monomer units in the segment.

The total difference between the principal polarizabilities of the chain molecule equals the sum of the three cited effects:

$$\gamma_1-\gamma_2=(\theta_i+\theta_{fs})\frac{h^2}{\bar{h}^2}+\theta_f(L_2-L_1), \qquad (25)$$

where θ_i, θ_f, and θ_{fs} are determined by Eqs. (21), (22), and (24), respectively.

We can easily see by comparing (22) and (24) that for a given macromolecule (M, M_0, n_k) in a certain solvent (n_s), the relative role of the macroform anisotropy θ_f and the microform anisotropy θ_{fs} depends on the conformation of the molecular chain.

As $\overline{h^2}$ increases, expression (22) decreases, while (24) increases, owing to the increase in the effective length of the segment. This means that the more open the structure of the molecular coil is (the less the molecule is coiled), i.e., the smaller the equilibrium flexibility of the chain, the greater the value of θ_{fs} and the smaller the value of θ_f in the total anisotropy of the molecule. Hence, the experimentally determined quantity θ_{fs}/θ_f can serve as a measure of the equilibrium rigidity of the chain molecule.

2. Hydrodynamic properties of chain molecules. Among the various models [1-10] used in describing the hydrodynamic properties of chain molecules in solution in treating the phenomenon of flow birefringence, those of fundamental importance are due to W. Kuhn, [86-88] B. Zimm, [89] and R. Cerf. [8,90,92]

Kuhn's model is the simplest. In it, the actual chain is replaced by a deformable (elastic) dumbbell of length h; the hydrodynamic force which should actually be exerted on a quarter of the molecular chain by the solvent is applied to each of the two endpoints. The hydrodynamic interaction of the parts of the chain is not calculated from theory, but is estimated from model experiments. [3] Only motion of the macromolecule in the plane of flow is considered (two-dimensional motion).

In addition to ideally flexible chains, Kuhn also treated the effect of kinetic rigidity of macromolecules on their hydrodynamic properties, and introduced for this purpose the concept of internal viscosity. [87,88] Internal viscosity (kinetic rigidity) characterizes the length of time the molecular chain takes to change in conformation, and is determined by the height of the potential barriers hindering free rotation of the atomic groups about the valence bonds of the chain.

Besides (owing to mathematical difficulties), Kuhn solved the problem of the dynamooptical properties of kinetically rigid chain molecules only in the limiting case of very high internal viscosity, which is equivalent to the case of absolutely rigid particles discussed in Section II, A. Hence the functions $\chi = \chi(g)$ and $\Delta n = f(g)$ for a solution of chains of high internal viscosity are expressed by the curves of Fig. 5. Zimm [89] uses a more refined hydrodynamic model of a chain molecule, a sequence of freely-linked subchains. [93,94] He treats the spatial (three-dimensional) motion of such a chain in a shear field by taking into account the hydrodynamic interactions of its parts by the Kirkwood-Riseman method. [95] However, here he takes the molecular chain to be ideally kinetically flexible, and ignores the internal viscosity. Cerf [90-92] uses the same model as Zimm (subchains) to describe the hydrodynamic properties of a chain molecule, but he supplements it by taking into account the effect of internal viscosity. Here he modifies the definition of internal viscosity introduced by Kuhn by bringing it closer to the idea of the viscosity η_i of a continuous liquid medium. Hence, the dynamic properties of Cerf's molecular model turn out to resemble the dynamics of the model of a viscoelastic sphere that he had used in previous studies. [96-98] According to Cerf, we can use the ratio of the internal viscosity coefficient η_i of the molecule to the viscosity η_0 of the solvent as a criterion for classifying molecules according to their rigidities. When $\eta_0 \ll \eta_i$ (in arbitrary units), the molecules are rigid, and the birefringence of the solution observed at small shear stresses ($\beta \to 0$) is the result of their orientation in the flow. When $\eta_0 \gg \eta_i$ (in the same units), the molecules are flexible, and the birefringence is due to their deformation in the flow, even at infinitesimally small shear stresses ($\beta \to 0$).

Thus, of the three models enumerated above, we can consider the hydrodynamic model of Cerf to be the most complete, and probably the most perfected. However, it is also the most complex. Hence, the problem of the dynamooptical properties of solutions of chain molecules has thus far been solved within the framework of this model only for the case of $g \to 0$, i.e., for infinitesimally small shear stresses.

On the contrary, by using the model of ideally flexible subchains (neglecting the internal viscosity), Zimm was able to solve the dynamooptical problem completely and derive the relations $\Delta n = f(g)$ and $\chi = \chi(g)$ for a broad range of velocity gradients g. However, here he did not take into account the form effect in the optical part of the problem, but kept only

the first term, $\theta_i h^2/\overline{h^2}$, in Eq. (25) for the polarizability difference of the molecule.

Finally, the use of the simplified hydrodynamic model of an elastic dumbbell without internal viscosity made it possible to solve the problem of the dynamooptic properties of flexible chain molecules for a wide range of velocity gradients, taking into account not only the intrinsic anisotropy [86] of the chains, but also their form anisotropy, [84,82,85] i.e., using all the terms of Eq. (25).

3. The magnitude and orientation of the birefringence in a solution of chain molecules. The theoretical results are summarized below for chain molecules of varying kinetic rigidities, as derived from the hydrodynamic and optical models mentioned above. All the formulas refer to infinitely dilute solutions ($C \to 0$) of a monodisperse polymer.

a) Ideally flexible chains (without internal viscosity). 1. Hydrodynamic model: elastic dumbbell. Optical properties given by Eq. (25). The magnitude of the birefringence is given by the expression [82,84,85]

$$\lim_{C\to 0}\left(\frac{\Delta n}{C}\right)\frac{3n_s}{4\pi}\frac{M}{N_A} = (\theta_i + \theta_{fs})\beta\sqrt{1+\beta^2} + \left(\frac{3}{2}\right)^2\theta_f\Phi(\beta), \tag{26}$$

where θ_i, θ_f, θ_{fs}, and β are defined respectively by Eqs. (21), (22), (24), and (12); $\Phi(\beta)$ is a function with limiting values:

$$\lim_{\beta\to 0}\Phi(\beta) = \beta \text{ and } \lim_{\beta\to\infty}\Phi(\beta) = \frac{4\pi}{3}.$$

The second term on the right-hand side of Eq. (26), which is determined by θ_f, is always positive. The first term (proportional to $\theta_i + \theta_{fs}$) can have either sign (θ_{fs} is positive, and θ_i can be either positive or negative). Hence, the relation $\Delta n = f(\beta)$ for the total birefringence is complicated in form, and in some cases (when $\theta_i < 0$), it can involve a change in the sign of the observed effect. Figure 7 shows the graphs of the relation $\Delta n = f(\beta)$ for the cases in which $\theta_i + \theta_{fs}$ and θ_f are positive (curve 4), or opposite in sign (curve 5).

The form of the curve for the orientation angle $\chi = \chi(\beta)$ depends essentially on the relative roles of the macroform θ_f and the intrinsic anisotropy θ_i effects in the observed birefringence. If we neglect the second term (the macroform effect) in (25) and (26), the value of the orientation angle will not depend on the optical properties of the system, will be determined by the hydrodynamic properties of the macromolecules, and will be expressed by the equation [86]

$$\operatorname{tg} 2\chi = \frac{1}{\beta}. \tag{27}$$

The overall form of the relation (27) qualitatively agrees with the curves for $\chi(\sigma)$ (Fig. 5). If we take into account the macroform effect (the term in (26) containing θ_f), the measured orientation angle is determined by the expression [99]

$$\operatorname{tg} 2(\chi - \chi_0) = \frac{1-x}{1+x}\operatorname{tg} 2\delta, \tag{28}$$

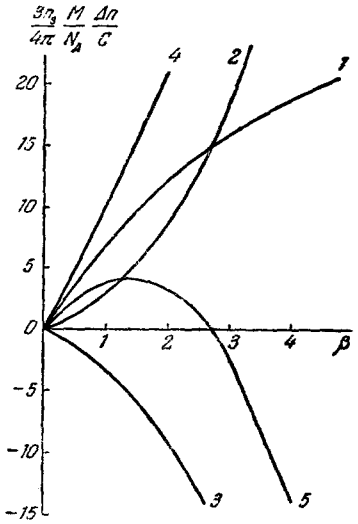

FIG. 7. The function $(\Delta n/C)(3n_s/4\pi)(M/N_A) = f(\beta)$ for solutions of flexible chain molecules. Curves: $1 - (3/2)^2\theta_f\Phi(\beta)$ for $\theta_f = 3$; $2 - (\theta_i + \theta_{fs})\beta\sqrt{1+\beta^2}$ for $\theta_i + \theta_{fs} = +2$; $3 - (\theta_i + \theta_{fs})\beta\sqrt{1+\beta^2}$ for $\theta_i + \theta_{fs} = -2$; 4 – additive effect of curves 1 and 2; 5 – additive effect of curves 1 and 3.

where

$$x = \frac{(\theta_i + \theta_{fs})\beta\sqrt{1+\beta^2}}{\left(\frac{3}{2}\right)^2\theta_f\Phi(\beta)}.$$

Here χ_0 is the value of the orientation angle characterizing the hydrodynamic properties of the system. It can be determined from Eq. (27). Furthermore,

$$\chi_0 = \frac{1}{2}(\chi_i + \chi_f)$$

and

$$\delta = \frac{1}{2}(\chi_f - \chi_i).$$

Here χ_i and χ_f are the extinction angles corresponding to the two parts into which the molecular system is arbitrarily divided. The first part gives the birefringence proportional to $(\theta_i + \theta_{fs})\beta\sqrt{1+\beta^2}$, and the second part is proportional to $(3/2)^2\theta_f\Phi(\beta)$.

It follows from Eq. (28) that in the range of β values where the birefringence changes sign ($x = -1$), the extinction-angle curves are discontinuous, and show an "anomalous" course. Thus, the value of the extinction angle for such systems reflects not only the hydrodynamic properties of the system, but also to a considerable extent its optical properties. Here, a minute hydrodynamic polydispersity (an insignificant value of δ) will result in quite appreciable changes in the experimental curve $\chi(\beta)$.

In the range of small shear stresses ($\beta \to 0$), Eq. (26) gives for the intrinsic value of the birefringence:

$$\lim_{\substack{C\to 0\\ g\to 0}}\left(\frac{\Delta n}{g\eta_0 C}\right) = [n] = [n]_i + [n]_{fs} + [n]_f, \tag{29}$$

where the three components of the birefringence, the effect of the intrinsic anisotropy $[n]_i$, the microform anisotropy $[n]_{fs}$, and the macroform anisotropy $[n]_f$ are, respectively:

$$[n]_i = \frac{4\pi}{45kT}\frac{(n_s^2+2)^2}{n_s}[\eta]_0(\alpha_1-\alpha_2), \quad (30)$$

$$[n]_{fs} = \frac{(n_s^2+2)^2(n_h^2-n_s^2)^2}{180\pi RTn_s^3\varrho}[\eta]_0 M_0 s(L_2-L_1)_s, \quad (31)$$

$$[n]_f = \frac{0{,}058\Phi(n_s^2+2)^2(n_h^2-n_s^2)^2}{\pi\varrho^2 N_A RTn_s^3}M. \quad (32)$$

Here, $\Phi \approx 2.1 \times 10^{23}$ is the Flory coefficient, and $[\eta]_0$ is the intrinsic viscosity of the solution for $g \to 0$.

For the intrinsic value of the orientation angle

$$\lim_{\substack{C\to 0\\ g\to 0}}\frac{\pi/4-\chi}{g} = \left[\frac{\varphi}{g}\right]$$

Eq. (27) gives

$$\left[\frac{\varphi}{g}\right] = a\frac{M[\eta]_0\eta_0}{RT}, \quad (33)$$

where a = 0.5.

If we take into account the form effect (the second term of Eq. (25)), Eq. (33) must be supplemented by the equation [84,100]

$$\left[\frac{\varphi}{g}\right]_z = \left[\frac{\varphi}{g}\right]\frac{1+C_1Z}{1+C_2Z}. \quad (34)$$

Here C_1 and C_2 are constant, unequal factors;

$$Z = \frac{1}{x_{\beta\to 0}} = \frac{9\theta_f}{4(\theta_i+\theta_{fs})};$$

$[\varphi/g]$ is the intrinsic value of the extinction angle in the absence of the form effect, as determined, e.g., from (33); $[\varphi/g]_Z$ is the same quantity in a system showing the form effect. In the region $C_2Z \approx -1$, the quantity $[\varphi/g]_Z$ essentially depends on the optical properties of the system.

2. Hydrodynamic model: freely-linked sequence of subchains. Optical properties of the molecule given by the first term of Eq. (25) (Zimm [89]). Correspondingly, the value of the birefringence is

$$\lim_{C\to 0}\left(\frac{\Delta n}{C}\right)\frac{3n_s}{4\pi}\frac{M}{N_A} = \theta_i\beta\sqrt{1+(0.5\operatorname{ctg}2\chi)^2}. \quad (35)^*$$

The orientation angle is determined by the expression

$$\operatorname{tg}2\chi = \frac{5}{2}\frac{1}{\beta} \quad (36)$$

in the case of weak hydrodynamic interaction (a hydrodynamically free-draining molecular coil) or by

$$\operatorname{tg}2\chi = \frac{4.88}{\beta} \quad (37)$$

in the case of strong hydrodynamic interaction (a non-free-draining coil).

Thus, the theory gives Eq. (30) for the intrinsic value of the birefringence [n], i.e., a result completely agreeing with that for an elastic dumbbell. The intrinsic value of the orientation angle $[\varphi/g]$ also can be expressed by Eq. (33), where we must assume: a = 0.2 for a free-draining coil, and a = 0.1 for a non-free-draining coil.

Thus, the use of the more refined hydrodynamic model of subchains, which leads to a considerable complication of the mathematical side of the problem, essentially makes no fundamental changes in the final result of the elastic-dumbbell theory (but changes only the values of the numerical coefficients). At the same time, the mathematical complications hinder the full utilization of the optical properties of the macromolecules, thus greatly limiting the possibilities of the theory. Hence, in spite of the apparent primitiveness of Kuhn's hydrodynamic model, its application in many cases seems fruitful and quite justified.

b) Molecular chains of large internal viscosity (kinetically rigid). In the limiting case of highly rigid chains, macromolecules do not undergo deformation in a flow. The birefringence is due to their orientation, and hence, independently of the model applied, the relations $\Delta n = f(\beta)$ and $\chi = \chi(\beta)$ qualitatively agree with the curves of Fig. 5.

The intrinsic value [n] is determined as before by Eqs. (29)—(32), both for rigid dumbbells and for rigid subchains.

The intrinsic orientation angle also is determined by Eqs. (33) and (34), but the proportionality coefficient differs for the two models.

In the rigid-dumbbell case,[87] a = 3/2. For rigid subchains: with complete hydrodynamic free draining, a = 0.9, and with complete lack of free draining, a = 0.7.

c) Flexible chains having a small but appreciable internal viscosity. We assume that $\eta_i \ll \eta_0$, and hence, the observed birefringence is of deformational type. However, the internal viscosity is not infinitesimally small (as in case (a)), and can exert an effect on the dynamooptical properties of the solution.

This intermediate case between absolutely rigid and ideally flexible molecules has been examined using a hydrodynamic model of subchains [90-92] and an optical model taking the macroform effect (Eq. (25)) into account.[100] The problem has been solved only in the region $\beta \to 0$, i.e., only the intrinsic values [n] and $[\varphi/g]$ were obtained.

The expression derived for [n] has a form similar to (29), and contains terms $[n]_i$ and $[n]_f$.[100] Here the part $[n]_i$ corresponding to the intrinsic anisotropy completely coincides with Eq. (30). Thus, the existence of an appreciable internal viscosity in the chain has no effect on the magnitude of the birefringence. On the contrary, the expression for $[\varphi/g]$ depends considerably on the internal viscosity. In the absence of a macroform effect ($\theta_f \approx 0$), the theory gives

$$\left[\frac{\varphi}{g}\right] = a\frac{M[\eta]_0\eta_0}{RT} + b\frac{F\overline{h^2}}{kT}, \quad (38)$$

where a = 0.2 and b = 0.0062 with weak hydrodynamic interaction, and a = 0.1, b = 0.0045 with strong hydrodynamic interaction; F is a constant coefficient

*ctg = cot

characterizing the internal viscosity η_i of the molecule that does not depend on M.

Zimm's result (for $\beta \to 0$) is a special case of Eq. (38) with $F \to 0$.

d) The extinction angle and kinetic rigidity of the chain. For all the discussed models of ideally flexible (Eq. (33)) and absolutely rigid (Eqs. (33) and (15)) macromolecules, the relation of $[\varphi/g]$ to $M[\eta]\eta_0$ is represented by a straight line passing through the origin (curve 1 in Fig. 8). For rigid molecules, such a relation means that the observed birefringence is of orientational nature. When there is a deformation effect showing the influence of internal viscosity (Eq. (38)), the corresponding relation has the form of curve 2 in Fig. 8, cutting the vertical axis at an intercept proportional to Fh^2/kT. The slopes of the straight lines 1 and 2 are determined by the values of the coefficient a in Eqs. (33) and (38), respectively.

For every real polymer, the relative roles of orientation and deformation in the Maxwell effect are determined by the ratio of coefficients of the internal viscosity η_i (or F) to the viscosity η_0 of the surrounding medium. As η_0 (and hence, also $M[\eta]\eta_0$) increases, the orientation process (curve 1) is replaced by the deformation process (curve 2). Hence, the relation of $[\varphi/g]$ to $M[\eta]\eta_0$ for the polymer chain is represented by curve 3, for which the straight lines 1 and 2 are asymptotes.

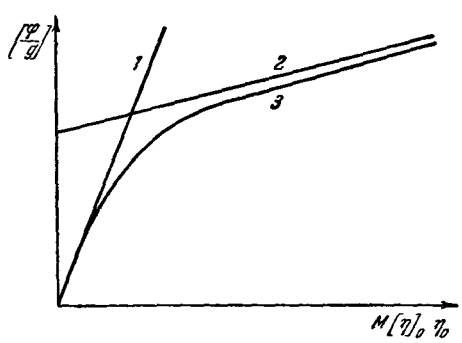

FIG. 8. The relation of $[\phi/g]$ to $M[\eta]\eta_0$ for chain molecules.[8] 1 – orientational birefringence; 2 – deformational birefrigence; 3 – the relation for a real molecule.

Thus, the form of the experimental curve for $[\varphi/g] = f(M[\eta]\eta_0)$, according to Cerf, can give information on the kinetic rigidity of a molecular chain and serve as a fundamental criterion for solving the problem of the relative roles of the effects of deformation and orientation in the birefringence observed in the region of small shear stresses, $\beta \to 0$. However, we must remember here that to obtain adequate hydrodynamic characteristics from measurements of the extinction angle, we must use a solvent in which the value of C_2Z in Eq. (34) differs appreciably from minus unity.

e) The magnitude of the birefringence and the anisotropy of the macromolecule. In distinction from the extinction angle, the expression for the intrinsic birefringence $[n]$ is practically independent of the hydrodynamic properties of the molecular model applied. In this sense Eqs. (29)—(32) are universal, and can be used to determine the optical characteristics of macromolecules independently of their mechanical properties. Here we can obtain from Eqs. (30) and (31) information on the parameters characterizing the microstructure of the chain (the segment anisotropy and the equilibrium rigidity), and from Eq. (32) we can find the asymmetry of the equilibrium form of the molecular coil. To do this, we must transform Eq. (32) into the form [80]

$$[n]_f = \left(\frac{n_s^2+2}{3}\right)^2 \frac{M}{120\pi\rho^2 RT} \frac{(n_k^2-n_s^2)^2}{n_s^3} [b_0 f_0 (L_2 - L_1)], \quad (39)$$

where f_0, b_0, and $L_1 - L_2$ are the functions taking part in Eqs. (9), (13), and (17), respectively. Equation (39) permits us to determine p from the experimental values of $[n]_f$ and M.

4. Concentration-dependence. None of the discussed theories pay any attention to intermolecular interactions, and hence are applicable only to experimental data extrapolated to infinite dilution. Peterlin [101,102] has proposed a semiempirical relation permitting one to take into account the intermolecular interactions in solution, and thus to limit the experimental procedure to the study of rather concentrated solutions, in which the technique of observing and measuring the Maxwell effect is considerably simpler. This relation is based on the assumption that the intermolecular interaction in a concentrated solution increases the effective hydrodynamic forces acting on the molecule in the flow to the same extent that it increases the reduced viscosity of the solution

$$[\eta]^* = \frac{\eta - \eta_0}{\eta_0 C}. \quad (40)$$

According to Peterlin, Eq. (27) and the part of (26) corresponding to the intrinsic anisotropy θ_i can be applied also to concentrated solutions if we replace $[\eta]$ by $[\eta]^*$ therein, and correspondingly, replace the parameter β by

$$\beta^* = \frac{Mg(\eta - \eta_0)}{RTC}. \quad (41)$$

Here, instead of Eqs. (27) and (26), we have

$$\operatorname{tg} 2\chi = \frac{1}{\beta^*}, \quad (42)$$

$$\frac{\Delta n}{g(\eta - \eta_0)} = \frac{4\pi}{45kT} \frac{(n_s^2+2)^2}{n_s} (\alpha_1 - \alpha_2) \sqrt{1+\beta^{*2}}, \quad (43)$$

from which it also follows that

$$\frac{\Delta n}{g(\eta - \eta_0)} \sin 2\chi = \frac{4\pi}{45kT} \frac{(n_s^2+2)^2}{n_s} (\alpha_1 - \alpha_2). \quad (44)$$

The latter equations are of great practical significance, since they permit us to determine the segment anisotropy $\alpha_1 - \alpha_2$ from the values of Δn, χ, and $\eta - \eta_0$ found experimentally in a solution of any concentration whatever, even if we do not know the concentration.

Equation (44) has also been derived by Lodge,[103,104] who considered a concentrated polymer solution as being a disordered network of tangled molecular chains that can be deformed in the shear field of the flow. Equations (42)—(44) refer to the case in which the solution shows no form effect.

The concentration-dependence of the form birefringence will be discussed in Sec. III.

III. EXPERIMENTAL DATA

In discussing the experimental data on flow birefringence, we cannot in all cases easily solve the problem of whether we should treat the solution being studied as a system of rigid particles, or must bear in mind their deformation in the flow.

Often the division of particles into two classes, rigid and deformable particles, is provisional, since one given macromolecule under different conditions (e.g., in different shear-stress ranges) can behave either as a highly rigid or a rather flexible body.

The following assumption can obviously serve as a general criterion for classification of a given system. If orientation of the molecules plays the basic role in an observed flow birefringence, then the molecules can be treated as being kinetically rigid, even if they indubitably exhibit deformability (flexibility) in other phenomena.

The equations of the theory of flow birefringence of rigid particles (Sec. II, A) are commonly applied to solutions of biopolymer molecules, although not nearly all of the latter can be considered to be completely rigid.

On the other hand, the fact that a molecule is kinetically rigid and the birefringence is due to orientation still does not imply that the most correct model for its geometric and optical properties is a rigid prolate ellipsoid or a straight rod, rather than a randomly coiled chain. This fact is not always taken into account sufficiently.

The section on biopolymers will take up several typical examples in which the hydrodynamic and optical properties of macromolecules can be represented by models of continuous ellipsoids or rods, and some cases are also given in which a randomly coiled chain is a more adequate model.

A. Biological polymers

The most characteristic representatives of high-molecular-weight substances whose solutions contain rigid particles of rodlike shape are the viruses, proteins, and polypeptides.

An essential point is that the dimensions and shapes of many of these particles can be directly determined with the electron microscope and compared with the values of the rotational diffusion coefficient obtained from measurements of the orientation angle of the birefringence.

1. Tobacco mosaic virus (TMV). Among the various viruses, the dynamooptical properties of TMV solutions have been studied in greatest detail, and the dimensions and shape of these particles have also been characterized rather fully by other methods.[105]

Sedimentation,[106-111] diffusion,[107,109] and partial specific volume measurements of TMV in solution indicate that the molecular weight of the particles $M \approx 40 \times 10^6$. If we represent the TMV particle by a solid ellipsoid of revolution,[5] we can conclude from these same data that it has the shape of a straight rod of length 3×10^{-5} cm and diameter 0.15×10^{-5} cm. The values found agree with the width found from the X-ray diffraction data,[112-114] and confirm well the direct determination of the mean length of the TMV rod from electron micrographs.[115-118] Determinations of the mean molecular weight and length of the TMV particles by the light-scattering method give the same results.[111,115]

Thus the hydrodynamic, optical, X-ray, and electron-microscope studies give a rather complete and consistent picture of the morphological properties of TMV particles. This permits us to use them as a convenient object for testing the orientation theory of flow birefringence.

In order to compare the relative roles of orientation and deformation in the birefringence phenomenon, Cerf[96] measured the orientation angles of TMV solutions, while varying the viscosity η_0 of the medium (by adding glycerol). The relation $[\varphi/g] = f(\eta_0)$ obtained is represented by a straight line passing through the origin, in complete agreement with Eq. (15) (or line 1 in Fig. 8), thus illustrating the rigidity of the TMV particles.

The overall course of the curve relating the orientation angle and the magnitude of the birefringence to the velocity gradient g has been studied in a number of references[19,39,46,110,111,120] for TMV solutions over a broad range of shear stresses. The range of stresses was extended particularly greatly (from 1 to 400 dyne/cm^2) in the study of Leray,[39] who constructed a special apparatus for this purpose.

The experimentally-obtained relation of the magnitude $\Delta n = f(g)$ and the orientation $\chi = \chi(g)$ of the birefringence agrees qualitatively in all cases with the orientation theory, resembling in form the curves of Fig. 5. However, if we use the experimental values of the orientation angle χ for various values of g to calculate the rotational diffusion coefficients D_r by the formulas of the rigid-ellipsoid theory (Eqs. (6) and (7) and the tables of[68]), we get values of D_r that increase with increasing g. The corresponding values of the particle length L (calculated by Eqs. (8), (9), and (10)) vary from $L = 5 \times 10^{-5}$ cm for infinitesimal g to $L = 3 \times 10^{-5}$ cm for large g. Thus, the dynamooptical data give satisfactory quantitative agreement with the results of other methods only at

large shear stresses, while at small g values, the experimental value of L turns out to be 1.5—2 times as large as the true length of the TMV particles.

This is illustrated by Fig. 9,[111] which shows the calculated particle lengths L as a function of the velocity gradient g. Such a result is characteristic of a polydisperse system. However, taking into account the actual length distribution of the particles (determined from electron micrographs) by using Sadron's formulas (19) and (20) for a polydisperse solution[119,39,110] does not make appreciable changes in the experimental values of the particle length, nor does the use of carefully prepared monodisperse samples.[111]

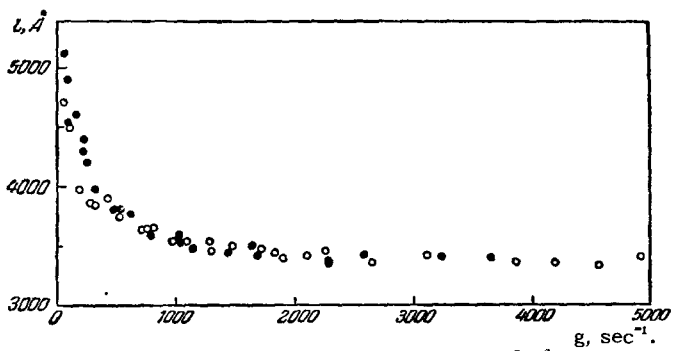

FIG. 9. The relation of L to g for TMV.[111]

We should note also a certain lack of agreement between the value of Δn and the orientation angle χ of the birefringence. At large g values, the curve $\Delta n = f(g)$ practically attains saturation, while χ has here a value differing from zero.

Possibly we should seek the reason for the observed differences between the electron-microscope and dynamooptical data in the differences in the morphological properties of the particles in a dried preparation and in solution,[121,122] or in the approximations made in calculating the length.[123,124] For particles of such great dimensions as the TMV particles, the effect of deviations from the conditions of the quasistatic theory in the optical problem is also not ruled out.[39] In any case, we should bear in mind the fact that a small proportion of associated particles in the solution can lead to a very appreciable lowering of the curve for the function $\chi(g)$ in the region of small g, whereas the breakdown of the aggregates and the destruction of the particles themselves in the flow must decrease the slope of the $\chi(g)$ curve at very high shear stresses.

Under these conditions, we can consider the L values obtained at moderately large g to be the most representative values of the true mean dimensions of TMV particles.

By using the experimental curve for the birefringence $\Delta n = f(g)$ and the rotational diffusion coefficient D_r in Eq. (13), we can calculate the difference between the two principal specific polarizabilities $g_1 - g_2$ of the particle. The experimental values of $g_1 - g_2$ for different samples lie in the range from 0.9×10^{-3} [110] to 4.6×10^{-3} [39].

It is hard to state reliably at present to what extent these $g_1 - g_2$ values express the intrinsic anisotropy of the material in the particles, or are a form effect, since the only study of the relation of the birefringence of TMV to the refractive index n_s of the solvent was made in an old investigation by Lauffer.[125] He used an experimental technique more suitable for qualitative than quantitative measurements. The refractive index was varied by changing the composition of the water-glycerol-aniline mixture used as the solvent. According to Lauffer, the curve $\Delta n = f(n_s)$ is of parabolic shape, and in the region of n_s near the refractive index of the virus ($n_k \approx 1.57$) it gives $\Delta n \approx 0$, which should correspond to particles of zero intrinsic anisotropy (see (17)). However, since the right-hand branch of the parabola (in the region $n_s > n_k$) was not obtained experimentally, the possibility is not eliminated that the observed solvent effect is due more to a change in the morphological properties of the virus particles than to the increase in the refractive index of the medium upon addition of aniline.

On the other hand, for an isotropic rodlike particle ($p = 20$) having a refractive index $n_k = 1.57$ in a glycerol-water mixture ($n_s = 1.4$), the theoretical $g_1 - g_2$ value corresponding to the form effect is $(g_1 - g_2) \approx 5 \times 10^{-3}$ according to Eq. (17). This is even somewhat greater than the above-mentioned experimental values for the total anisotropy of the particle.

Thus the experimentally-found value of the birefringence of the TMV solution can be completely ascribed to the form effect, in agreement with Lauffer's result.

A final quantitative solution of the problem of the anisotropy of TMV particles will require further special experiments.

2. Proteins. Numerous studies of the dynamooptical properties of solutions of a number of protein polymers can be found in the articles of Edsall and his associates,[1,126,127] and also in the monographs [4,6]. The results have been interpreted in terms of the rigid-ellipsoid model. They show good agreement of the geometric parameters of the particles obtained by the birefringence method with the data found by other methods,[128-130] thus favoring the orientational character of the observed birefringence. For illustration, we can cite the result of Boedtker and Doty,[131] who studied the dimensions and shape of particles of soluble collagen by various methods in solution, including flow birefringence.

At collagen concentrations below 0.1 g/100 cm^3 in buffer solutions, the intrinsic value and the orientation of the birefringence are practically independent

Table I. The molecular weight M, length L, and diameter d of particles of soluble collagen, as obtained by various methods (from Boedtker and Doty [131])

Method	M	L	d
Osmotic pressure (M_n)	$3.10 \cdot 10^5$	—	—
Light-scattering (M_w)	$3.45 \cdot 10^5$	$3.1 \cdot 10^{-5}$	$13.0 \cdot 10^{-8}$
Viscosity and M_w	—	$2.97 \cdot 10^{-5}$	$13.6 \cdot 10^{-8}$
Sedimentation and viscosity	$3.00 \cdot 10^5$	—	$12.8 \cdot 10^{-8}$
Birefringence and viscosity	$3.50 \cdot 10^5$	$2.90 \cdot 10^{-5}$	$13.5 \cdot 10^{-8}$

of the concentration. The particle length L calculated from the orientation angle in the range of gradients from 0 to 5500 sec^{-1} varied from 3×10^{-5} cm to 2.5×10^{-5} cm, respectively, indicating that the polydispersity of the sample was negligible.

The trend of the birefringence Δn with varying g corresponded to the theory of orientation of rigid particles, and the sign of the effect was positive. The found value of the specific anisotropy of the particles was $g_1 - g_2 = 2.4 \times 10^{-3}$. Using the experimental values of the refractive increment $dn/dC = 0.187$ of collagen solutions and the partial specific volume $\bar{v} = 0.7$, the authors found from Eq. (18) the ratio of the principal refractive indices of the particle $n_1/n_2 = 0.998$. Thus they concluded that collagen particles are optically isotropic, and the observed birefringence is a form effect.

The birefringence data are to be compared with the results obtained by other methods. The final results are given in Table I. They show completely satisfactory agreement among the data obtained by the various methods. The direct determination of the length distribution of collagen particles that Hall [132] has made by the electron-microscope method also corroborates these data. Thus, on the one hand, the study of the dynamooptical properties of collagen solutions confirms the correctness of the ideas that its molecules show considerable rigidity, are of rod-like form, and of triple-helical structure.[133] On the other hand, it illustrates the applicability of the equations of the orientation theory to such systems.

3. Polypeptides. The development of methods of synthesizing polypeptide chains [134,135] has made it possible to study dynamooptical properties using structures that can serve as models for the rigid helical conformations of native proteins, while at the same time having an assigned chain structure (identity of the repeating units, molecular weight, polydispersity of samples, etc.)

Among the known synthetic polypeptides, the most complete information on hydrodynamic and morphological properties has been obtained for poly-γ-benzyl-L-glutamate [134] (PBG). The conformation of this molecule in solutions has been studied by the methods of light scattering,[136,137] viscosimetry,[136,138] spectroscopy,[139] polarimetry,[137,134] diffusion and sedimentation,[140] and also by the method of orientation in an electric field.[141-146,260] All these studies give analogous results, according to which PBG molecules in a number of organic solvents (e.g., m-cresol) are reinforced by intramolecular hydrogen bonds, and thus can exist as rigid α-helices [147] having the "hydrodynamic" shape of a cylinder of diameter ~ 15 Å and length 1.5 Å per monomer unit in the chain. The length of the cylindrical particle is thus $L = 1.5\ M/M_0$ Å, where M is the molecular weight of the chain, and $M_0 = 219$ is the monomer unit. These conclusions are corroborated by data obtained by studying the angular distribution of X-ray scattering [148] of PBG in the solid state.

Yang [149] has studied the flow birefringence of solutions of a PBG sample ($M_w = 2.08 \times 10^5$, L = 1430 Å) in cresol, and of another sample of higher molecular weight ($M_w = 3.34 \times 10^5$, L = 2300 Å) in dichloroethane (ethylene dichloride) and obtained similar results. The relation $\Delta n = f(g)$ in m-cresol is shown in Fig. 10. The curves have the usual form for an orientation effect in a system of rigid particles. The initial slopes of the $\Delta n/g$ curves corresponding to different concentrations are given in Table II. By using the data on the viscosity η of

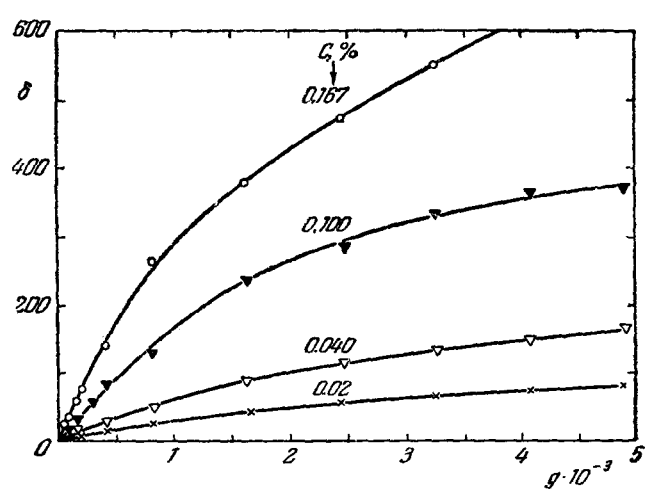

FIG. 10. The birefringence of poly-γ-benzyl-L-glutamate in m-cresol[149] ($\delta = 1.39 \times 10^{-6}\ \Delta n$).

the same solutions,[138] we can calculate the intrinsic value of the birefringence $\Delta n/g\ (\eta - \eta_0)$ corresponding to different concentrations. The obtained values (the last column in the table) agree within the limits of error for all concentrations. The same regularity is illustrated by the graphs in Fig. 11,[146] which shows the relation of Δn to $g(\eta - \eta_0)$ for the PBG sample in three solvents. Thus Peterlin's theory of the concentration-dependence of the birefringence (Eq. (43)) proves to be applicable to solutions of rigid rodlike particles. The concentration-dependence of the orientation angle also agrees with Eq. (42). The function $\chi(g)$ reduced to zero concentration generally agrees with the orientation theory. However, the length L of the cylindrical particles for the sample of Table II, as calculated from the angles χ as g was varied from zero to 5000 sec^{-1}, varied from 2300 to 1380 Å, thus indicating a considerable polydispersity of the sample.

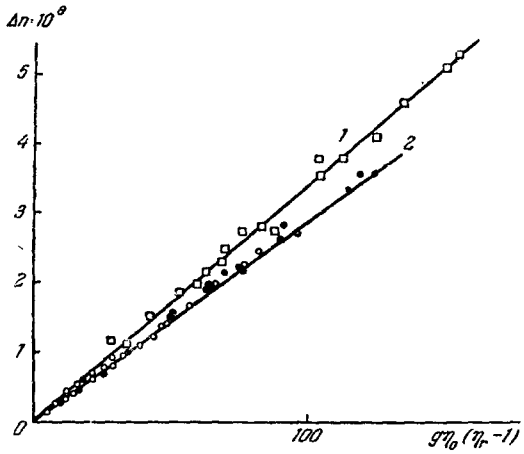

FIG. 11. The relation of Δn to the shear stress $g(\eta - \eta_0)$ for a sample of PBG ($M = 10^5$)[146] in dichloroethane (○), dimethylformamide (●), and chloroform (□).

In studying the morphological properties of PBG molecules, it is useful to combine the methods of flow birefringence and electric birefringence.[146,261]

In distinction from flexible chain molecules having no secondary structure, the rigid PBG helices in solution exhibit a strong positive birefringence in an electric field,[145] thus indicating the high degree of order of their internal structure.

In an alternating electric field one observes a sharp frequency-dependence of the Kerr constant, indicating the dipole nature of the process of orientation and relaxation. This is illustrated by Fig. 12, which shows the relation $\Delta n_\omega = f(\nu)$ for solutions of the sample of Fig. 11 in chloroform.[146]

By using these curves and the theory [2], we can calculate the relaxation time of dipole orientation τ_ϵ and the rotational diffusion coefficient $D_r = 1/2\tau_\epsilon$, and thereby also the length L of the rodlike molecule (by Eq. (10)). The corresponding data are given in Table III.

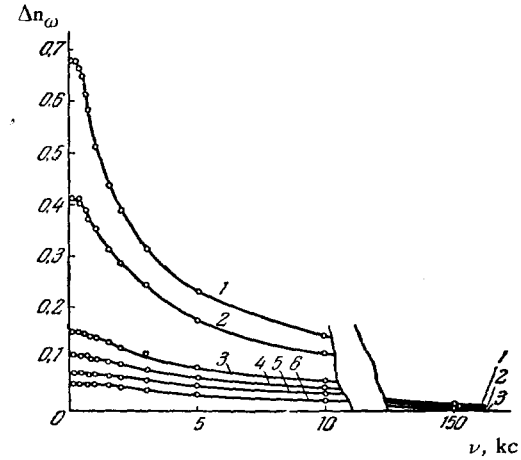

FIG. 12. The relation of the magnitude of the electrical birefringence (in relative units) of solutions of PBG in chloroform to the frequency $\nu = \omega/2\pi$ of the applied field.[145] 1: C = 1.5%; 2: C = 1.0%; 3: C = 0.5%; 4: C = 0.3%; 5: C + 0.2%; 6: C = 0.15%.

Table II. Birefringence and viscosity of solutions of PBG in m-cresol at 25°C [149]

C, g/100 cm³	$(\Delta n/g)_{g\to 0}\cdot 10^{12}$	$(\eta-\eta_0)\cdot 10^2$	$\left[\frac{\Delta n}{g(\eta-\eta_0)}\right]_{g\to 0}\times 10^{10}$
0.02	500	0.9	556
0.04	1080	1.84	587
0.10	2600	4.97	525
0.167	5560	9.0	615

If we assume the basic molecular structure to be the α-helix (1.5 Å per monomer unit), we can determine from the length L the molecular weight M, whose value is also given in Table III. It agrees well with the value obtained by viscosimetry ($M_\eta \approx 0.95 \times 10^5$), thus corroborating the hypothesis of the α-helical structure.

The second and third columns of the table give the data on the optical anisotropy of the same sample obtained from the flow-birefringence measurements. The difference between the principal polarizabilities of the molecule (in vacuo) $\gamma_1 - \gamma_2$ is calculated by Eq. (16), in which the Lorentz factor $((n^2 + 2)/3)^2$ has been introduced, and it has been assumed that $b_0/F(p) = 1$. The fourth column of the table gives the experimental values of the specific [150] Kerr constant K_S of PBG in a direct-current field.

By comparing these quantities with the value of $\gamma_1 - \gamma_2$, we can calculate [151] the axial component μ of the dipole moment of the molecule. The values of μ are also given in Table III. The last column gives the value of $\mu(M_0/M) = \mu_0$, the dipole moment per monomer unit of the molecule. The value of μ_0 agrees with the value obtained by measuring the dielectric constant of PBG solutions.[144] This means that the directions of the valence bonds N-H and C=O (linked by the intramolecular hydrogen bonds) are near the axis of the helix.

The polarizability difference $\gamma_1 - \gamma_2$ given in

Table III. Dynamooptic, electrooptic, and morphological properties of PBG molecules in solution [146]

Solvent	$\frac{\Delta n}{g(\eta-\eta_0)}\cdot 10^{10}$	$(\gamma_1-\gamma_2)\cdot 10^{25}$, cm³	$K_s\cdot 10^8$	$\tau\cdot 10^5$, sec	$D_r\cdot 10^{-3}$, sec^{-1}	L, Å	$M\cdot 10^{-5}$	$\mu\cdot 10^{18}$	$\frac{\mu M_0}{M}\cdot 10^{18}$
Dichloroethane	295	3600	7,6	1,0	50	700	1,02	1390	3,0
Chloroform	342	4200	9,6	1,3	38	880	1,30	1650	2,8

Table III includes both the intrinsic anisotropy of the molecule and the form effect.

By using Yang's data (Table II) obtained in m-cresol (in which $n_k \approx n_s$), we can estimate the intrinsic anisotropy (from Eq. (16)). For the sample of $M_w = 2.08 \times 10^5$, we find $\gamma_1 - \gamma_2 = 7000 \times 10^{-25}$ cm³ (in vacuo). This value is two orders of magnitude greater than the anisotropy of flexible chain molecules of synthetic polymers having no secondary structure (see Sec. III, B). However, the anisotropy per monomer unit with respect to the principal axes of the helix

$$a_{\parallel} - a_{\perp} = (\gamma_1 - \gamma_2)\frac{M_0}{M} = 7\cdot 10^{-25} \text{ cm}^3$$

is quite small.

For a monomer unit of PBG of absolutely rigid structure $[(-NH-CHR-CO-)_n$, where R is $-(CH_2)_2-COO-CH_2-C_6H_5]$, the anisotropy $a_{\parallel} - a_{\perp}$ should be negative. The fact that it actually has a small positive value indicates that the ester side-chain is considerably more flexible than the helical main chain, which is reinforced by hydrogen bonds.

Thus, the combination of the two cited methods permits us to obtain rather full information on the geometrical, optical, and electric parameters of PBG molecules. This information agrees well with the α-helical structure.

The data obtained in chloroform agree somewhat more poorly with the properties of the α-helix model than the results obtained in dichloroethane. This fact can result either from phenomena of molecular association in chloroform, or from some change in the conformation of the molecules upon substitution of the one solvent for the other.

The study of the frequency-dependence of the electrooptic effect shows that the relaxation time τ and the corresponding effective lengths L can be considered to be frequency-independent only in a first approximation, and only in the range of sufficiently high frequencies ν. On the contrary, as ν decreases, τ and L increase appreciably.

This is illustrated by Fig. 13. This phenomenon resembles the effect of variation of D_r and L observed in the study of the orientation angles χ (see Fig. 9), and is obviously due to the polydispersity of the sample.

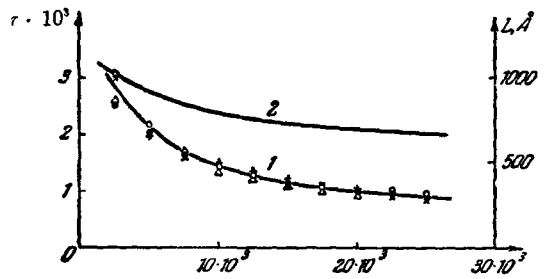

FIG. 13. The relation of the relaxation time τ of the Kerr effect and the corresponding effective molecular length L to the electric-field frequency ν for solutions of various concentrations of PBG in dichloroethane.[146] 1: $\tau = \tau(\nu)$; ○ – 0.3%; ● – 0.25%; + – 0.20%; Δ – 0.13%, × – 0.10%; 2: L = L(ν).

4. Nucleic acids. Recently, much attention has been attracted to the study of the structures of the nucleic acid molecules,[177] deoxyribonucleic acid (DNA) and ribonucleic acid (RNA), in connection with the important biological functions of these polymers.

a) DNA. A number of studies [152-174] have dealt with the dynamooptical properties of DNA solutions. In all cases, a large effect of negative sign has been found, with a value increasing with the velocity gradient, in accordance with the theory of orientation of rigid particles (see Fig. 5).

The high rigidity of the dissolved macromolecules is also manifested in the insignificant influence of the ionic state of the solution on the hydrodynamic properties of the molecules. Figure 14 [155] shows the relation of the orientation angle χ to the velocity gradient g for aqueous solutions of DNA having various concentrations of added salt (NaCl).

In distinction from the behavior of solutions of flexible polyelectrolytes, the points remained clustered about a single curve as the ionic strength was varied by a factor of 10^4, indicating the invariability of the dimensions of the DNA molecule under these conditions, and thus illustrating their considerable rigidity.

Studies of the rigidity of DNA molecules by Cerf's method have been made by Cerf [154] and by Leray. [165,166,173] The final results are given by the graph of Fig. 15,[173] where the intrinsic value of the orientation angle $[\varphi/g]$ is shown as a function of the viscosity η_0 of the solvent or as a function of the parameter $M[\eta]\eta_0$ for three DNA samples (Nos. 2, 3, and 4 of

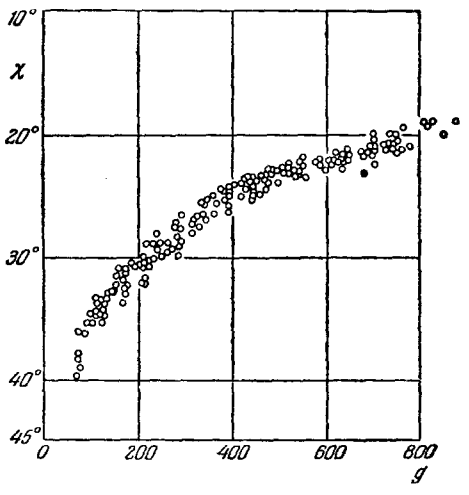

FIG. 14. The relation of the orientation angle χ to the velocity gradient g for aqueous solutions of DNA for various ionic strengths of the solutions.[155] The points correspond to intervals of variation of the DNA concentration from 8×10^{-3} to 20×10^{-3} g/100cm³, and salt concentrations from 1×10^{-3} to 10000×10^{-3} g/100 cm³.

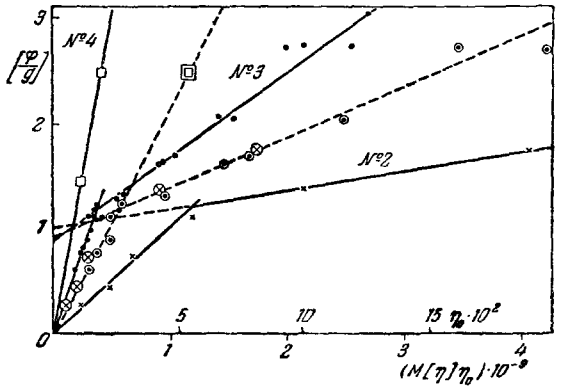

FIG. 15. The relation of $[\phi/g]$ to the viscosity of the solvent for three DNA samples.[173]

Table IV). In all cases in the region of small η_0, the points lie on straight lines passing through the origin. As η_0 was increased, the curve $[\varphi/g] = f(\eta_0)$ for two of the samples showed a sharp break, while this range of η_0 values was apparently not attained with the third sample.

Such a trend in the function, according to Cerf, corresponds to the case of semirigid macromolecules (see Fig. 8), for which the observable birefringence is an orientation effect in the region of small η_0, but a deformation effect in the region of large η_0. In "normal" coordinates (with $M[\eta]\eta_0$ as abscissa), the initial slopes of the curves for all three samples agree, in accordance with the theory.

At the same time, according to the data obtained, the kinetic rigidity (internal viscosity) of the third sample (No. 4) must be considerably higher than for the first two, since it did not exhibit a break in the straight line graph. Here the greater kinetic rigidity of the sample is accompanied by a lesser equilibrium rigidity (though having a greater molecular weight, sample No. 4 gives practically the same viscosity as sample No. 3). In itself, this fact compels us to treat with caution any attempts to interpret the presented data quantitatively, in any case, in the sense of establishing a relation between the rigidity and molecular structure of different DNA samples. However, the obtained results indisputably show that in the region of small velocity gradients when the viscosity of the solvent is not too great, the dynamooptical effect in DNA solutions can be described within the framework of the theory of orientation of rigid particles.

Table IV gives the dynamooptical parameters for some DNA samples. Here $D_0 = D_r\eta_0$, and a is the numerical coefficient in Eqs. (33) and (38). The a coefficients agree in order of magnitude with the value predicted by theory (a does not depend greatly on the model characteristics of the particle), but they differ rather greatly for different DNA samples. D_0 systematically (and very sharply) declines with increasing molecular weight, in qualitative agreement with the theory. It would seem premature at present

Table IV. Characteristic constants of the birefringence of some samples of native DNA (thymus) from the data of different authors

Author	$M \cdot 10^{-6}$	$[\eta] \cdot 10^{-3}$, cm³/g	D_r, $cm^{-1}sec^{-1}$	a	$(g_1-g_2)10^3$	$\frac{[n]}{[\eta]} \cdot 10^3$	$M_s \cdot 10^{-3}$	A, Å
1. Wissler[152]	—	—	2.03	—	—	—	—	—
2. Schwander and Cerf[154]	6	1.5	0.48	0.48	−0.88	−4.3	400	2100
3. Leray[173]	6	5.7	0.12	0.49	—	—	—	—
4. Leray[175]	11	6.5	0.06	0.47	−0.29	−1.56	144	760
5. Goldstein	6.85	4.8	0.046	1.43	−1.0	−6.7	620	3200
6. and	5.9	5.1	0.18	0.38	−1.5	−2.4	220	1170
7. Reichmann	5.85	5.34	0.21	0.35	−1.0	−1.25	116	600
8. [162,163]	3.5 (2.5)	3.07	2.83	0.1	−4.1	−0.8	75	400
9. Andreeva and Tsvetkov*	6.5	5.0	0.10	0.62	−0.40	−1.4	130	680
10. Frisman[174]	5	4.0	—	—	—	−5	460	2400

*Unpublished

to speak of quantitative agreement, in view of the insufficient number of systematic experimental studies. If we represent the DNA molecule by the model of a rigid continuous ellipsoid (as was usually done in the earlier studies), and use the experimental D_r values and Eqs. (8)—(10), we obtain lengths exceeding tens of thousands of Ångström units in a number of cases. Here the model ellipsoid is transformed into a thin straight rod with the enormous asymmetry of $p \approx 500$. The stable existence of molecules of such a configuration in solution is improbable, since it is hard to imagine even for the Watson-Crick double helix that such a shape would not be destroyed by the thermal motion of the parts of the molecule and by defects in the secondary structure. Besides, such a conformation does not agree with the optical properties of the macromolecules.

The great spread in the values of $g_1 - g_2$ and $[n]/[\eta]$ obtained by different authors cannot be ascribed to experimental errors. It is apparently due to actual differences in the morphological properties of the studied samples, since we know that a change in the morphology (e.g., denaturation) shows a more marked influence on the optical anisotropy than on the hydrodynamic properties of DNA molecules.[174]

The values of $[n]/[\eta]$ (which are negative in sign) are two orders of magnitude greater than the $[n]/[\eta]$ values usually obtained from flexible chain polymers, thus indicating the high degree of order of the structural elements of the DNA chain.

These properties fully agree with the generally accepted molecular model of Watson and Crick,[178] in which the rigid double-helix structure is reinforced by hydrogen bonds linking the purine and pyrimidine bases of the DNA chains. Here the planes of the optically-anisotropic bases are normal to the axis of the double helix, giving rise to the large negative anisotropy of the entire molecule.

On the other hand, a theoretical estimate[175] of the anisotropy of the monomer unit (or nucleotide pair) of DNA with respect to the helical axes gives a value $a_{\parallel} - a_{\perp} \approx -190 \times 10^{-25}$ cm^3. Assuming this value of $a_{\parallel} - a_{\perp}$, if we represent the DNA molecule by the model of a rigid rod, we get a value for its anisotropy $\gamma_1 - \gamma_2$ exceeding the experimental value by a factor of tens (or even hundreds).

Nevertheless, we can interpret the experimental values of $[n]/[\eta]$ reasonably by representing the DNA molecule by the model of a random coil of great rigidity.[175] If we take into account the fact that for a rigid chain such as DNA, the macroform effect $[n]_f$ constitutes an insignificant fraction of the observed birefringence $[n]$ (see Table V), we can reduce Eqs. (29), (30), and (31) to the form

$$\frac{[n]}{[\eta]} = \frac{4\pi}{45kT} \frac{(n_s^2+2)^2}{n_s} s \left[a_{\parallel} - a_{\perp} + \frac{M_0}{2\pi N_A \bar{\nu}} \left(\frac{dn}{dC} \right)^2 \right]. \quad (45)$$

Table V gives the results obtained by using the experimental data of Table IV and Eq. (45) for sample No. 9, while the last column of Table IV gives the results for all the others. They show that, in order to explain the experimental values of the optical anisotropy, we can represent the DNA molecule by the model of a chain of freely-linked linear segments. The molecular weight M_S of each of these segments amounts to hundreds of thousands, while its length A amounts to hundreds or thousands of Ångström units.

The quantity s characterizes the average number of nucleotide pairs joined in an ordered double-helix structure, while A is the average length of such an ordered helical region. Thus, these quantities give information on the dimensions of the regions in the DNA chain through which the "long-range order" in the orientation of the planes of the bases extends; this order is responsible for the negative anisotropy of the chain, and is maintained by the intramolecular hydrogen bonds. The ordered structural elements are linked by regions where the secondary structure of the molecule (the hydrogen bonds of the bases) is weakened for some reason, thus causing a certain flexibility of the chain (Fig. 16).[258] At the same time, the dynamooptical properties of DNA obviously do not correspond to the model of a straight rod, since in this case the number s of monomers per segment would simply be equal to the degree of polymerization. The anisotropy of the molecule, e.g., for the sample given in Table V, would correspondingly be $M/M_S = 50$ times as great as the value found ex-

Table V. Birefringence and the mean dimensions of the ordered regions of double-helical chain of DNA

Experimental data					
M	$[\eta]_0$	$[n]$	M_0	dn/dC	$\bar{v}$[176]
$6.5 \cdot 10^6$	$5 \cdot 10^3$	$-0.71 \cdot 10^{-3}$	660	0,172	0.56
Calculated					
$[n]_f$	$a_{\parallel} - a_{\perp}$	s	M_s	A	$[n]_{fs}$
$+1 \cdot 10^{-6}$	$-190 \cdot 10^{-25}$	200	$130 \cdot 10^3$	680 Å	$+0.64 \cdot 10^{-3}$

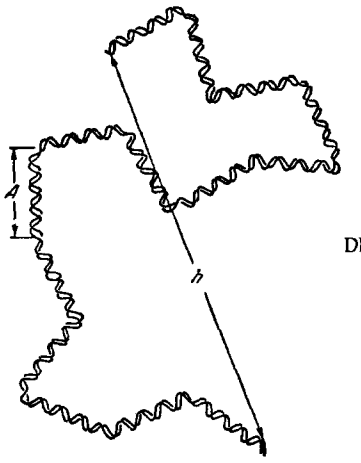

FIG. 16. Optical model of the DNA molecule.

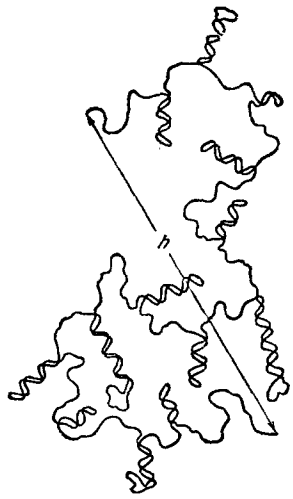

FIG. 17. Model of the RNA molecule (according to Doty).

perimentally. The hydrodynamic properties of DNA solutions also agree better with the molecular model of a random coil than with that of a rigid rod.[179]

The values cited for s and A were obtained under the assumption that the planes of the bases within the ordered elements are strictly normal to the axis of the helix. Local defects in the double-helix regions only slightly affecting the overall geometry of the chain can decrease appreciably the optical anisotropy of these regions, and hence also the experimental values of s and A. This would seem to explain the great divergence in the values obtained from different samples (Table IV).

This fact shows that the birefringence can be used as a sensitive method of comparative analysis of DNA samples of differing origins, and in particular, of studying the degree of order of their helical structures. This method has actually been applied in several instances, e.g., in studying processes of denaturation of DNA.[168-172,174]

What has been said is also illustrated by the fact that the effects of heat and changes in the ionic strength of the solution have a weaker influence on the hydrodynamic characteristics[155,179] (Fig. 14) of DNA solutions than on the optical anisotropy.[174]

b) RNA. The information on the morphological properties of RNA is more scanty than for DNA. In spite of the great similarity in the chemical structures of these two polynucleotides, the hydrodynamic properties of their solutions differ greatly. In the case of RNA, they agree with the properties of ordinary flexible polyelectrolytes, and depend greatly on the ionic strength, the pH, and the temperature of the solution.[180-183]

At the same time, the presence of a hypochromic effect [sic!] (an increase in the ultraviolet absorption) upon heating or upon decreasing the ionic strength of the solution indicates the existence of imperfect helical regions in the chain. When the helical structure is destroyed (by the action of heat or by decrease in ionic strength), the dimensions of the RNA molecules in solution expand, in distinction from DNA. Hence we can conclude[177] that the helical regions

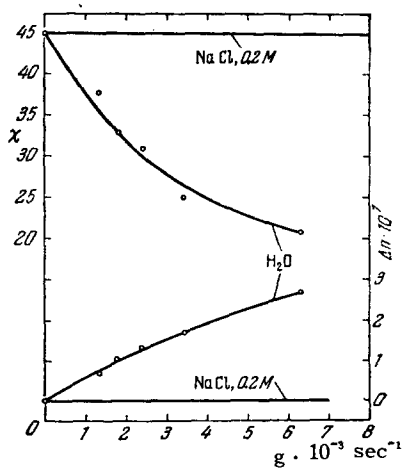

FIG. 18. The orientation angle and the magnitude of the birefringence for RNA solutions. RNA concentration $C = 2.8 \times 10^{-3}$ g/cm³.

are linked by single molecular chains of RNA having the conformation of randomly coiled flexible chain molecules (Fig. 17).

The data on the dynamooptical properties of RNA are as yet very sparse.[184,185]

Figure 18 shows the results[184] obtained in a neutral aqueous solution of an RNA sample from Escherichia coli. The birefringence is positive and considerably smaller in magnitude than that in DNA solutions. The $\Delta n = f(g)$ graph is curved toward the horizontal axis, as is typical of flexible chains of polyelectrolytes in solutions of low ionic strength.[257] An increase in the ionic strength of the solution results in coiling of the flexible RNA chain, and sharply reduces the magnitude of the birefringence.

Analogous results were obtained in[185] from RNA samples of a different origin, and a study was made of the concentration-dependence of the effect for various ionic strengths (rather small, not exceeding 0.01) of the solution. The nature of the concentation-dependence also resembles that of flexible polyelectrolytes in the ionized state. At a moderate ionic

strength (buffered 0.01 M NaCl), the value of the anisotropy of the molecule $\gamma_1 - \gamma_2 = +1100 \times 10^{25}$ cm^3 for a sample from TMV. If we assume the model of Fig. 17, we can take this large value (for a flexible chain polymer) as consisting of three components: the negative anisotropy of the single coiled chains of the molecule (like polystyrene or poly-β-vinylnaphthalene), the slight (probably positive) anisotropy introduced by the helical regions (whose axes are oriented practically at random), and the positive form anisotropy. At small salt concentrations (as in the discussed cases), the form effect is of decisive importance [186,257] for a flexible polyelectrolyte chain, and results in a positive total birefringence (cf. the data of Table XVII).

Thus the currently known dynamooptical properties of RNA solutions do not contradict the model of Fig. 17. However, they cannot prove it beyond question, since they are fundamentally determined by the electrostatic interactions of the charged chain, which blur out the effect of the secondary structure. To study the latter, we must screen the interaction of the charges by increasing the ionic strength of the solution. Here, however, owing to the coiling of the molecules, the birefringence declines sharply, and the experiment requires increase in the concentration of the solutions, improvement of their purification, and an increase in the sensitivity of the apparatus.

B. Polymers with flexible chain molecules

Even the first systematic studies of the relations $\Delta n = f(g)$ and $\chi = \chi(g)$ in the solutions of a number of synthetic polymers [187,79] showed that the deformation of the macromolecules in the flow plays the basic role in the dynamic birefringence of these systems (at least at appreciable shear stresses). Hence, in the quantitative interpretation of the experimental data for polymers having flexible chain molecules, we must rely on a theory taking this deformation into account (Sec. II, B).

In comparing theory with experiment, we must take into account the influence of concentration effects, which commonly play a very essential role in the systems being discussed.

1. Concentration-dependence (in the absence of a form effect). Among the proposed methods [187,188,96] for extrapolating the experimental data to zero concentration, the one deserving greatest attention is that of Peterlin, based on Eqs. (40)—(44). In this method, the experimental data on Δn and χ obtained from solutions of a given polymer at various concentrations C are to be plotted in the form of the relations $\Delta n/\Delta\tau = f(\Delta\tau/C)$ and $\chi = \chi(\Delta\tau/C)$, where $\Delta\tau = (\eta - \eta_0)g$ is the effective shear stress, and η is the viscosity of the solution of concentration C at a velocity gradient of g. Here, according to (43) and (42), the data corresponding to different concentrations must lie on a single curve.

a) The relation of Δn to C. In the region of small shear stresses ($g \to 0$), Eq. (43) implies the constancy of $\Delta n/\Delta\tau$ for all concentrations. This result is confirmed by voluminous experimental material, and is illustrated by Figs. 19 and 20, where the relation $(\Delta n/\Delta\tau)_{g\to 0} = f(C)$ is shown for a series of solutions under the condition $n_k \approx n_s$. The points for

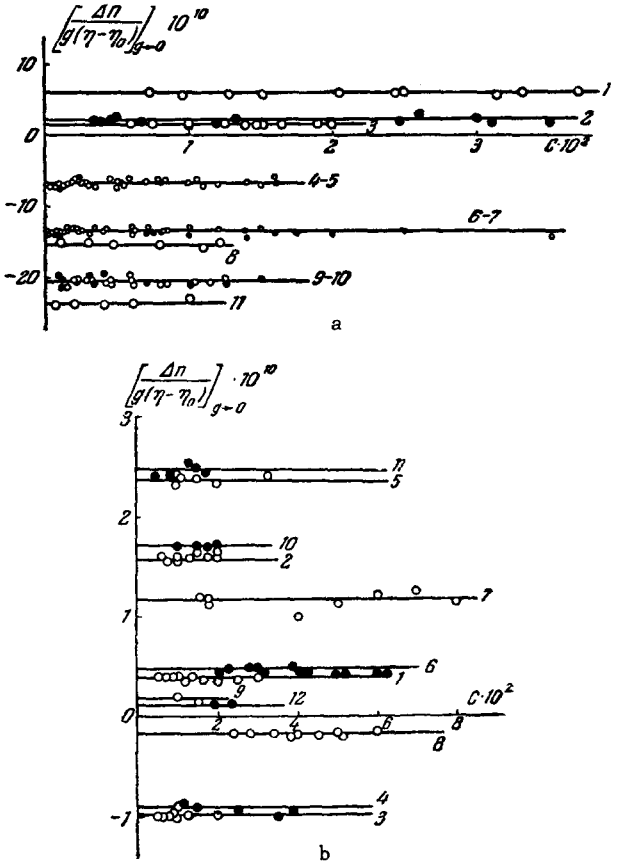

FIG. 19. Anisotropy of solutions at various concentrations. a) 1 – polyethyleneterephthalate in a 1:1 dichloroethane-phenol mixture, M = 3 × 10^4; 2 – PMMA (atactic) in toluene, M = (0.004 – 4) × 10^6; 3 – PMA (polymethylacrylate) in benzene; 4 – ● – polyvinylpyrrolidone in benzyl alcohol; 5 – ○ – poly-p-tert-butylphenylmethacrylate in bromobenzene, M = (0.2 – 20) × 10^6; 6 – ○ – polystyrene (atactic) in bromoform, M = (0.2 – 17) × 10^6; 7 – poly-p-methylstyrene in bromoform, M = (0.3 – 0.7) × 10^5; 8 – poly-2,5-dimethylstyrene in bromoform; 9 – ● – isotactic polystyrene in bromoform; 10 – ○ – poly-p-chlorostyrene in bromoform, M = (0.55 – 9) × 10^6; 11 – poly-2,5-dichlorostyrene in bromoform. b) 1 – polydimethylsiloxane in benzene, M = (1.8 – 0.7) × 10^6; 2 – polymethylmethacrylate in toluene; 3 – polybutylmethacrylate in benzene; 4 – ● – polyphenylmethacrylate in bromobenzene; 5 – polypropylene in carbon tetrachloride; 6 – ● – polyvinylacetate in benzene; 7 – polyvinylacetate in toluene; 8 – polymethylphenylsiloxane in benzene; 9 – poly-tert-butylmethacrylate (atactic) in benzene; 10 – poly-tert-butylmethacrylate (isotactic) in benzene; 11 – isotactic PMMA in benzene; 12 – syndiotactic PMMA in benzene.

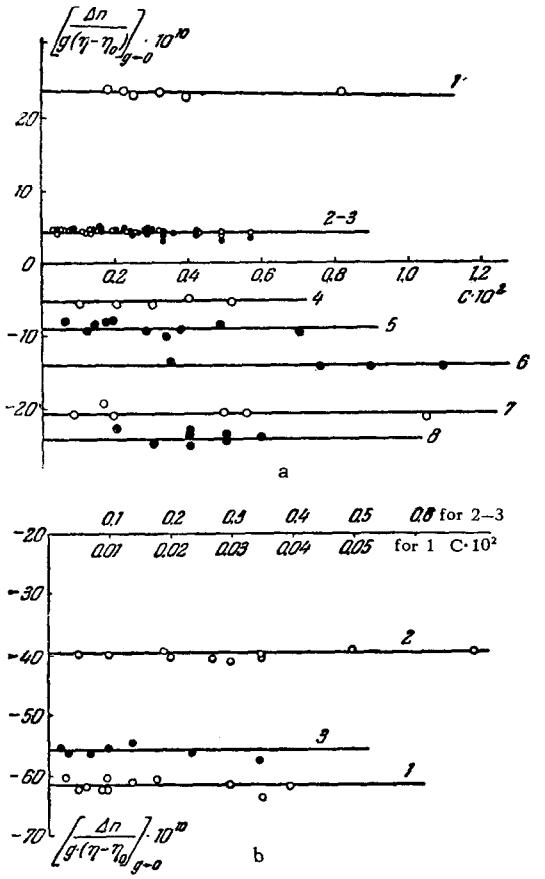

FIG. 20. Anisotropy of solutions at various concentrations. a) 1 – ethylcellulose in carbon tetrachloride, M = (0.3 – 1) × 10^4; 2 – ● – polyisobutylene in benzene; 3 – ○ – natural rubber, M = (2.6 – 26) × 10^5 in benzene; 4 – polynaphthylmethacrylate in tetrabromoethane; 5 – polyphenylmethacrylamide in o-toluidine; 6 – polychlorophenylmethacrylamide in o-toluidine; 7 – polycarbethoxyphenylmethacrylamide in o-toluidine; 8 – poly-3,4-dichlorostyrene in tetrabromoethane; b) 1 – nitrocellulose (γ = 2.8), lower scale (in cyclohexanone), M = 1 × 10^6; 2 – poly-β-vinylnaphthalene in tetrabromoethane; 3 – cellulose tribenzoate in bromobenzene.

a given polymer-solvent system lie on a single straight line parallel to the concentration axis, independent not only of the concentration of the solution, but also of the molecular weight of the dissolved sample and its degree of polydispersity.

This means that the birefringence in all the studied systems not only shows a concentration-dependence following Eq. (43), but also varies with the molecular weight M of the polymer in accordance with Kuhn's theory.

Thus, from measurements of the value of the birefringence of the solution and its viscosity made under the condition g → 0, using Eq. (43), we can reliably determine the segment anisotropy $\alpha_1 - \alpha_2$ of a polymer molecule without recourse to studies of the concentration-dependences of Δn and η. The experimental data on the concentration-dependence of the birefringence are considerably less complete in the region of large shear stresses, where a deviation from proportionality between Δn and $\Delta\tau$ is clearly manifested. Hence, in order to get the value of $(\Delta n/C)_{C\to 0}$ in the region of large g, we must resort to the ordinary graphical extrapolation of the experimental data to zero concentration.

b) The orientation angle. The concentration-dependence of the orientation angle has been studied in a number of references [149,187-193] whose results can be summarized as follows.

At low enough concentrations of solutions in low-viscosity solvents, the experimental points plotted in coordinates of $\chi = \chi(\Delta\tau/C)$ practically all cluster about a single curve (Fig. 21). With increase of concentration we observe a deviation from this rule that increases with increasing velocity gradient and solvent viscosity (Fig. 22). Experiment shows that for every actual polymer-solvent system, we can choose an experimentally-attainable region of concentrations

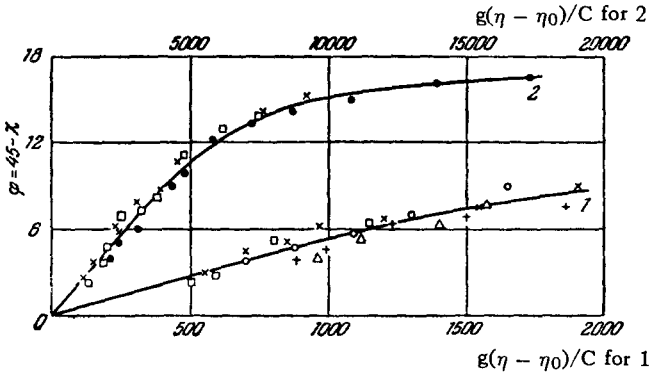

FIG. 21. The variation of the orientation angle $\phi = \phi(\Delta\tau/C)$ for polymethylmethacrylate fractions (M = 2.3 × 10^6) in two solvents.[192] 1 – solvent: acetone, η_0 = 0.3 × 10^{-2}; x – C = 0.98 × 10^{-2}, + – C = 0.81 × 10^{-2}, ○ – C = 0.67 × 10^{-2}, Δ – C = 0.55 × 10^{-2}, □ – C = 0.28 × 10^{-2} g/cm³; 2 – solvent: bromoform-tetrabromoethane mixture, η_0 = 3 × 10^{-2}; ● – C = 0.23 × 10^{-2}, × – C = 0.18 × 10^{-2}, □ – C = 0.12 × 10^{-2} g/cm³.

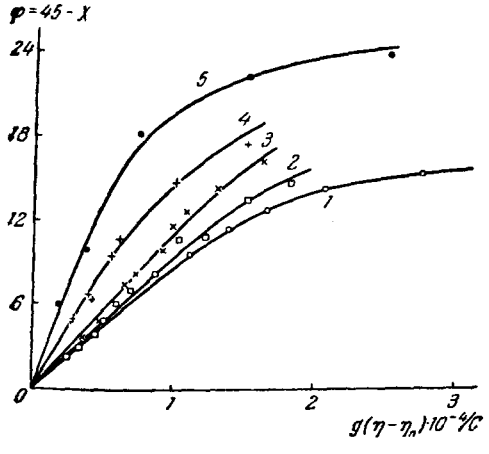

FIG. 22. The variation of the orientation angle $\phi = \phi(\Delta\tau/C)$ for polymethylmethacrylate fractions (M = 2.3 × 10^6) in tetrabromoethane (η_0 = 15.3 × 10^{-2}) at the temperature 7°C.[192]

1 – ○ – C = 0.03 · 10^{-2}; 2 – □ – C = 0.08 · 10^{-2}; 3 – × – C = 0.12 · 10^{-2}; 4 – + – C = 0.18 · 10^{-2}; 5 – ● – C = 0.363 · 10^{-2} g/cm³.

and velocity gradients for which the concentration-dependence of the orientation angle will approximate Eq. (42). Hence the drawing of $\chi = \chi(\Delta\tau/C)$ curves is a useful method for simplifying the extrapolation of the experimental values to zero concentration.

2. The relation of χ and Δn to the shear stress. It was found in even the first studies [79] and later confirmed [29,31,42,44,189-193] that the experimental relation $\chi_{C\to 0} = \chi(g)$ for an infinitely dilute solution qualitatively resembles the theoretical relations (27), (36) or (37), but does not agree with them quantitatively. If we fit the initial slopes of the theoretical and experimental curves for $\chi = \chi(\beta)$, the latter curves will be flatter with further increase in β than the former. Figure 23 is presented as an illustration. Apparently, one of the basic reasons for this discrepancy is polydispersity (see Figs. 9 and 13), which is practically unavoidable in any actual polymer fraction. In addition, we must also bear in mind the possible effect of kinetic rigidity of the molecular chain [as is not taken into account in Eqs. (27), (36), or (37)]. In Kuhn's dumbbell model the internal viscosity not only increases the initial slope of the $\chi(\beta)$ curve, but also causes the curve to be flatter at large β, thus bringing the theoretical $\chi(\beta)$ curve closer to the experimental.[87]

By representing the molecule by the model of a viscoelastic sphere, Cerf [97] showed that one can get a theoretical $\chi(\beta)$ curve similar to the experimental curve by assuming certain properties of the model.

Thus the fact that the theoretical relation $\chi(\beta)$ given by Eqs. (36) or (37) only qualitatively agrees with the experimental relation does not seem paradoxical, since Zimm's theory does not take into account such an important kinetic factor as the internal viscosity of the molecule.

An analogous situation occurs in the relation of the value of the birefringence to the shear stress. This is illustrated by Fig. 24, which shows, in addition to the theoretical curve (from Eq. (26) with $\theta_f = 0$), the experimental values of $(\Delta n/C)_{C\to 0}$ for a high-

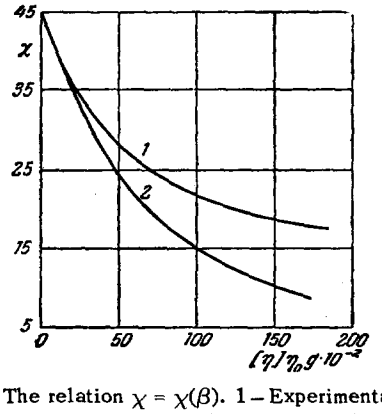

FIG. 23. The relation $\chi = \chi(\beta)$. 1 – Experimental curve for a fraction of poly-p-tert-butylphenylmethacrylate (PptBPMA, M = 7.4 × 10⁶) in bromobenzene [200,208]; 2 – from Eq. (27), with initial slopes fitted by choice of the coefficient in Eq. (27).

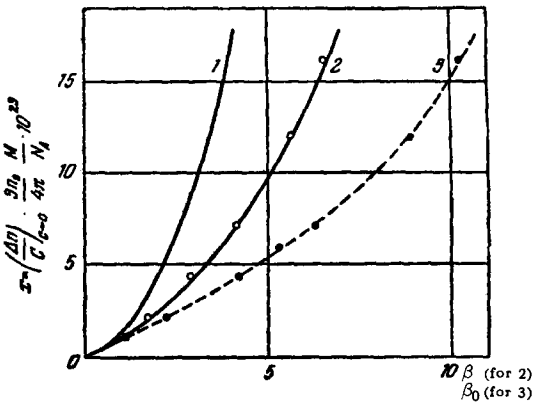

FIG. 24. The relation of the birefringence $(\Delta n/C)_{C\to 0}$ to the shear stress. 1 – From Eq. (26); 2 – experimental data for a PptBPMA fraction (M = 24 × 10⁶) in bromobenzene [193,200] as a function of $\beta = M[\eta]\eta_0 g/RT$; 3 – the same, as a function of $\beta = M[\eta]_0\eta_0 g/RT$ where $[\eta]_0 = \lim_{g\to 0}[\eta]$.

molecular-weight fraction of poly-p-tertiary-butylphenylmethacrylate (PptBPMA) as a function of β or β_0. While the forms of the theoretical and experimental curves are qualitatively similar, however, at large β values the experimental curves rise considerably less steeply than the theoretical (with equal initial slopes).

The experimental data approach the theoretical if we take into account the dependence of $[\eta]$ on the shear stress (curve 2). Peterlin has recently discussed this fact.[194,195]

The discrepancy between theory and experiment in the region of large β might be due either to the inadequacy of the hydrodynamic parameters of Kuhn's model or to the neglect of the influence of the internal viscosity. A comparison of the experimental data with Eq. (35), which is based on a more refined model, gives better results, but it does not completely eliminate these discrepancies.

We should point out that, although each of the experimental relations $\Delta n = f(\beta)$ and $\chi = \chi(\beta)$ by itself diverges from the theoretical relations (26) and (27), the direct relation between Δn and χ expressed by Eq. (44) is confirmed well by the experimental data over a broad range of concentrations and shear stresses.[58,196-198] This fact indicates that the discrepancies between theory and experiment found in the orientation and the magnitude of the birefringence are caused by similar mechanisms. Perhaps the essential role in these mechanisms is played by the kinetic rigidity of the molecular chains, which hinders their uncoiling in the flow.

3. The relative roles of orientation and deformation at small shear stresses. While we can reliably state on the basis of the existing data that the Maxwell effect in solutions of chain molecules at large shear stresses is fundamentally due to the deformation of the macromolecules, the problem of the relative roles

of deformation and orientation at low flow rates requires special treatment.

A number of studies [96,173] have dealt with the relation of the intrinsic value of the orientation angle $[\varphi/g]$ to the solvent viscosity η_0. The objects of study were solutions of polystyrene fractions. The interval of measurement of η_0 covered the range from 0.6 to 4 centipoise.

The found relation $[\varphi/g] = f(\eta_0)$ in all cases has the form of an inclined straight line intersecting the $[\varphi/g]$ axis at a finite intercept. That is, it corresponds to Eq. (38) or curve 2 in Fig. 8. This result shows that for the studied polystyrene samples in the stated range of variation of η_0, deformation of the molecules plays the fundamental role in the birefringence.

A number of other studies have taken up the relation of $[\varphi/g]$ to M at constant η_0 in solvents of low viscosity ($\eta_0 < 2 \times 10^{-2}$). Fractions of polystyrene, [44,189,191] polyisobutylene, [190] PptBPMA, [99] rubber, [199] and nitrocellulose [200] have been studied. It was found that at constant η_0, the value of $[\varphi/g]$ increases proportionally to $M[\eta]_0$. This is illustrated by Fig. 25, which gives the relation of $[\varphi/g]/M$ to $[\eta]_0\eta_0$ for the first three of the cited polymers. In these cases the birefringence is an orientation effect, and the relation between $[\varphi/g]$ and M corresponds to line 1 in Fig. 8. A complete $[\varphi/g] = f(\eta_0)$ curve (of the type of curve 3 in Fig. 8) including both asymptotic branches has been obtained from solutions of polymethylmethacrylate ($M = 2.3 \times 10^6$) in a range of solvent viscosities η_0 from 0.3×10^{-2} to 15×10^{-2} poise. The results are shown in Fig. 26. [192] They illustrate the transition from orientational to deformational birefringence as η_0 increases. The values of the coefficient a in Eq. (33) calculated from the

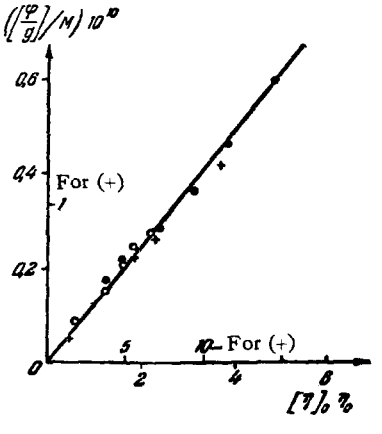

FIG. 25. $[\phi/g]/M$ as a function of $[\eta]_0\eta_0$ for solutions of fractions of certain polymers. ● – Polystyrene in benzene[189] (M from 0.9×10^6 to 5.2×10^6), $\eta_0 = 0.65 \times 10^{-2}$; ○ – polyisobutylene in hexane[190] (M from 1.24×10^6 to 9.8×10^6), $\eta_0 = 0.32 \times 10^{-2}$; + – poly-p-tert-butylphenylmethacrylate (PptBPMA) in bromobenzene[99] (M from 1.1×10^6 to 24×10^6 to 24×10^6), $\eta_0 = 1.3 \times 10^{-2}$ (on the small scale).

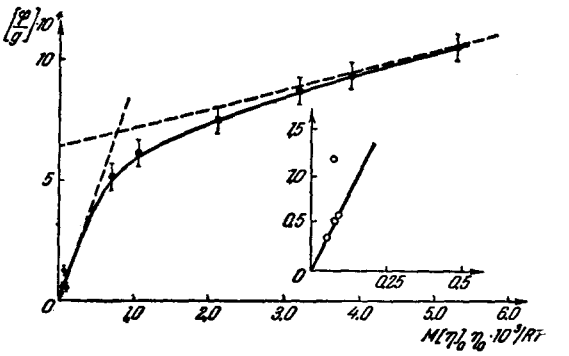

FIG. 26. The relation $[\phi/g] = f(M[\eta]_0\eta_0/RT)$ for PMMA fractions ($M = 2.3 \times 10^6$). Range of η_0 from 0.3×10^{-2} to 15×10^{-2} poise.[192]

experimental data on the slopes of the initial straight lines in Figs. 25 and 26 are given in Table VI. In order of magnitude they lie within the limits predicted by theory for the various models, and are also close to the a values given in Table IV. The lack of systematic experimental material at present does not permit us to say how much the differences in the found values of a express structural characteristics of the studied polymer-solvent systems, rather than involving experimental errors.

However, the data presented undoubtedly show that the dynamic birefringence of a solution of a chain polymer in solvents of low viscosity η_0 in the range of small shear stresses $\Delta\tau$ is an orientation effect that goes over into a deformation effect as η_0 or $\Delta\tau$ increases. This fact is of considerable importance, since it permits us to apply the theory of orientation of rigid particles to solutions of chain macromolecules under conditions of small η_0 and g. It also permits us to use the experimental values of $[\varphi/g]$ to determine rotational diffusion coefficients of molecules and thus to obtain information on their dimensions in solution. Besides, in a number of cases these data can be used to determine the molecular weight. As for the quantitative agreement of the theory of internal viscosity of chain molecules with the experimental data, in particular the relation of the second term in Eq. (38) to the molecular parameters M and $[\eta]$, this problem still requires further study.

4. The intrinsic value of the birefringence and the optical anisotropy of macromolecules. Table VII gives the values of the segment anisotropy $\alpha_1 - \alpha_2$ for a number of polymers, as calculated from the experimental values of $(\Delta n/\Delta\tau)_{g\to 0}$ or $[n]/[\eta]_0$ (obtained under the condition $n_k = n_s$, see Figs. 19 and 20) using Eq. (43) or (30). The value of $\alpha_1 - \alpha_2$ is an important characteristic of the microstructure of the chain, and does not depend on its length (provided the latter is great enough). The problem of the effect of the nature of the solvent on the measured value of $[n]/[\eta]$, and hence also on $\alpha_1 - \alpha_2$, has been discussed in [201]. The temperature-dependence

Table VI. The value of the coefficient a in Eq. (33) for certain polymers in solution

Polymer	Solvent	$\eta_0 \cdot 10^2$	$M \cdot 10^{-6}$	a
Polystyrene[42 44]	Toluene	0.60	0.45—1.9	0.85
	Methylethylketone	0.40		1.0
Polystyrene[189]	Benzene	0.65	0.9—5.2	0.33
Polystyrene[191]	Bromoform	2.0	0.57—4.3	0.32
PptBPMA[99]	Bromobenzene	1.13	1.1—24	0.3
Polyisobutylene[190]	n-hexane	0.32	1.2—9.8	0.34
Nitrocellulose[200]	Ethyl acetate	0.45		2.0
	Butyl acetate	0.22	0.15—1.0	1.0
	Cyclohexanone	2.15		0.85
Rubber[199]	Benzene	0.65		0.30
Polymethylmethacrylate [192]	Acetone	0.30		0.60
	Methylethylketone	0.40	2.3	0.60
	Butyl acetate	0.72		0.60
	Bromoform	2.0		0.70

Table VII. The segment $(\alpha_1 - \alpha_2)$ and monomer-unit $(a_{\parallel} - a_{\perp})$ anisotropies of the macromolecules of certain polymers

Polymer	Formula	Solvent	$(\alpha_1-\alpha_2) \times 10^{25}$ cm^3	$(a_{\parallel}-a_{\perp}) \times 10^{25}$ cm^3
1. Polyethylene (PET)	$-CH_2-CH_2-$	Xylene	+50	+7
2. Polypropylene (PP) (atactic and isotactic)	$-CH(CH_3)-CH_2-$	Carbon tetrachloride	+30	+3.5
3. Polyisobutylene (PIB)	$-C(CH_3)_2-CH_2-$		+50	+8.2
4. Polybutadiene (PB)	$-CH_2-CH=CH-CH_2-$	Benzene	+30	+4.3
5. Natural rubber (NR)	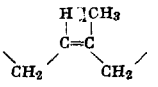	Benzene, toluene	+50	
6. Gutta percha (GUT)	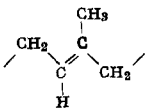	Benzene	+85	
7. Polyethyleneterephthalate (TEN)	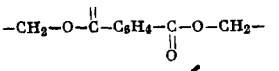	1:1 dichloroethane-phenol	+70	
8. Poly-1,4-diisopropenylbenzene	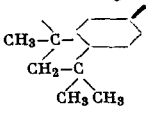	Bromoform	+78	
9. Poly-4,4′-diisopropenyldiphenylethane	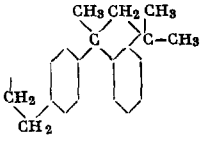	Bromoform	+142	
10. Polydimethylsiloxane (PDMS)	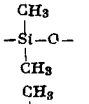	Benzene	+4.7	+0.96
11. Polymethylphenylsiloxane (PMPS)		Benzene	−66	−13.5
12. Polyacrylonitrile (PAN)		Dimethylformamide	−23	−1.8
13. Polyvinylpyrrolidone (PVP)	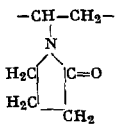	Benzyl alcohol	−75	−10

Table VII (continued)

Polymer	Formula	Solvent	$(\alpha_1-\alpha_2)$ $\times 10^{25}$ cm^3	$(\alpha_\parallel-\alpha_\perp)$ $\times 10^{25}$ cm^3
14. Polystyrene (atactic) (PS)	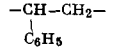	Bromoform	−145	−18
15. Polystyrene (isotactic) (PSI)	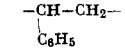	Bromoform	−224	−23
16. Poly-p-methylstyrene (atactic) (PpMS)	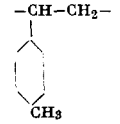	Bromoform	−147	−20
17. Poly-p-methylstyrene (isotactic) (PpMSI)	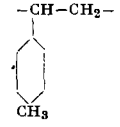	Bromoform	−140	−19
18. Poly-p-chlorostyrene (PpCS)	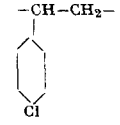	Bromoform	−230	−35
19. Poly-2,5-dimethylstyrene (P-2,5-DMS)	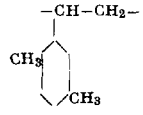	Bromoform	−180	−25
20. Poly-2,5-dichlorostyrene (P-2,5-DCS)	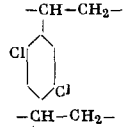	Bromoform	−265	−30
21. Poly-3,4-dichlorostyrene (P-3,4-DCS)	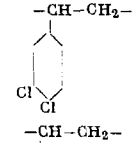	Tetrabromoethane	−300	−25
22. Poly-β-vinylnaphthalene (PβVN)	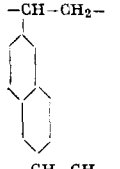	Tetrabromoethane	−430	−30
23. Polyvinylacetate (PVA)	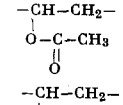	Benzene Toluene	+5.4 +13.5	+0.8 +2.0
24. Polymethylacrylate (PMA)	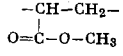	Benzene Toluene	+17 +26	+2.5 +3.6

Polymer	Formula	Solvent	$(\alpha_1-\alpha_2)$ $\times 10^{25}$ cm^3	$(\alpha_\parallel-\alpha_\perp)$ $\times 10^{25}$ cm^3
25. Poly-n-butylacrylate (PnBA)	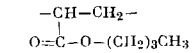	Benzene Toluene	−11 −6.5	−1.5 −0.87
26. Polymethylmethacrylate (PMMA)	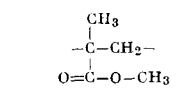	Benzene	+2	+0.3
27. Polymethylmethacrylate (isotactic) (PMMAI)	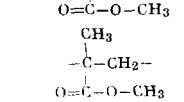	Benzene	+25	+3.5
28. Poly-n-butylmethacrylate (atactic) (PnBMA)	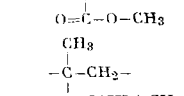	Benzene	−14	−2.1
29. Poly-n-butylmethacrylate (isotactic) (PnBMAI)	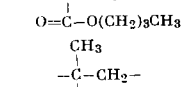	Benzene	−2	−0.3
30. Poly-tert-butylmethacrylate (PtBMA)	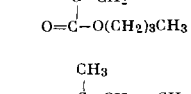	Benzene	+2.1	+0.3
31. Poly-tert-butylmethacrylate (isotactic) (PtBMAI)	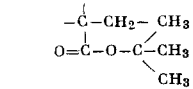	Benzene	+19.8	+3.0
32. Polyphenylmethacrylate (PPMA)	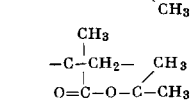	Bromobenzene	−10.5	−1.5
33. Poly-p-tert-butylphenylmethacrylate (PptBPMA)	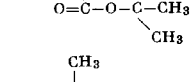	Bromobenzene	−90	−7.5
34. Poly-β-napthylmethacrylate (PβNMA)	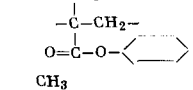	Tetrabromoethane	−60	−8.5
35. Polyphenylmethacrylamide (PPMAM)	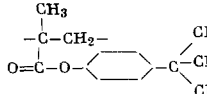	o-Toluidine	−103	−13
36. Polychlorophenylmethacrylamide (PCPMAM)	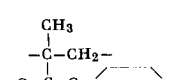	o-Toluidine	−160	−20

Table VII (continued)

Polymer	Formula	Solvent	$(\alpha_1-\alpha_2)$ $\times 10^{25}$ cm^3	$(\alpha_{\parallel}-\alpha_{\perp})$ $\times 10^{25}$ cm^3
37. Polycarbethoxyphenylmethacrylamide (PCEPMAM)	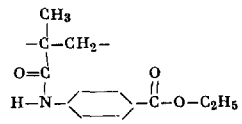	o-Toluidine	−230	−23
38. Ethylcellulose (EC)	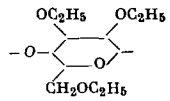	Carbon tetrachloride	+430	+21
39. Nitrocellulose (NC)	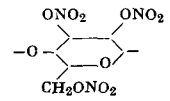	Cyclohexanone	−300	−18
40. Cellulose tribenzoate (CTB)	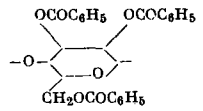	Bromobenzene	−914	−90

was studied in solutions of polyisobutylene (M = 5 × 10^6) in benzene (an ideal solvent at 24°C) and poly-3, 4-dichlorostyrene (M = 2 × 10^5) in tetrabromoethane (an ideal solvent at 41°C). In both cases the increment dn/dC in the system did not exceed 0.003. Thus an influence of the form effect was ruled out.

The results obtained are given in Table VIII.

A more than twofold increase in $[\eta]$ with increasing temperature was accompanied in both cases by a proportional increase in $[n]$. Here $[n]/[\eta]$ and the segment anisotropy $\alpha_1 - \alpha_2$ remained constant within the experimental limits of error.

This result shows that to a first degree of approximation the value of $\alpha_1 - \alpha_2$ does not depend on the thermodynamic interaction of the molecular chain with the solvent. It implies that the process of swelling of the molecular coil in a good solvent must be represented, to a first degree of approximation, by a model in which the nature of the segment distribution changes from Gaussian to non-Gaussian, rather than by a change in the length of the segments. Here the size of the segment and its optical anisotropy remain practically constant, being determined by short-range action, i.e., the skeletal rigidity of the molecular chain. However, we must note that cases are known of specific interaction of a solvent with a molecular chain. Here, while the conformational properties (equilibrium flexibility) are not altered appreciably, the interactions result in quite considerable changes in the anisotropy of the monomer unit, and hence, in the segment anisotropy.

5. The macroform effect. a) Relation to the refractive index n_S of the solvent. A parabolic relation of the birefringence to the refractive index of the solvent has been established experimentally for a number of polymers.[81,79,187,29,202-204,219,220] As illustrative examples, Fig. 27 gives the curves for $[n] = f(n_S)$ for polymethylmethacrylate (whose intrinsic anisotropy is positive) and PptBPMA (whose intrinsic anisotropy is negative). In agreement with Eqs. (29), (31), and (32), the minimum of the parabola on both curves corresponds to the condition n_k

Table VIII. Characteristic hydrodynamic and optical constants of polymers at various temperatures [201]

$t°$, C	$\eta_0 \cdot 10^2$	$[\eta] \cdot 10^{-2}$	$[n] \cdot 10^8$	$\frac{[n]}{[\eta]} \cdot 10^{10}$	n_s	$(\alpha_1-\alpha_2)$ $\times 10^{25}$
Poly-3,4-dichlorostyrene in tetrabromoethane						
41	6.35	0.15	−3.9	−24.9	1.6265	−304
45	5.79	0.25	−6.6	−25.2	1.6241	−312
50	5.20	0.36	−9.6	−26.5	1.6221	−321
Polyisobutylene in benzene						
24	0.625	2.4	10.3	4.3	1.499	51
30	0.562	3.5	14.0	4.0	1.494	52
40	0.492	4.9	20.6	4.2	1.488	54
50	0.437	5.6	24.1	4.3	1.480	56

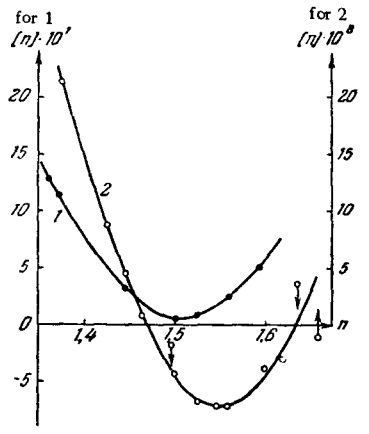

FIG. 27. The relation $[n] = f(n_s)$: 1 – for PptBPMA[203] ($M = 0.57 \times 10^6$, $n_k = 1.55$); 2 – for PMMA[202] ($M = 4.2 \times 10^6$, $n_k = 1.50$).

$= n_s$. The scatter of the experimental points sometimes observed involves not only experimental errors, but may also be due to the differing nature of the interaction of the polymer with different solvents (cf. Sec. III, B, 9, g). For this reason, one should not use mixtures of two solvents of differing n_s.[79] The quantity $[n]_f$ (see Eq. (32)) is determined from the experimental values of $[n]$ and $[n]_k$ by using the expression [202]

$$[n]_f = [n] - [n]_k \frac{[\eta]}{[\eta]_k} \frac{n_k}{n_s} \left(\frac{n_s^2+2}{n_k^2+2} \right)^2, \qquad (46)$$

where the quantities with the subscript k refer to a solvent in which the form effect is absent.

Table IX gives the results for polymethylmethacrylate (PMMA) fractions. The axial ratios p of the molecular coils and the Flory coefficients Φ were calculated from the experimental data by Eqs. (39) and (32), respectively. The found asymmetry of shape of the macromolecules agrees well with the calculated value ($p \approx 2$) predicted by the statistical theory of chain molecules,[3] while the values of the coefficient Φ correspond to the values ordinarily found by the light-scattering method.

b) Relation to the molecular weight. A characteristic peculiarity of the macroform effect is its dependence on the molecular weight, which differs from the corresponding dependence of the intrinsic anisotropy effect. If we plot the total quantity $[n]/[\eta]$ determined experimentally for a series of fractions of the same polymer in a given solvent as a function of $M/[\eta]$, then according to Eqs. (29)—(32) and (39), the points must lie on a straight line. From the slope of this line we can determine Φ or $p = H/Q$, while from the intercept on the vertical axis we can determine the segment anisotropy (including the microform anisotropy as well). This is illustrated by Fig. 28, which shows the given relation for certain polymers. The essential point is that the fact that the line $[n]/[\eta] = f(M/[\eta])$ is inclined directly indicates that the macroform effect plays an appreciable role in the observed birefringence, since not only the intrinsic anisotropy but also the microform effect give a relation of $[n]/[\eta]$ to M (or to $M/[\eta]$) having the form of a straight line parallel to the horizontal axis) [see Eq. (31)]. This fact can be used in practice to distinguish the macroform effect in the total birefringence. The horizontal dotted lines in Fig. 28 represent the corresponding relation as obtained for the same polymers in solvents in which the form effect is absent. The inclined lines and the corresponding horizontal lines intersect the vertical axis at practically the same point. This means that the form effect observed in solutions of flexible chain polymers of molecular weight above 10^5 can be considered practically to be the macroform effect $[n]_f$, without consideration of the considerably smaller microform effect $[n]_{fs}$.

Table X gives the values of the asymmetry factors p and the Flory coefficients Φ calculated for certain polymers from the slopes of the straight lines of Fig. 28.

The scatter in the found values of Φ is quite considerable. However, a much more important point is that the absolute value of these quantities is near 2×10^{23}, the most probable value of Φ. This fact shows that the hydrodynamic and optical properties of the molecular model on which Eqs. (32) and (39)

Table IX. The asymmetry of form p of the molecular coil and the Flory coefficient Φ as calculated from the experimental values of the form birefringence $[n]_f$ for polymethylmethacrylate fractions ($M = 4.2 \times 10^6$) in various solvents.[202] (The function $f(p) = b_0 f_0(L_2 - L_1)$ is that entering into Eq. (39)).

Solvent	n_s	$\eta_0 \cdot 10^2$	$[\eta]$, cm³/g	$[n] \cdot 10^7$	$[n]_f \cdot 10^7$	$f(p)$	p	$\Phi \cdot 10^{-23}$
Acetone	1.359	0.35	370	13.0	12.5	27	2.4	2.6
Ethyl acetate	1.372	0.51	445	11.5	11.0	27	2.4	2.6
Chloroform	1.450	0.59	845	3.34	2.3	31	2.5	3.0
Toluene	1.498	0.59	387	0.48	0	—	—	—
Chlorobenzene	1.523	0.80	595	0.87	0.11	13	1.9	1.3
Bromobenzene	1.560	1.17	565	2.55	1.81	21	2.2	2.0
Bromoform	1.598	2.08	592	5.00	4.22	18	2.0	1.8

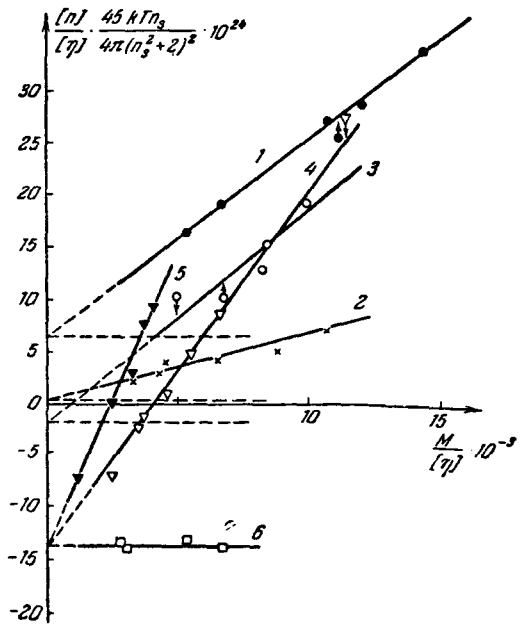

FIG. 28. The relation of $([n]/[\eta]) \cdot [45kTn_s/4\pi(n_s^2 + 2)^2]$ to $M/[\eta]$. 1 – ● – PIB in hexane[190]; 2 – × – PDMS in toluene[205]; 3 – ○ – PBMA in ethyl acetate[207]; polystyrene[210]; 4 – ▽ – in dioxan, $n_k - n_s = 0.18$; 5 – ▼ – in butanone, $n_k - n_s = 0.22$; 6 – □ – in bromoform, $n_k - n_s \approx 0$.

are based adequately reflect the behavior of chain polymer molecules in solution.

c) Concentration-dependence. The concentration-dependence of the form birefringence is especially specific.

If, as suggested by Peterlin, we take into account the increase in the hydrodynamic interaction of the macromolecules with increasing concentration by replacing β by β^* (Eq. (41)), then in the region $\beta \to 0$ we obtain instead of Eq. (26):

$$\left(\frac{\Delta n}{\Delta \tau}\right)_{g\to 0} = \left[\frac{\Delta n}{g(\eta-\eta_0)}\right]_{g\to 0} = \frac{4\pi}{3n_s kT}\left(\theta_i^* + \theta_{fs}^* + \frac{9}{4}\theta_f^*\right), \quad (47)$$

where the asterisk indicates that the quantity thus denoted has been obtained for a solution of finite concentration. $\theta_i^* = \theta_i$, independently of the concentration (see Sec. III, B, 1). At concentrations C < 10%, we can practically neglect the concentration-dependence of θ_{fs}^* as well, and assume $\theta_{fs}^* \approx \theta_{fs}$. On the contrary, as C increases, θ_f^* rapidly decreases from the value $\theta_f^* = \theta_f$ (for $C \to 0$) to zero (at large enough C). This effect is quite general [203,209-214,190] for all polymer-solvent systems. For polymers having a negative intrinsic anisotropy, it can bring about a sign change of the birefringence as C increases. [210,212] The observed decrease in θ_f^* can be explained [210] by the filling of the volume of the solution with molecular coils, their mutual penetration, and the concomitant decrease in the optical inhomogeneity of the system as C increases. The observed effect is determined by the quantity $[\eta]C$, which characterizes the fraction of the volume occupied by the coils in the solution, and can be expressed by the equation

$$\theta_f^* = \theta_f(1 - k_1[\eta]C + k_2[\eta]^2C^2 + \ldots), \quad (48)$$

where k_1 and k_2 are constant coefficients.

The correctness of Eq. (48) has been shown experimentally for a number of polymers. This is illustrated by Fig. 29, which shows the relation of θ_f^*/θ_f to $[\eta]C$ for a series of poly-p-carbethoxyphenylmethacrylamide (PCEPMAM) fractions in ethyl acetate [209] and of polyisobutylene in hexane. [190] The points, which correspond to samples of molecular weights covering the range from 0.2×10^6 to 10×10^6, cluster about a single curve. For many of the studied systems, the observed values of k_1 lie between the limits from 0.3 to 0.4.

The photoelastic method as applied to a polymer swollen in solvents of differing refractive indices has proved useful in determining the form anisotropy in the high-concentration range. [215] Here the form anisotropy is clearly manifested even in systems in which the polymer concentration is as great as 50% or greater. One can show [215] that under these conditions it is practically reduced to the microform effect.

Figure 30 shows the total effective anisotropy of

Table X. The asymmetry of form of the molecular coil p = H/Q and the Flory coefficient Φ, calculated from the experimental value of the macroform effect

Polymer	$M \cdot 10^{-6}$	Solvent	p	$\Phi \cdot 10^{-23}$
Polydimethylsiloxane[205]	0.15—3.0	Toluene	1.6	0.9
Polyisobutylene[190]	0.6—9.8	Hexane	2.0	1.6
Polystyrene[81,211]	0.45—1.92	Toluene, butanone	2.1	1.8
		Butanone	1.9	1.5
Polymethylmethacrylate [202,81,206]		See Table IX	2.2	2.1
Poly-n-butylmethacrylate[207]	0.96—2.2	Ethyl acetate	2.0	1.6
Poly-p-tert-butylphenylmethacrylate[208]	0.2—9.3	Carbon tetrachloride	2.3	2.5
Polyphenylmethacrylamide[209]	0.16—1.6	Ethyl acetate	2.1	1.8
Poly-p-carbethoxyphenylmethacrylamide[209]	0.22—1.14	Ethyl acetate	2.2	2.0

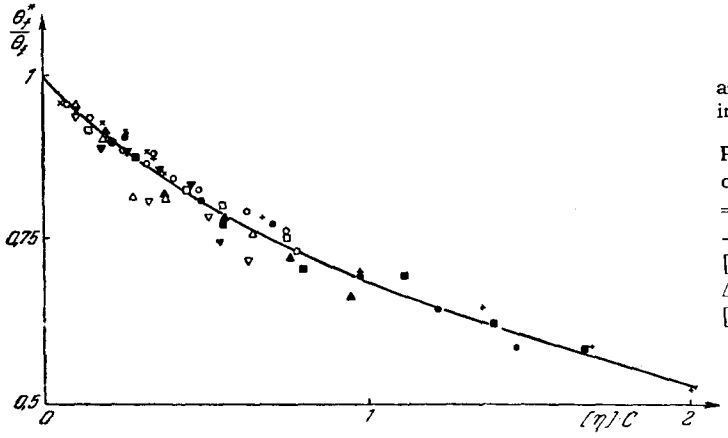

FIG. 29. The concentration-dependence of the relative form anisotropy θ_f^*/θ_f for fractions of PIB in hexane[190] and PCEPMAM in ethyl acetate.[209]

PIB: + – M = 9.8 · 10^6 [η] = 680 cm³/g; ■ – M = 6.9 · 10^6, [η] = 590 cm³/g; ▲ – M = 5.3 · 10^6, [η] = 490 cm³/g; ▲ – M = 4.3 · 10^6, [η] = 380 cm³/g; ▼ – M = 1.2 · 10^6, [η] = 180 cm³/g. PCEPMAM □ – M = 1.136 · 10, [η] = 1.09 · 10^2 cm³/g; × – M = 1.045 · 10^6, [η] = 1.02 · 10^2 cm³/g; o – M = 0.760 · 10^6, [η] = 0.79 · 10^2cm³/g; △ – M = 0.539 · 10^6, [η] = 0.60 · 10^2 cm³/g; ▽ – M = 0.226 · 10^6, [η] = 0.30 · 10^2 cm³/g.

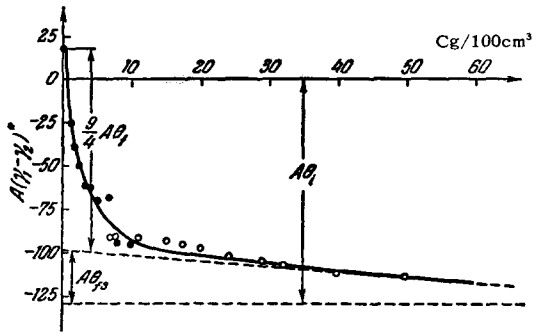

FIG. 30. The concentration-dependence of the form anisotropy of polystyrene in dioxan,

$$A(\gamma_1-\gamma_2)^*=\frac{3nkT}{4\pi}\left(\frac{\Delta n}{\Delta\tau}\right),\quad A=\frac{5}{3}\left(\frac{3}{n^2+2}\right)^2\cdot 10^{25}.$$

●– flow birefringence,[212] M = 0.7 × 10^5, o – photoelastic effect in the swollen polymer.[215]

the polystyrene macromolecule (M = 0.7 × 10^5)

$$(\gamma_1-\gamma_2)^*=\frac{3nkT}{4\pi}\left(\frac{\Delta n}{\Delta\tau}\right)_{g\to 0}$$

Table XI. The intrinsic viscosity [η], form birefringence $[n]_f$, asymmetry p, and form anisotropy θ_f of the macromolecules of polybutylmethacrylate in isopropyl alcohol at various temperatures t [262]

Fraction	t, °C	$[\eta]\cdot 10^{-2}$, cm³/g	$[n]_f\cdot 10^8$	p	$\theta_f\cdot 10^{25}$ cm³
1. $M = 6.4\cdot 10^6$	45	2.72	55	2.06	152
	30	1.68	50	2.00	223
	25	1.17	45	1.95	288
	21.5	0.74	44	1.90	405
2. $M = 2.2\cdot 10^6$	45	1.51	27	2.30	134
	30	0.98	24	2.20	184
	25	0.76	22	2.15	217
	21.5	0.54	20	2.10	278
3. $M = 2.0\cdot 10^5$	52	0.29	1.82	2.10	47
	25	0.174	1.69	2.00	73
	21	0.151	1.77	2.06	88

in dioxan at different concentrations of the solvent, from data on flow birefringence and the photoelasticity of the gel. Even at concentrations C > 10%, the observed form effect is practically due to the microform of the chain alone.

d) Relation to the nature of the solvent. While the choice of a thermodynamically better solvent brings about a parallel increase in the intrinsic birefringence $[n]_i$ and the viscosity [η] of the solution (see Table VIII), we find a completely different result with regard to the form effect.

This is illustrated by Table XI, which gives the results of measurements of the intrinsic viscosity and the birefringence of polybutylmethacrylate fractions in isopropyl alcohol [262] (an ideal solvent at t = 21.5°C). The volume effects, while markedly altering the dimensions of the molecular coils in the solution (i.e., [η]), have little effect on the value of the form birefringence $[n]_f$.

This result corresponds to Eq. (39), according to which $[n]_f$ can only change upon going to better solvents to the extent that the form asymmetry function $b_0f_0(L_2 - L_1)$ changes. The values of p calculated from (39) using the experimental $[n]_f$ values show that the volume effects, while greatly increasing the dimensions of the macromolecules, change their asymmetry of shape only very slightly. A theoretical calculation has confirmed this conclusion.[216]

Thus, the swelling of the molecular coil in solution owing to long-range forces occurs practically isotropically, both in the sense of the invariance of the segment anisotropy of the macromolecule and with regard to its geometric shape. Here the swelling of the macromolecule is accompanied by a decrease in its macroform anisotropy θ_f (see Eq. (47) and Table XI), as is predicted by Eq. (22).

6. The microform effect and rigidity of the chain. Figure 30 graphically illustrates that in dilute solutions (C → 0), even for a polymer of relatively low molecular weight (M = 7 × 10^4), the ratio θ_{fs}/θ_f does not exceed 20%. For samples of higher molecular weight it is even smaller, and for a flexible chain, when M is of the order of several hundred thousand,

the role of the microform in the total effect can be practically neglected.

The situation changes radically for a rigid chain. A comparison of Eq. (22) with (24), or (31) with (32), shows that an increase in the dimensions of the macromolecule (i.e., an increase in v, s, and $[\eta]_0$) with M remaining constant entails an increase in the relative values of θ_{fs} and $[n]_{fs}$ as compared with θ_f and $[n]_f$. Hence, for a chain having a large equilibrium rigidity, the form birefringence is practically determined by the microform effect, while we can neglect the macroform effect.

An example of such polymers are the cellulose derivatives.

In Fig. 31, curves 1—6 give the value of $(\Delta n/\Delta\tau)_{g\to 0}$ for nitrocellulose fractions in butyl acetate ($n_k - n_s = 0.10$) as a function of $[\eta]C$. The dotted lines represent the same relation for the same samples in a solvent in which the form effect is absent (cyclohexanone).[200,208] In distinction from the graphs shown in Fig. 29 and 30, the form anisotropy for nitrocellulose is practically independent of the concentration, and hence must be ascribed to the microform effect.

We can convince ourselves of this from the results of applying Eqs. (30), (31), (32), and (39) to the obtained experimental data. If we assume that the experimentally-determined form anisotropy is due to the macroform effect $[n]_f$, the values of p calculated from (39) prove to be tens of times greater, and the values of Φ (calculated from (32)) hundreds of times greater than the value for Gaussian coils. This completely invalidates the assumptions made.

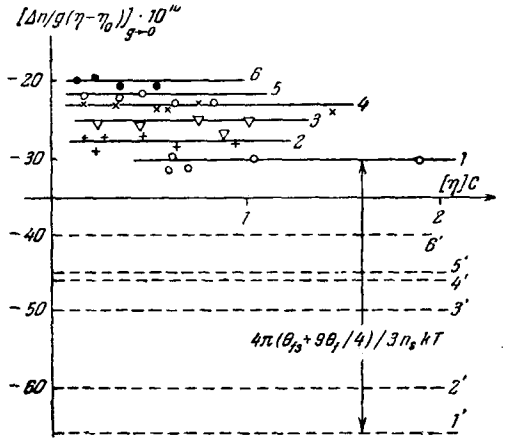

FIG. 31. The relation of $(\Delta n/\Delta\tau)$ to $[\eta]C$ for nitrocellulose fractions in butyl acetate.[200,208]

1 — $M=1.03\cdot10^6$; 2 — $M=8.14\cdot10^5$; 3 — $M=7.78\cdot10^5$; 4 — $M=5.2\cdot10^5$; 5 — $M=4.25\cdot10^5$; 6 — $M=1.53\cdot10^5$.

On the contrary, the assumption that the entire observed form effect is practically the microform effect $[n]_{fs}$ gives (from Eq. (31)) quite reasonable values of s (see Table XII) agreeing with the results from other methods.[217,218]

Here the value of $[n]_f$ (calculated from (32) with a value $\Phi = 2\times10^{23}$) proves to be two orders of magnitude smaller than the value of $[n]_{fs}$.

Analogous results have been obtained for ethylcellulose [204] and cellulose tribenzoate,[200] as well as for DNA.[174,175] The systematic increase of the effective segment length with increasing M indicates a deviation of the molecular configuration from the conformation of an ideal Gaussian chain.

Thus the microform anisotropy depends on the equilibrium rigidity of the chain, and can be used to characterize it.

7. The form effect at high shear stresses. The results of the theory of these phenomena have been discussed in Sec. II, B, 3, a, 1, and are represented by Eqs. (26) and (28). Form birefringence can be observed in its pure form in a polymer whose intrinsic anisotropy is insignificantly small, such as, e.g., polymethylmethacrylate ($\alpha_1 - \alpha_2 = 2\times10^{-25}$ cm^3). In this case, with an appropriate solvent, the curve $\Delta n = f(\beta)$ (Fig. 32) has a form [29,192] qualitatively agreeing with the theoretical relation (26) or curve 1 of Fig. 7, thus sharply differing from the experimental relation $\Delta n = f(\beta)$ observed in the absence of a form effect (e.g., Fig. 24).

In a polymer-solvent system showing a negative intrinsic anisotropy and an appreciable form effect, the relation $\Delta n = f(\beta)$ can involve a sign change in Δn.[221,193] This is illustrated by Fig. 33, which shows the corresponding curves for a series of PptBPMA fractions in carbon tetrachloride.[193,208] The overall course of the experimental curves corresponds to the theoretical relation (26) or curve 5 of Fig. 7. However, theory and experiment agree quantitatively only in the region of small β. The curves bend

Table XII. The form anisotropy and the thermodynamic rigidity parameter (s) for nitrocellulose fractions in butyl acetate

$M\cdot10^{-6}$	$[\eta]\times10^{-2}$	$[n]\cdot10^8$	$[n]_f\times10^8$	$[n]_{fs}\times10^8$	s*	$M\cdot10^{-6}$	$[\eta]\times10^{-2}$	$[n]\cdot10^8$	$[n]_f\times10^8$	$[n]_{fs}\times10^8$	s*
1.03	37	—1160	6.1	1170	32	0.525	21.3	—500	3.1	430	20
0.814	28.9	—750	4.8	680	24	0.425	13.0	—270	2.5	280	22
0.778	27.6	—650	4.6	580	21	0.153	5.75	—113	0.9	100	18

*Number of monomer units (of length 10.3 Å) per segment.

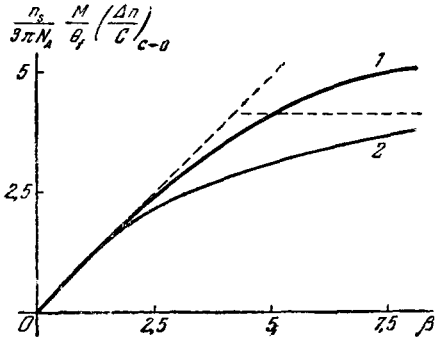

FIG. 32. The relation of the form birefringence to the shear stress. 1 – experimental curve for a PMMA sample ($M = 2.5 \times 10^6$) in tetrabromoethane;[192] 2 – the theoretical relation according to Eq. (26) (corresponding to curve 1 in Fig. 7).

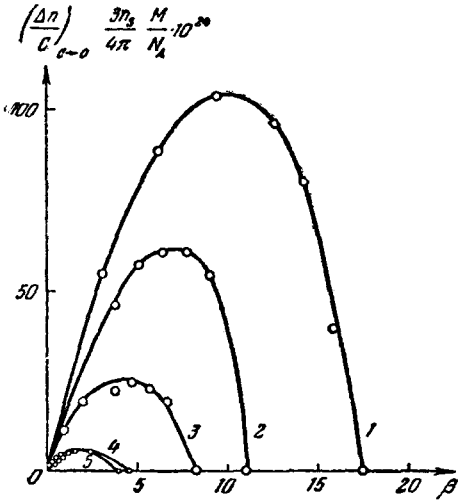

FIG. 33. The relation of the birefringence to β for PptBPMA fractions in carbon tetrachloride.[193,208]

1 — $M = 13.2 \cdot 10^6$; 2 — $M = 7.4 \cdot 10^6$; 3 — $M = 6.0 \cdot 10^6$; 4 — $M = 2.2 \cdot 10^6$; 5 — $M = 1.67 \cdot 10^6$.

further and cross the horizontal axis at considerably higher shear stresses (larger β) than the theory predicts.

This fact might involve either the imperfection of the hydrodynamic model of the molecule (an elastic dumbbell) or the manifestation of internal viscosity, which is not taken into account in Eq. (26). Hence we can suppose that further experimental studies of the effect of sign inversion of Δn at large β will be useful in extending our knowledge on the kinetic rigidity and dynamics of macromolecules in solution.

The sign inversion of Δn is accompanied by an "anomalous" dependence of the extinction angle on the velocity gradient.[222,193,99] This phenomenon can be explained by the effect of the polydispersity of the shapes of the molecules and described by Eq. (28). We give as an illustration Fig. 34, where the circles represent the experimental data, and the curves are calculated by Eq. (28).

These results show that in solutions in which a

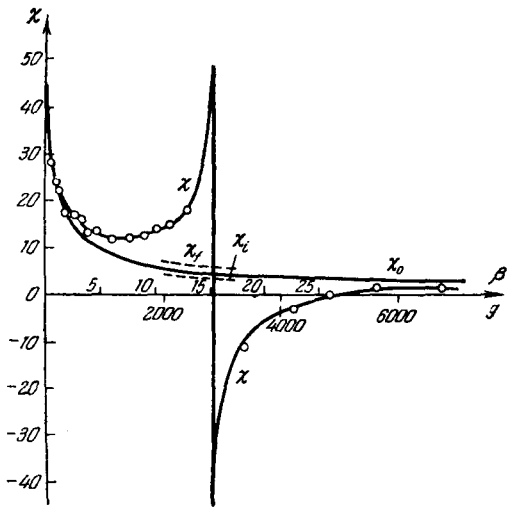

FIG. 34. The relation of the orientation angle χ to g (or β) for solutions of a PptBPMA fraction ($M = 7.4 \times 10^6$) in carbon tetrachloride. Circles – experimental data;[193] curves calculated by Eq. (28), assuming that $\delta = 2.2°$.

negative anisotropy of the molecule compensates a positive form effect, a very small "natural" polydispersity in the chain conformations can lead to marked anomalies in the experimental data on the orientation angles.

This fact must be taken into account in using experimental χ values to characterize the hydrodynamic properties of macromolecules.

8. Optical anisotropy and equilibrium rigidity of the molecular chain. As the data of Table VII illustrate, the segment anisotropy for various polymers can vary within very broad limits and can have either sign. This means that the anisotropy of a molecular chain is sensitive to its structure. The fundamental parameters determining the polarizability difference of a segment are the anisotropy of the monomer unit and the equilibrium rigidity of the chain.

The latter is characterized by the segment length A (or the number s of monomer units per segment), and is experimentally determined from the statistical dimensions of the chain in an ideal solvent (i.e., the root-mean-square distance between its ends $(\overline{h_\theta^2})^{1/2}$, according to the formula

$$A = s\lambda = \frac{\overline{h_\theta^2}}{L}, \qquad (49)$$

where L is the length of the fully-extended chain, and λ is the length of the monomer unit in the direction of L.

For the simplest case of a chain consisting of valence bonds of the same length linked with one another at a valence angle v:

$$s = \frac{\overline{h_\theta^2}/\overline{h_0^2}}{v \cos^2 \frac{\nu}{2}}, \qquad (50)$$

where $\overline{h_0^2}$ is the mean-square statistical length for completely free rotation about the bonds, and ν is the number of bonds per monomer unit.

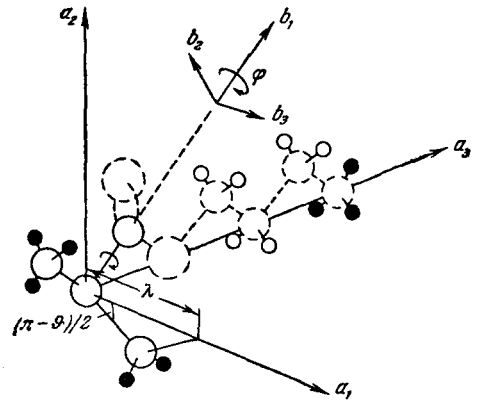

FIG. 35. The monomer unit of poly-n-butylmethacrylate.

The polarizability of the monomer unit along the principal axes 1, 2, and 3 of a fully-extended trans-chain can be characterized by the three components along these axes: a_1, a_2, a_3 (Fig. 35). While these quantities may turn out not to be the principal polarizabilities of the monomer (the polarizability tensor of the monomer may not be diagonal with respect to the axes 1, 2, 3), however, it is precisely these components that are of fundamental significance in the anisotropy of the entire chain. A measure of the anisotropy of the monomer unit is the difference in its polarizability in the directions parallel ($a_{\parallel} = a_1$) and perpendicular ($a_{\perp} = (a_2 + a_3)/2$) to the chain: $a_{\parallel} - a_{\perp}$. From the definition of a segment,

$$\alpha_1 - \alpha_2 = s'(a_{\parallel} - a_{\perp}) = \frac{A(a_{\parallel} - a_{\perp})}{\lambda}, \qquad (51)$$

or, taking (49) into account,

$$a_{\parallel} - a_{\perp} = \frac{\lambda L(\alpha_1 - \alpha_2)}{h_0^2}. \qquad (52)$$

In a number of theoretical studies,[223-233] calculations have been made of the anisotropy and statistical dimensions of chain molecules using a model more adequate than the segmented chain of Kuhn. These calculations have shown that for all the models, the relations between the dimensions of the chain and its anisotropy practically maintain the form of the simple relation (52) based on Kuhn's statistics.

The values of $a_{\parallel} - a_{\perp}$ calculated by Eq. (52) from the experimental data ($\alpha_1 - \alpha_2$, h_0^2, and L) are given in Table VII. They are a characteristic of the structure of the monomer unit of the chain, and in distinction from $\alpha_1 - \alpha_2$, they do not depend on its rigidity. Thus, for example, the great segment anisotropy of ethylcellulose in comparison with other polymers results from its rigidity, while the value of $a_{\parallel} - a_{\perp} = 21 \times 10^{-25}$ obtained for it is close to the anisotropy of the monomer units of a number of other chain molecules. In its positive sign and order of magnitude, it agrees with the value that we might expect on the basis of a theoretical estimate (the anisotropy of a pair of rigidly linked cyclohexane rings is about 50×10^{-25} cm^3).

What has been said above is true also of nitrocellulose, for which some results of studies are given in Table XIII.

In distinction from all other linear polymers with flexible chains, the segment anisotropy of nitrocellulose increases somewhat with the molecular weight, as is illustrated by the deviation of its properties from those of Gaussian chains. At the same time, this increase is accompanied by a proportional increase in the effective segment length calculated from viscosimetry and light-scattering data. Owing to such a correlation in the hydrodynamic and optical properties of the molecule, the anisotropy of the monomer unit $a_{\parallel} - a_{\perp}$ calculated from (52) remains constant as the molecular weight varies (within the limits of experimental error).

9. Optical anisotropy and structure of the chain. Experiment shows that the anisotropy of the monomer unit of the chain is a sensitive indicator of its structure, and thus can often be used to analyze this structure.

In this aspect, we can make some general remarks from an examination of the data of Table VII.

The molecules of carbon-chain polymers not containing large side-chain groups usually show a positive anisotropy, e.g., Nos. 1—6.

The introduction into the main chain of cyclic structures, especially aromatic ones, increases the positive anisotropy of the chain, since the benzene ring has minimum polarizability in a direction normal to itself (Nos. 7—9). This property can prove useful in solving the problem of how benzene rings are arranged in chains being studied.[234,235]

The polysiloxane chain (No. 10) is very weakly

Table XIII. The geometric and optical parameters of nitrocellulose molecules (with constant degree of substitution = 2.75; 13.4% nitrogen) from viscosimetric and dynamooptical data [208]

$M \cdot 10^{-5}$	$\overline{h^2} \times 10^{11}$	A, Å	$(\alpha_1-\alpha_2) \times 10^{25}$	$(a_{\parallel}-a_{\perp}) \times 10^{25}$	$M \cdot 10^{-5}$	$\overline{h^2} \times 10^{11}$	A, Å	$(\alpha_1-\alpha_2) \times 10^{25}$	$(a_{\parallel}-a_{\perp}) \times 10^{25}$
10.32	77.1	426	—824	—19.6	4.25	23.8	320	—556	—17.9
8.14	61.4	430	—647	—15.5	2.85	14.3	290	—541	—19.3
7.78	55.2	405	—583	—14.9	2.15	9.8	260	—491	—21.6
5.50	33.6	350	—620	—18.0	1.53	6.2	230	—490	—19.4
5.25	33.9	368	—573	—16.0	1.47	5.9	230	—498	—22.3

anisotropic, which is explained by the closeness of the values of the anisotropies of the SiO and SiC bonds.[205]

a) The effect of the side-chain groups. As the length of the side-chain radicals increases, the positive anisotropy of the chain decreases, changes sign, and then increases in negative value (Nos. 1, 2, 12, 13 or 23–25, or 26, 28). The introduction into the side-chain radicals of anisotropically polarized bonds and atomic groups, e.g., rings containing conjugated bonds, has an especially strong effect on the negative anisotropy (No. 10, 11 or 14–22, or 26, 32–34, or 35–37, or 38–40).

Figure 36 illustrates[208] the effect of the number of side-chain nitrate groups per glucose ring on the mean anisotropy of the monomer unit of nitrocellulose. As the nitrogen content (degree of nitration) increases, the negative anisotropy of the monomer $a_{\parallel} - a_{\perp}$ increases in line with the greater polarizability of the

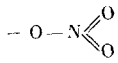

group in the direction of its symmetry axis. These results permit us to estimate the hindrance of rotation of the nitrate groups about the valence bonds linking them to the main chain. They can also be used to determine the degree of nitration of cellulose.

b) Flexibility of the side-chain groups. The negative anisotropy of the chain introduced by the side-chain groups depends on the flexibility of the latter. Thus, for example, the negative anisotropy created by an aromatic ring introduced into the side chain

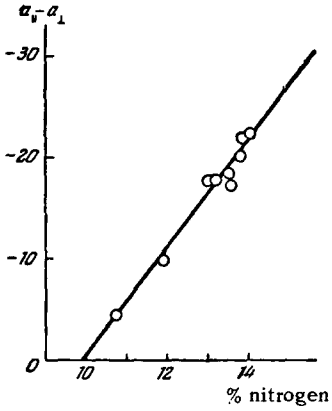

FIG. 36. The relation of the anisotropy of the monomer unit of nitrocellulose to the degree of nitration $(a_{\parallel} - a_{\perp}) \cdot 10^{25}$ cm^3.

proves to diminish, the farther this ring is removed from the main chain, since then the flexibility of the side-chain imparts to it a greater freedom to rotate. Hence the negative anisotropy of polyphenylmethacrylate (No. 32) is much less than that of polystyrene (No. 14), although in both cases the polarizability difference of the molecule is mainly due to the anisotropy of the benzene ring. For the same reason, poly-β-naphthylmethacrylate (No. 34) is considerably less anisotropic than poly-β-vinylnaphthalene (No. 22), although the polarizability of the naphthalene ring plays the decisive role in the anisotropy of both molecules. Obviously, this fact can be used to study the flexibility of the side chain.

If we consider the side group as a rigid chain (an aromatic ring or a rigid trans-chain) having a certain freedom of rotation about the valence bond joining it to the main chain (the b_1 axis in Fig. 35), we can easily derive the expression [205,206]

$$a_{\parallel} - a_{\perp} = (a_{\parallel} - a_{\perp})_0 + b_2 - \frac{1}{2}[b_1 + b_3 + 3(b_3 - b_2)\sin^2\varphi], \quad (53)$$

relating the anisotropy $a_{\parallel} - a_{\perp}$ of the monomer unit to the angle φ between the plane of the group and the main-chain direction. Here $(a_{\parallel} - a_{\perp})_0$ is the portion of the anisotropy of the monomer due to all its bonds except for the side group; b_1, b_2, and b_3 are the principal polarizabilities of the side group along the axes of the rotating coordinate system. $(a_{\parallel} - a_{\perp})_0$, b_1, b_2, and b_3 can usually be calculated from the known polarizabilities of the bonds constituting the monomer unit. Then the experimental value of $a_{\parallel} - a_{\perp}$ permits us to determine the angle φ. The deviation of the angle φ from the value $\pi/2$ characterizes the inclination of the plane of the side group from the position corresponding to a rigid trans-configuration.

As an example of the application of Eq. (53), Table XIV gives data for some polymers having aromatic side radicals. In the calculation, the values of $a_{\parallel} - a_{\perp}$ are taken from Table VII, and the bond polarizabilities are taken from Denbigh.[237] The obtained results show that in all the cases examined, the rotation of the phenyl groups is rather weakly hindered (free rotation corresponds to $\varphi = 45°$), and in a number of cases (except Nos. 16, 17, 11, 15, and 20), it varies little upon introducing substituents into

Table XIV. The angle between the plane of the side group and the molecular chain direction

No. in Table VII	Polymer	φ°	No. in Table VII	Polymer	φ°
14	PS (atactic)	52	20	P-2,5-DCS	58
15	PS (isotactic)	59	21	P-3,4-DCS	52
16	PpMS (atactic)	45.5	19	P-2,5-DMS	51
17	PpMS (isotactic)	44,7	22	PβVN	50
			11	PMPS	45
18	PpCS	53			

the ring. The great hindrance of the benzene ring in No. 20 is apparently due to the closeness of one of the chlorine-atom substituents to the main chain. In No. 15, the reason for it is the stereospecificity of the chain. The weakened hindrance in No. 11 can be explained by the great distances between the benzene rings in the phenylmethylsiloxane chain.

c) The effect of isomerism. The optical anisotropy of the chain is also sensitive to cis-trans isomerism. Thus, for example, the trans configuration of polyisoprene (No. 6) corresponds to a greater anisotropy than the cis form, No. 5.

When we go from a side group of linear structure (No. 28) to the branched tertiary isomer (No. 30), we find a decrease in the positive anisotropy of the side chain (in its own coordinate axes), resulting in a decrease in the negative anisotropy of the molecule (in the coordinate axes of the main chain) and a sign change in $a_{\parallel} - a_{\perp}$ from negative to positive.

d) Deformation of valence angles. In the case of No. 3 of Table VII, the experimental data deviate from the general rule that the positive anisotropy of the chain decreases with increase in the size of the side groups. The replacement of the C-H side linkage by the more anisotropic CH_3 group in going from polypropylene (No. 2) to polyisobutylene (No. 3) increases the anisotropy $\alpha_1 - \alpha_2$. Further, the presence of a considerable anisotropy in polyisobutylene is quite paradoxical when we consider the tetrahedral symmetry of its structure.

These departures from the general rule can be ascribed to partial non-additivity of the various bonds (the anisotropy of a C-C bond in the chain is greater than the anisotropy of the same bond in a side group). However, perhaps, it can be ascribed in greater degree to the deformation of the valence angle of the main chain of the polymer,[201,190] owing to interaction of the side methyl groups. Apparently an analogous phenomenon occurs in the chains of the polymethacrylate series.[206]

e) Graft polymerization and anisotropy of the chain. The increase in the negative anisotropy of a molecule as the side groups are lengthened is due to the fact that a long side group itself has a positive anisotropy (i.e., a maximum polarizability in its own chain direction). However, another situation is possible, and has been realized in the grafting of polystyrene chains onto a polymethylmethacrylate [241] or polybutylmethacrylate chain. In this case, the side chain being grafted on is optically negatively anisotropic (No. 14, Table VII). That is, it has maximum polarizability in a direction normal to the side chain, or in a direction parallel to the main chain. Hence, the graft polymer obtained has a very large positive anisotropy,[242] although its main chain in itself is optically almost isotropic (No. 26, Table VII), while the polystyrene chain, which comprises nine-tenths of its mass, is negatively anisotropic.

This is illustrated by Table XV.

These results show that optical anisotropy can be used as a method of studying the structure of graft polymers, as well as branched macromolecules.

The huge positive value of $\alpha_1 - \alpha_2$ observed in the graft polymer indicates that its chains are more rigid than those of the component being copolymerized.

f) Stereospecificity and optical anisotropy of molecules.[243,244] Experiment shows that stereospecificity of molecular chains has practically no effect on their statistical dimensions in solution.[245-247] Hence, the study of the geometric and hydrodynamic properties of macromolecules in solution cannot give information on their microtacticity.

On the other hand, optical anisotropy of chain molecules has proved in a number of cases to be very sensitive to their stereospecificity. Some appropriate examples are given in Table VII (Nos. 14 and 15, or 26 and 27, or 28 and 29, or 30 and 31).

In all the studied cases, the anisotropy of the atactic and syndiotactic stereoisomers turned out practically to coincide, indicating the similarity in structure of these two isomers.

On the other hand, the anisotropy of an isotactic sample can be either considerably larger in absolute value (polystyrene, polymethylmethacrylate, poly-tert-butylmethacrylate) or considerably smaller (poly-n-butylmethacrylate) than that of an atactic sample.

The difference in anisotropy of the monomer unit in the stereoisomers is due to the differing nature of the rotation of their side groups.

Here the approach of the plane of the side group to the direction of the main chain will increase the positive anisotropy of the monomer and of the entire chain (or decrease their negative anisotropy). This

Table XV. Composition and segment anisotropy $\alpha_1 - \alpha_2$ of PMMA-PS graft polymers [242]

Molecular weight of the main PMMA chain	Molecular weight of the grafted PS chains	Average number of grafts per molecule	Number of grafted chains per 100 monomer units of the main chain	% (by mass) styrene in the polymer	Molecular weight of the graft polymer	$(\alpha_1 - \alpha_2) \times 10^{25}$ cm^3
$7 \cdot 10^4$	$2 \cdot 10^3$	315	45	90	$7 \cdot 10^5$	+870
$58 \cdot 10^4$	$2 \cdot 10^3$	1850	32	86	$41.5 \cdot 10^5$	+750
$58 \cdot 10^4$	$10 \cdot 10^3$	420	7	88	$48 \cdot 10^5$	+7000

Table XVI

Polymer	In solution (flow birefringence)	In bulk (photoelasticity)				
	φ°	T, °C	$\epsilon \cdot 10^{12}$ cm²/dyne	$(\alpha_1 - \alpha_2) \times 10^{25}$ cm³	φ°	Crystallizability
PMMA atactic	52,5 (benzene)	110	from −3.0 to +4.8	from −3.0 to +4.8	from 53.5 to 52.5	Amorphous
PMMA isotactic	45 (benzene)	50	14.6	4.0	52	Crystalline
PnBMA atactic	50.5 (benzene)	30	−10	−2.6	49	Amorphous
PnBMA isotactic	49 (benzene)	15	30	8.0	47,8	Amorphous
PtBMA atactic	52.5 (benzene)	118	14	4.1	52	Amorphous
PtBMA isotactic	46 (benzene)	70	77	14	48	Amorphous

situation occurs in all the studied polymers of the methacrylate series. Table XVI gives the corresponding values of φ calculated from the experimental values of $a_{\parallel} - a_{\perp}$ using Eq. (53).

The opposite situation occurs with polystyrene: φ is greater for the isotactic polymer than for the atactic (see Table XIV).

The decrease in φ with increasing microtacticity observed in the polymethacrylates implies a decrease in the rigidity of the side groups when the chain structure is rearranged from atactic to stereospecific. The data given agree with the results of a study of the photoelasticity of the same samples,[236,248] as are given in Table XVI.

Stereospecificity not only lowers the glass-transition temperature T_0, i.e., makes the polymer chain softer, but it also shifts the value of the photoelastic coefficient ϵ and the corresponding values of α_1 and α_2 and φ in the same direction as for the molecule in solution.

The study of the time-dependence of the photoelasticity also permits us to detect the slight effects of stereoblock structure (microcrystallites), which cannot be detected by x-ray diffraction analysis.

The great sensitivity of the molecular anisotropy to stereospecificity is apparently a general property of the esters of the polymethacrylate series. In these molecules, the positive anisotropy of the main chain is appreciably compensated by the negative anisotropy of the side groups. Hence, small variations in the flexibility of the side groups and the corresponding changes in their anisotropy can sharply displace this compensation equilibrium in the molecule and lead to changes in the magnitude and sign of the anisotropy.

At the same time, a change in the stereospecificity in the polypropylene chain, which has the symmetric CH_3 side group, does not alter the optical anisotropy of the macromolecule, since the nature of the rotation of this group can have no effect on the polarizability difference of the chain. The effect of stereospecificity on the anisotropy is also weakened by the introduction of a methyl group in the para-position in the benzene ring of polystyrene (Tables VII and XIV, Nos. 16 and 17).

The found relation of $\alpha_1 - \alpha_2$ to the microtacticity of the chain does not involve the ability of the polymer to crystallize. It can occur both in amorphous and crystallizable samples (see Table XVI).

g) The effect of the surrounding medium. It was shown above (III, B, 4) that the segment anisotropy of a chain is a characteristic of its microstructure, and does not depend on the thermodynamic nature of the solvent.

Experiment also shows that for polymers of sufficiently large intrinsic anisotropy (polystyrene and its halogenated derivates, PptBPMA, polyisobutylene, rubber, etc.), the segment anisotropy $\alpha_1 - \alpha_2$ of the chain found from the birefringence in solution (see Table VII) is near the value of $\alpha_1 - \alpha_2$ obtained from photoelasticity measurements of the same samples.[227,228,240,199,81,250] Thus, in these cases the change of the medium from the low-molecular-weight solvent to that of the polymer itself does not alter the anisotropy of the chain significantly.

Likewise, the swelling of rubber or polystyrene in appropriate solvents ($n_K = n_S$) has practically no effect on the segment anisotropy of these polymers.[251,215]

However, cases are known in which a variation in the surrounding medium entails considerable changes in the magnitude and sometimes even in the sign of the intrinsic anisotropy of the macromolecule.

Thus, for example, for the polymers Nos. 23—25 of Table VII, a change of the solvent from benzene to toluene increases the positive (or decreases the negative) anisotropy of the chain by a factor of two. Also, for samples Nos. 23, 24, and 29, the anisotropy in solution and in bulk differs even in sign (cf. Table XVI).

The sensitivity of the anisotropy of polyvinylacetate to changes in the medium is also illustrated by

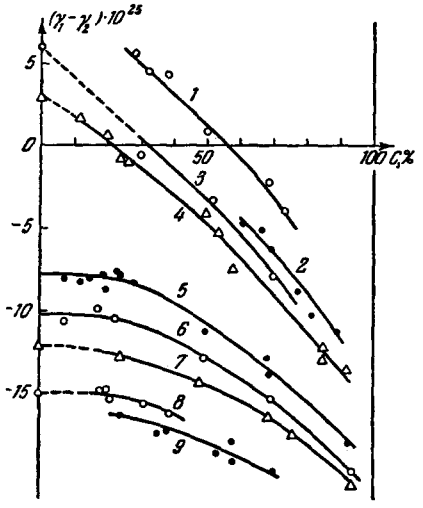

FIG. 37. The relation of the anisotropy of PVA swollen in various solvents to the degree of swelling (from the photoelasticity of the gels).[215] 1 – bromobenzene; 2 – xylene; 3 – toluene; 4 – benzene; 5 – bromoform; 6 – chloroform; 7 – acetone; 8 – tetrabromoethane; 9 – carbon tetrachloride.

Fig. 37, which gives the values of $\gamma_1 - \gamma_2 = (3/5) \times (\alpha_1 - \alpha_2)$ (obtained from measurements of the photoelasticity of the gel) as a function of the degree of swelling in different solvents.[215] The points on the vertical axis correspond to the data in dilute solutions (flow birefringence).[252,224] Such a strong dependence of the anisotropy on the properties of the surrounding medium is specific for the molecules of the polyacrylate and methacrylate series. It is probably due to changes in the rotation of the side groups with change in the interaction with the surrounding medium (just as in the case of the effect of stereospecificity). Here, as was pointed out above (see Table XVI), very small differences in the angles φ can lead to large changes in the anisotropy observed experimentally.

Obviously, these phenomena can be used as a sensitive method for studying interactions in a polymer-solvent system.

10. Polyelectrolytes. The problem of the dynamic birefringence in solutions of flexible chain polyions is highly complex and poorly worked out.

The difficulty of the problem is due not so much to its hydrodynamic aspect as to its optical aspect. Since polyelectrolytes are soluble practically only in an aqueous medium, we cannot use solvents of differing refractive indices. Hence, the experimental distinction of the form effects from the intrinsic anisotropy by the direct methods applicable to solutions of nonelectrolyte polymers is ruled out in this case. This fact greatly hinders the quantitative interpretation of the results. A number of studies have dealt with the dynamooptical properties of certain polyelectrolytes: polymethacrylic [253,263] and polyacrylic [255,257] acids, poly-4-vinyl-n-butylpyridinium bromide,[254,256] sodium alginate, [256] and poly-4-vinylpyridinium chloride.[186]

Increase in the degree of ionization and decrease in the ionic strength of the buffer solution, which lead to uncoiling of the chain and increase in the dimensions of the polyion, sharply reduce the orientation angle and increase the magnitude of the birefringence. The decrease in the orientation angles qualitatively agrees with the increase in viscosity of the solution observed here.

For all the studied polyelectrolytes at low enough ionic strengths of the solution (when the molecular coil is uncoiled enough), the birefringence is positive. This fact is of fundamental significance, since it shows that the anisotropy of a sufficiently uncoiled polyion chain is determined by the form effect.

This is graphically shown by Table XVII, which gives the anisotropy of polyvinylpyridine

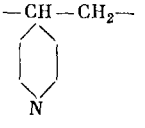

in ethanol (non-polyelectrolyte) and its quaternary salt

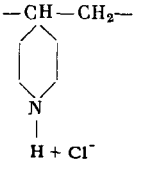

in aqueous solution (polyelectrolyte).[256,186]

The intrinsic negative anisotropy of the polyvinylpyridine molecule (cf., e.g., No. 14 of Table VII) is

Table XVII. Anisotropy of polyvinylpyridine in ethanol and of its quaternary salt in aqueous solution [186,256]

Polyvinylpyridine	Polyvinylpyridinium chloride —CH—CH₂— (N, H + Cl⁻)				
$(\alpha_1 - \alpha_2)\cdot10^{25}$	$C\cdot10^2$, g/ml	$\left(\frac{\Delta n}{g}\right)\cdot10^{10}_{g\to0}$	$(\eta_{sp})_{g\to0}$	$\frac{\Delta n}{\Delta\tau}\cdot10^{10}$	$(\alpha_1-\alpha_2)\cdot10^{25}$
+ 630	1.05	29.1	25	115	1820
	0.63	21.2	17.8	123	1860
	0.08	7.4	3.35	221	3450
	0.01	1.2	0.45	265	4120

obviously overcompensated by the form effect, and the effective segment polarizability difference $\alpha_1 - \alpha_2$ (calculated from (30)) has a large positive value. The intrinsic anisotropy of the quaternary salt should have an even greater negative value (cf. Nos. 14 and 18 in Table VII). Nevertheless, in aqueous solution (in which polyelectrolyte effects are large), its effective anisotropy is positive and very large.

Thus, the uncoiling of a polyion chain under the action of the electrostatic repulsion forces of the charged groups entails a sharp increase in the positive form effect overbalancing the role of the intrinsic (negative) anisotropy of the molecule. A decrease in the concentration of the solution entails a decrease in its ionic strength (non-isoionic dilution), a weakening of the screening effect of the counterions, and a still greater uncoiling of the molecules. The latter results in an increase in the reduced viscosity η_{sp}/C and the anisotropy $\alpha_1 - \alpha_2$ (see Table XVII), as well as a decrease in the orientation angles with dilution.

The use of the method of isoionic dilution [259] permits us to weaken the influence of concentration effects on the shape of the polyion molecules and to get data that reflect their optical properties more adequately.

This is illustrated by Fig. 38, which shows the relation of $\Delta n/g(\eta - \eta_0)$ to the concentration for solutions of several fractions of polymethacrylic acid (PMA) (0.012 M NaCl).[263] The reduced anisotropy depends very slightly on the polymer concentration, indicating the prevailing role of the microform effect in the birefringence (compare with the curves of Figs. 29 and 31).

The large value of the microform effect at low ionic strengths of the solution corresponds to Eqs. (22) and (24), which predict a decrease in the relative value of the quantity θ_f (in comparison with θ_{fs}) as the volume v of the molecular coil is increased.

The data of Table XVIII indicate the same. At a constant ionic strength I, the quantity $[n]/[\eta]$ is practically independent of the molecular weight, indicating the segment character of the observed anisotropy. As the molecule goes from the uncharged to the charged state, a certain decline in $[n]/[\eta]$ takes place in the first stages of ionization. This can be

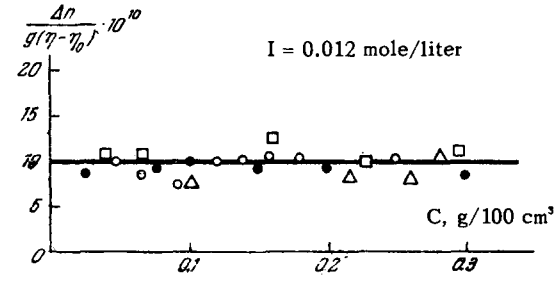

FIG. 38. The concentration-dependence[263] of $\Delta n/g(\eta - \eta_0)$ for PMA fractions in buffer solution (I = 0.012 M) (isoionic dilution).

● — $M = 8.3 \cdot 10^5$; □ — $M = 5.0 \cdot 10^5$; △ — $M = 0.6 \cdot 10^5$; ○ — $M = 2.3 \cdot 10^5$;

explained by the decrease in the relative role of the macroform effect as the coil is unwound (cf. Table XI). Further increase in the dimensions of the molecule (at an ionic strength of 0.0012 M in NaCl) involves an increase in $[n]/[\eta]$ owing to the increase in the effective segment length, and correspondingly, of the microform anisotropy.

Further analysis of the experimental data [263] shows that the dynamooptical properties of PMA solutions are complicated by the influence of hydrogen bonds and their partial rupture upon ionization of the molecule.

While in solutions of ionized PMA the overall effect of the intrinsic (positive) anisotropy and the macroform and microform effects result in a large positive birefringence, in solutions of polyacrylic acid (PAA), the overall effect proves to be considerably smaller (Fig. 39).[257]

Apparently, a mutual compensation of a negative intrinsic anisotropy of the chain and a positive form effect takes place here.

As the concentration of the solution increases, the relative role of the form effect declines, and the birefringence changes sign from positive to negative.[255,257] Thus, the PAA molecule in the ionized state in sufficiently concentrated solutions shows a negative intrinsic anisotropy. However, this does not mean that in the un-ionized state (or in another solvent) this anisotropy would also be negative. Solutions in dioxan (Table XIX) show a positive anisotropy, which decreases very sharply, however, with decreasing

Table XVIII. Dynamooptical data on solutions of PMA fractions in the un-ionized and ionized states (α = degree of ionization)[263]

$M \cdot 10^{-5}$	0.002 M HCl		$M \cdot 10^{-5}$	$\alpha = 0.6$, $I = 0.012$ M		$\alpha = 0.6$, $I = 0.0012$ M	
	$[\eta] \cdot 10^{-2}$	$\frac{[n]}{[\eta]} \cdot 10^{10}$		$[\eta] \cdot 10^{-2}$	$\frac{[n]}{[\eta]} \cdot 10^{10}$	$[\eta] \cdot 10^{-2}$	$\frac{[n]}{[\eta]} \cdot 10^{10}$
7.2	0.51	15.8	8.3	19	9.5	40	34
4.4	0.44	15.0	5.0	10	10.0	—	—
2.0	0.30	14.2	2.3	7.0	11.4	20	34
1.0	0.21	13.6	0.6	2.8	10.0	5	36
0.4	0.07	11.0	0.13	0.65	12.3	—	—

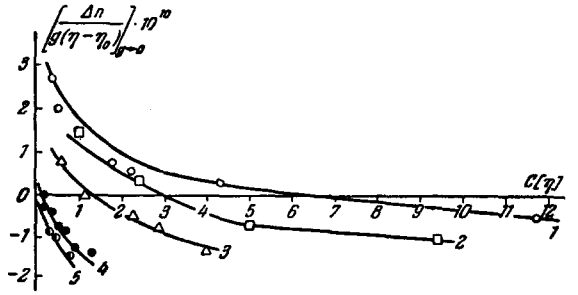

FIG. 39. The concentration-dependence of $\Delta n/g(\eta - \eta_0)$ (as a function of $C[\eta]$) for PAA fractions in buffer solution (I = 0.012 M,[257] isoionic dilution).

1 — $M = 1.8 \cdot 10^6$; 2 — $M = 1.3 \cdot 10^6$; 3 — $M = 0.53 \cdot 10^6$; 4 — $M = 0.16 \cdot 10^6$; 5 — $M = 0.38 \cdot 10^6$.

Table XIX. Dynamooptical properties of solutions of PAA fractions in dioxan (in un-ionized state), T = 30°C

$M \cdot 10^{-5}$	$[\eta] \cdot 10^{-2}$	$\frac{[n]}{[\eta]} \cdot 10^{10}$
13	0.97	2.68
8.3	0.77	1.93
5.3	0.62	1.88
1.56	0.34	0.89

molecular weight (macroform effect).

For PMA, just as for its esters (see Sec. III, B, 9, g), we should expect the intrinsic anisotropy of the chain to be very sensitive to interaction with the surrounding medium (and even more so to electrostatic interactions), since small changes in the rotation of the side groups in polymers of this class result in quite appreciable differences in the optical properties of the monomer unit. Hence the observed changes in the magnitude and sign of the birefringence of PAA solutions as the ionic strength, the degree of ionization, and the concentration are varied might be due not only to conformational changes in the chain, but also to the direct influence of the electrostatic interactions on the anisotropy of the monomer unit.

It seems likely that we could choose a more suitable model than PAA for studying the general dynamooptical properties characteristic of a broad class of polyelectrolytes, e.g., the quaternary salts of polyvinylpyridine and its derivatives. Unfortunately, the experimental material obtained for this class of polymers is not yet sufficient. In any case, the first problem that we must solve in studies of this sort is how to distinguish reliably the effects of the intrinsic anisotropy and the (macro- and micro-)form effects.

The relation of the magnitude of the birefringence to the velocity gradient $\Delta n = f(g)$ in polyion solutions at low enough ionic strengths is usually given by a graph curved toward the horizontal axis, like the curves of Fig. 5.[255-257,263] This shows that the electrostatic repulsion of the charged groups of the macromolecule not only unwinds the molecular chain, but also increases its kinetic rigidity appreciably. Hence, the birefringence under these conditions is to a considerable extent an orientation effect.

At the same time, while the effective values of the chain anisotropy are large, according to the data of Tables XVII and XVIII, they are many times smaller than the values that we could obtain if the molecular chain were unfolded to a shape similar to a straight rod. Hence, in describing the hydrodynamic and optical properties of a chain polyion in solution, the conformation of a slightly-coiled stiff random coil is a much better model than one in the form of a rod-like particle.

NOTATION

A—segment length,
D_r—rotational diffusion coefficient of the particles,
$D_0 = D_r\eta$,
F—coefficient characterizing the internal viscosity,
L—longitudinal axis of the particle, length of the completely extended molecular chain,
L_1, L_2—optical form factor (functions of the axial ratio p of the coil),
M_0—molecular weight of the monomer unit,
M_S—molecular weight of the segment,
M—molecular weight of the polymer,
M_n—number-average molecular weight,
M_w—weight-average molecular weight,
N—number of particles per cm^3,
N_A—Avogadro's number,
R—universal gas constant,
R—mean radius of the dynamooptimeter cylinder,
ΔR—width of the gap in the dynamooptimeter,
s—number of monomer units per segment,
T—absolute temperature,
T_g—glass-transition temperature,
Φ—Flory coefficient,
θ_i—intrinsic anisotropy of the chain,
θ_f—macroform anisotropy,
θ_{fS}—microform anisotropy,
a—proportionality coefficient,
$a_{\parallel} - a_{\perp}$—polarizability difference of the monomer unit,
b_0—a function of p,
C—concentration of the solution in g/cm^3,
C_V—volume concentration of the solution,
d—transverse axis of the particle,
f_0—a function of p,
$f(\sigma, p)$—mechanical factor (a function of the orientation),
g—velocity gradient of flow,
g_k—critical velocity gradient,
$g_1 - g_2 = (\gamma_1 - \gamma_2)/v$—specific anisotropy of the substance of the particle,
h—distance between the ends of the macromolecule,

$\overline{h^2}$—mean square distance between the ends of the chain,
$\overline{h_\theta^2}$—the same in an ideal solvent,
h_0^2—the same, with free rotation about the valence bonds,
k—the Boltzmann factor,
$[n]$—intrinsic value of the birefringence,
$[n]_i$—intrinsic value of the intrinsic birefringence
$[n]_{fs}$—intrinsic value of the microform birefringence,
$[n]_f$—intrinsic value of the macroform birefringence,
$n_1 - n_2 = \Delta n$—difference between the two principal refractive indices of the liquid,
n_s—refractive index of the solvent,
n_k—refractive index of the dry polymer,
p—axial ratio of the particle,
u—velocity of flow,
v—volume of the particle,
v_0—hydrodynamic volume of the particle,
$\bar{v}$—partial molar volume of the particle,
$\alpha_1 - \alpha_2$—polarizability difference of the segment,
$\beta = M[\eta]\eta_0 g/RT$—a parameter,
$\gamma_1 - \gamma_2$—difference between the two principal polarizabilities of the particle,
δ—phase difference due to the solution,
δ_0—phase difference due to the compensator,
ϵ—photoelastic coefficient,
η, η_0—viscosities of the solution and solvent, respectively,
$[\eta]$—intrinsic viscosity of the polymer,
$[\eta]_0$—intrinsic viscosity of the polymer extrapolated to zero velocity gradient,
η_i—internal viscosity of the molecule,
$[\eta]^*$—reduced viscosity of the solution,
λ—wavelength of light, length of the monomer unit in the direction of the axis of the chain molecule,
ν—number of bonds per monomer unit,
ρ—density of the polymer,
$\sigma = g/D_r$—orientation factor,
τ—relaxation time,
$\Delta\tau = (\eta - \eta_0)g$—effective shear stress,
$[\varphi/g]$—intrinsic value of the orientation angle,
φ—angle between the plane of a side group and the chain direction in the macromolecule,
χ—extinction angle,
ω—vibration frequency (circular).

[1] J. T. Edsall, Advances Colloid Sci. 1, 269 (1942).
[2] A. Peterlin and H. A. Stuart, Hand. u. Jahrb. chem. Phys., Bd. 8(1), 1 (1943).
[3] Kuhn, Kuhn, and Buchner, Ergeb. exact. Naturwiss. 25, 1 (1951).
[4] R. Cerf and H. A. Scheraga, Chem. Revs. 51, 185 (1952).
[5] A. Peterlin and H. A. Stuart, Die Physik der Hochpolymeren, Ed. H. A. Stuart, Vol. 2, p. 569, Springer, Berlin (1953).
[6] H. A. Scheraga and R. Signer, in Physical Methods of Organic Chemistry, 3rd Edition Vol. 1, Part 3, Chap. 34, (Ed. A. Weissberger), Interscience, New York (1960).
[7] A. Peterlin, in Rheology (Ed. F. R. Eirich), Vol. 1, p. 615, Academic Press, New York (1956).
[8] R. Cerf, Fortschr. hochpolym. Forsch. 1, 382 (1959), Springer-Verlag, Berlin.
[9] H. G. Jerrard, Chem. Revs. 59, 345 (1959).
[10] J. T. Edsall, Fortschr. chem. Forsch. 1, 119 (1949).
[11] G. I. Taylor, Phil. Trans. Roy. Soc. (London) A223, 289 (1923); Proc. Roy. Soc. (London) A157, 546, 565 (1936); A146, 501 (1934).
[12] H. G. Jerrard, J. Appl. Phys. 21, 1007 (1950).
[13] C. Sadron, J. phys. radium, Ser. 7, 7, 263 (1936).
[14] C. Sadron, Schweiz. Arch. angew. Wiss. u. Tech. 3, 8 (1937).
[15] Buchheim, Stuart, and Menz, Z. Physik 112, 407 (1939).
[16] G. Boehm, Handbuch der biologischen Arbeitsmethoden, Vol 24, 3939 (1939).
[17] J. W. Mehl, Biol. Bull. 79, 488 (1940).
[18] O. Snellman and Y. Björnståhl, Koll. Beihefte 52, 403 (1941).
[19] H. Nitschmann and H. Guggisberg, Helv. Chim. Acta 24, 434 (1941).
[20] A. J. de Rosset, J. Chem. Phys. 9, 766 (1941).
[21] M. Gerendas, Enzymologia 9, 123 (1941).
[22] E. Winkler, Z. Physik 118, 232 (1941).
[23] V. N. Tsvetkov and A. I. Petrova, ZhTF 12, 423 (1942).
[24] Edsall, Gordon, Mehl, Scheinberg, and Mann, Rev. Sci. Instr. 15, 243 (1944).
[25] Lawrence, Needham, and Shen, J. Gen. Physiol. 27, 201 (1944).
[26] E. Fredericq and V. Desreux, Bull. Soc. chim. Belges 56, 223 (1947).
[27] J. T. Edsall, [10].
[28] V. R. Gray and A. E. Alexander, J. Phys. Coll. Chem. 53, 9 (1949).
[29] V. Tsvetkov and A. Petrova, Zhur. Fiz. Khim. 23, 368 (1949).
[30] V. Tsvetkov and M. Sosinskiĭ, JETP 19, 543 (1949).
[31] Tsvetkov, Petrova, and Poddubnyĭ, Zhur. Fiz. Khim. 24, 994 (1950).
[32] H. A. Scheraga, J. Chem. Phys. 19, 983 (1951).
[33] Edsall, Eich, and Goldstein, Rev. Sci. Instr. 23, 846 (1952).
[34] A. G. Ogston and J. E. Stanier, Biochem. J. 53, 4 (1953).
[35] Kuhn, Oswald, and Kuhn, Helv. Chim Acta. 36, 1209 (1953).
[36] V. N. Tsvetkov and S. Ya. Magarik, Vestnik LGU 8, 163 (1954).

[37] W. Philippoff and F. H. Gaskins, Ind. Eng. Chem. 51, 871 (1959).
[38] F. H. Gaskins and W. Philippoff, J. Appl. Polymer Sci. 2, 143 (1959).
[39] J. Leray, J. chim. phys. 58, 316 (1961).
[40] E. Winkler and W. Kast, Naturwiss. 29, 288 (1941).
[41] V. N. Tsvetkov and N. A. Kibardina, DAN SSSR 62, 223 (1948).
[42] E. V. Frisman and V. N. Tsvetkov, JETP 23, 690 (1952).
[43] V. N. Tsvetkov, International Symposium on Macromolecular Chemistry, Milan (1954).
[44] E. V. Frisman and V. N. Tsvetkov, ZhTF 25, 448 (1955).
[45] Y. Björnståhl, Z. Physik 119, 245 (1942).
[46] J. Leray, J. chim. phys. 52, 755 (1955).
[47] E. V. Frisman and Hsü Mao, Vysokomolekulyarnye Soedineniya 3, 276 (1961).
[48] G. Szivessy, in Handbuch der Physik (Ed. H. Konen), Vol 19, p. 917, Springer-Verlag, Berlin (1928).
[49] D. B. Brace, Phys. Rev., Ser. 1, 18, 70 (1904); 19, 218 (1904).
[50] Y. Björnståhl, J. Opt. Soc. Am. 29, 201 (1939).
[51] G. Szivessy and A. Dierkesmann, Ann. der Physik 11, 949 (1931).
[52] R. Cerf, Rev. optique 29, 200 (1950).
[53] B. H. Zimm, Rev. Sci. Instr. 29, 360 1154 (1958).
[54] J. Leray and G. Scheibling, Compt. rend. 251, 349 (1960).
[55] S. N. Pen'kov and V. Z. Stepanenko, Optika i Spektroskopiya 14, 156 (1963).
[56] C. Sadron, J. phys. 9, 381, 384 (1938).
[57] V. Tsvetkov and E. Frisman, Zhur. Fiz. Khim. 21, 261 (1947).
[58] W. Philippoff, Trans. Soc. Rheol. 4, 159 (1960).
[59] J. Leray and G. Scheibling, J. chim. phys. 58, 797 (1961).
[60] W. Haller, Kolloid Z. 61, 26 (1932).
[61] P. Boeder, Z. Physik 75, 258 (1932).
[62] W. Kuhn, Z. phys. Chem. 161A (1), 427 (1932).
[63] W. Kuhn, Kolloid Z. 62, 269 (1933).
[64] C. Sadron, J. phys. radium, Ser. 7, 8, 481 (1937).
[65] A. Peterlin and H. A. Stuart, Z. Physik 112 (1), 129; 113, 663 (1939).
[66] D. Edwards, Quart. J. Math. 26, 70 (1893).
[67] I. M. Burgers, Second Report on Viscosity and Plasticity, Academy of Sciences at Amsterdam, Vol. 16, Chap. 3 (1938).
[68] Scheraga, Edsall, and Gadd, J. Chem. Phys. 19, 1101 (1951).
[69] H. G. Jerrard, J. Opt. Soc. Am. 88, 35 (1948).
[70] [32].
[71] M. Goldstein, J. Chem. Phys. 20, 677 (1952).
[72] R. Simha, J. Phys. Chem. 44, 25 (1940).
[73] F. Perrin, J. phys. radium 5 (7), 487 (1934).
[74] C. G. Le Fèvre and R. J. W. Le Fèvre, in Physical Methods of Organic Chemistry, 3rd Edition (Ed. A. Weissberger), Vol. 1, Part 3, Chap. 36, Interscience, New York (1960).
[75] W. Kuhn, Kolloid Z. 68, 2 (1934).
[76] H. Kuhn, Experientia 1, 28 (1945).
[77] H. Kuhn, Helv. Chim. Acta 31, 1677 (1948).
[78] W. Kuhn and F. Grün, Kolloid Z. 101, 248 (1942).
[79] V. N. Tsvetkov and E. V. Frisman, Acta Physicochim. USSR 20, 363 (1945).
[80] V. N. Tsvetkov and E. V. Frisman, DAN SSSR 97, 647 (1954).
[81] V. N. Tsvetkov, J. Polym. Sci. 23, 151 (1957).
[82] Tsvetkov, Frisman, Ptitsyn, and Kotlyar, ZhTF 28, 1428 (1958), Soviet Phys.-Technical Physics 3, 1325 (1958).
[83] M. Čopič, International Symposium on Macromolecular Chemistry, Milan, 1954.
[84] M. Čopič, J. Chem. Phys. 26, 1382 (1957).
[85] V. N. Tsvetkov, Vysokomolekulyarnye Soedineniya 5, 740 (1963).
[86] W. Kuhn and H. Kuhn, Helv. Chim. Acta 26, 1394 (1943).
[87] W. Kuhn and H. Kuhn, ibid. 28, 1533 (1945); 29, 39, 71, 830 (1946).
[88] W. Kuhn and H. Kuhn, J. Colloid Sci. 3, 11 (1948).
[89] B. H. Zimm, J. Chem. Phys. 24, 269 (1956).
[90] R. Cerf, Compt. rend. 240, 531 (1955); 241, 496, 1458 (1955); 243, 1875 (1956).
[91] R. Cerf, J. Polym. Sci. 20, 216 (1956); 23, 125 (1957); 25, 247 (1957).
[92] R. Cerf, J. phys. radium, 19, 122 (1958).
[93] V. A. Kargin and G. L. Slonimskiĭ, Zhur, Fiz. Khim. 23, 563 (1948).
[94] P. E. Rouse Jr., J. Chem. Phys. 21, 1272 (1953).
[95] J. G. Kirkwood and J. Riseman, J. Chem. Phys. 16, 565 (1948).
[96] R. Cerf, J. chim. phys. 48, 59, 85 (1951); 52, 53 (1955).
[97] R. Cerf, J. phys. radium 13, 458 (1952); 15, 145 (1954).
[98] R. Cerf, J. Polym. Sci. 12, 35 (1954).
[99] V. N. Tsvetkov and I. N. Shtennikova, Vysokomolekulyarnye Soedineniya 5, (1963).
[100] R. Koyama, J. Phys. Soc. Japan 16, 1366 (1961).
[101] A. Peterlin, Bull. Sci. Youg. 1, 40 (1953).
[102] A. Peterlin, J. Polym. Sci. 12, 45 (1954).
[103] A. S. Lodge, Nature 176, 838 (1955).
[104] A. S. Lodge, Trans. Faraday Soc. 52, 120 (1956).
[105] Franklin, Klug, and Holmes, The Nature of Viruses, Boston, Mass., (1957).
[106] M. A. Lauffer, J. Am. Chem. Soc. 66, 1188 (1944).
[107] G. Schramm and G. Bergold, Z. Naturforsch. 2b, 108 (1947).
[108] H. K. Schachman, J. Am. Chem. Soc. 73, 4808 (1951).
[109] I. Watanabe and Y. Kawade, Bull, Chem. Soc. Japan 26, 294 (1953).
[110] J. W. Rowen and W. Ginoza, Biochim. Biophys. Acta 21, 416 (1956).

[111] H. Boedtker and N. S. Simmons, J. Am. Chem. Soc. 80, 2550 (1958).
[112] J. Bernal and I. Fankuchen, J. Gen. Physiol. 25, 111, 147 (1941).
[113] D. L. D. Caspar, Nature 177, 475 (1956).
[114] R. E. Franklin and A. Klug, Biochim. Biophys. Acta 19, 403 (1956).
[115] G. Oster, J. Gen. Physiol. 33, 445 (1950).
[116] R. C. Williams and R. L. Steere, J. Am. Chem. Soc. 73, 2057 (1951).
[117] G. Schramm and M. Wiedemann, Z. Naturforsch. 66, 379 (1951).
[118] C. E. Hall, J. Am. Chem. Soc. 80, 2556 (1958).
[119] J.-B. Donnet, Compt. rend. 229, 189 (1949).
[120] J. T. Yang, J. Am. Chem. Soc. 83, 1316 (1961).
[121] M. Joly, Trans. Faraday Soc. 48, 279 (1952).
[122] M. Joly, Rheologica Acta 185, 180 (1958).
[123] A. J. Haltner and B. H. Zimm, Nature 184, 265 (1959).
[124] S. Broersma, J. Chem. Phys. 32, 1626 (1960).
[125] M. Lauffer, J. Phys. Chem. 42, 935 (1938).
[126] see [10].
[127] Edsall, Gilbert, and Scheraga, J. Am. Chem. Soc. 77, 157 (1955).
[128] C. Hall, J. Biol. Chem. 179, 857 (1949).
[129] R. F. Steiner and K. Laki, J. Am. Chem. Soc. 73, 882 (1951).
[130] Hocking, Laskowski, and Scheraga, J. Am. Chem. Soc. 74, 775 (1952).
[131] H. Boedtker and P. Doty, J. Am. Chem. Soc. 78, 4267 (1956).
[132] C. E. Hall and P. Doty, J. Am. Chem. Soc. 80, 1269 (1958).
[133] A. Rich, Revs. Modern Phys. 31, 65 (1959).
[134] Blout, Karlson, Doty, and Hargitay, J. Am. Chem. Soc. 76, 4492 (1954); Doty, Holtzer, Bradbury, and Blout, ibid., 4493.
[135] P. Doty, Proc. Natl. Acad. Sci. USA 42, 791 (1956).
[136] Doty, Bradbury, and Holtzer, J. Am. Chem. Soc. 78, 947 (1956).
[137] P. Doty and J. T. Yang, ibid. 78, 498 (1956).
[138] J. T. Yang, ibid. 80, 1783 (1958).
[139] Luzzati, Cesari, Spach, Masson, and Vincent, J. Mol. Biol. 3, 566 (1961).
[140] L. Freund, Theses (Strasbourg, 1961).
[141] M. L. Wallach and H. Benoit, J. Polym. Sci. 57, 41 (1962).
[142] O'Konski, Yoshioka, and Orttung, J. Phys. Chem. 63, 1558 (1959).
[143] C. T. O'Konski and A. J. Haltner, J. Am. Chem. Soc. 78, 3604 (1959).
[144] A. Wada, J. Chem. Phys. 31, 495 (1959).
[145] I. Tinoco Jr., J. Am. Chem. Soc. 79, 4336 (1957).
[146] Tsvetkov, Mitin, Glushenkova, Grishchenko, Boĭtsova, and Lyubina, Vysokomolekulyarnye soedineniya 5, 453 (1963).
[147] Pauling, Corey, and Branson, Proc. Natl. Acad. Sci. 37, 205, 235 (1951).
[148] U. Arndt and D. Riley, Phil. Trans. Roy. Soc. (London) 247A, 409 (1955).
[149] J. T. Yang, J. Am. Chem. Soc. 80, 5138 (1958).
[150] see [74], p. 2481.
[151] V. N. Tsvetkov and V. A. Marinin, JETP 18, 641 (1948).
[152] A. Wissler, Dissertation (Bern, 1940).
[153] O. Snellman and G. Widstrom, Arkiv Kemi, Mineral., Geol. 19A, No. 31 (1945).
[154] H. Schwander and R. Cerf, Helv. Chim. Acta 32, 2356 (1949); 34, 436 (1951).
[155] H. Schwander and R. Signer, Helv, Chim. Acta 34, 1344 (1951).
[156] Edsall, Scheraga, and Rich, 119th Meeting, Am. Chem. Soc., 1951.
[157] Horn, Leray, Pouyet, and Sadron, J. Polym. Sci. 9, 531 (1952).
[158] R. F. Steiner, Trans. Faraday Soc. 48, 1185 (1952).
[159] J. W. Rowen, Biochim. Biophys. Acta 10, 391 (1953).
[160] Reichmann, Bunce, and Doty, J. Polym. Sci. 10, 109 (1953).
[161] J. W. Rowen and A. Norman, Arch. Biochem. Biophys. 51, 524 (1954).
[162] Reichmann, Rice, Thomas, and Doty, J. Am. Chem. Soc. 76, 3047 (1954).
[163] M. Goldstein and M. E. Reichmann, J. Am. Chem. Soc. 76, 3337 (1954).
[164] L. R. Rey, J. chim. phys. 51, 85 (1954).
[165] J. Leray, Compt. rend. 241, 1741 (1955).
[166] J. Leray, J. Polym. Sci. 23, 167 (1957).
[167] A. R. Mathieson and S. Matty, J. Polym. Sci. 23, 747 (1957).
[168] E. Barbu and M. Joly, Bull, Soc. chim. Belg. 65, 17 (1956).
[169] E. Barbu and M. Joly, Trans. Faraday Soc. 53, 249 (1957).
[170] Barbu, Basset, Joly, and Wahl, J. Polym. Sci. 23, 717 (1957).
[171] E. Barbu and M. Joly, J. chim. phys. 53, 951 (1956); 54, 700 (1957); 55, 799 (1958).
[172] M. Joly, J. Polym. Sci. 29, 77 (1958).
[173] J. Leray, J. chim. phys. 37, 323 (1960).
[174] Frisman, Vorob'ev, Shchagina and Yanovskaya, Vysokomolekulyarnye Soedineniya 4, 762 (1962); 5 (1963); Engl. Transl. of former article, Polymer Science USSR (Pergamon Press) 3, 978 (1962).
[175] V. N. Tsvetkov, Vysokomolekulyarnye Soedineniya 5, 752 (1963).
[176] H. Kahler, J. Phys. Chem. 52, 676 (1948).
[177] P. Doty, J. Polym. Sci. 55, 1 (1961).
[178] J. D. Watson and F. H. C. Crick, Nature 171, 737 (1953).
[179] H. Eisenberg, J. Polym. Sci. 25, 257 (1957).

[180] Doty, Boedtker, Fresco, Haselkorn, and Litt, Proc. Natl. Acad. Sci. USA 45, 482 (1959).
[181] H. Boedtker, Biochim. Biophys. Acta 32, 519 (1959).
[182] Fresco, Alberts, and Doty, Nature 188, 98 (1960).
[183] R. A. Cox and U. Z. Littauer, J. Mol. Biol. 2, 166 (1960).
[184] U. Z. Littauer and H. Eisenberg, Biochim. Biophys. Acta 32, 320 (1959).
[185] Frisman, Vorob'ev, Yanovskaya, and Shchagina Biokhimiya 28, 137 (1963).
[186] D. O. Jordan and T. Kurucsev, Polymer 1, 202 (1960).
[187] V. N. Tsvetkov and A. Petrova, ZhTF 14, 289 (1944).
[188] B. Schmidli, Dissertation (Zürich, 1952).
[189] V. N. Tsvetkov and S. M. Savvon, ZhTF 26, 349 (1956); Soviet Phys.-Technical Physics 1, 342 (1956).
[190] Tsvetkov, Boĭtsova, and Grishchenko, Vestnik LGU 4, 59 (1962).
[191] S. Ya. Magarik and P. P. Baranov, Vysokomolekulyarnye soedineniya 5, (1963).
[192] V. N. Tsvetkov and V. P. Budtov, ibid. 5, (1963).
[193] V. N. Tsvetkov and I. N. Shtennikova, ibid. 2, 640 (1960).
[194] A. Peterlin, J. Phys. radium 22, 407 (1961).
[195] A. Peterlin, Polymer 2, 257 (1961).
[196] W. Philippoff, J. Appl. Phys. 27, 984 (1956).
[197] W. Philippoff, Trans. Soc. Rheology 1, 95, 109 (1957).
[198] W. Philippoff, J. Polym. Sci. 57, 141 (1962).
[199] S. M. Savvon and Kao Yu-shu, Vysokomolekulyarnye Soedineniya 5, (1963).
[200] I. N. Shtennikova, Dissertation (Leningrad, 1963).
[201] Tsvetkov, Bychkova, Savvon, and Nekrasov, Vysokomolekulyarnye Soedineniya 1, 1407 (1959); Engl. Abstract, Polymer Sci. USSR 1, 584 (1960).
[202] Tsvetkov, Frisman, and Mukhina, JETP 30, 649 (1956); Soviet Phys. JETP 3, 492 (1956).
[203] V. N. Tsvetkov and I. N. Shtennikova, ZhTF 29, 885 (1959); Soviet Phys.-Technical Physics 4, 800 (1960).
[204] V. N. Tsvetkov and I. N. Shtennikova, Vysokomolekulyarnye Soedineniya 2, 808 (1960).
[205] Tsvetkov, Frisman, and Boĭtsova, ibid. 2, 1001 (1960).
[206] V. N. Tsvetkov and N. N. Boĭtsova, ibid. 2, 1176 (1960).
[207] V. N. Tsvetkov and S. Ya. Lyubina, ibid. 1, 856 (1959); Engl. Abstract, Polymer Sci. USSR 1, 334 (1960).
[208] V. N. Tsvetkov and I. N. Shtennikova, ibid. 5, (1963).
[209] V. E. Bychkova, ibid. 5, (1963).
[210] E. V. Frisman and V. N. Tsvetkov, J. Polym. Sci. 30, 297 (1958).
[211] Frisman, Garmonova, and Bychkova, ZhTF 29, 198 (1959); Soviet Phys. Technical Physics 4, 171 (1959).
[212] Frisman, Sibileva, and Krasnoperova, Vysokomolekulyarnye soedineniya 1, 597 (1959); Engl. Transl., Polymer Sci. USSR 1, 209 (1960).
[213] H. Jeneschitz-Kriegl, Macromol. Chem. 33, 55 (1959); 40, 120 (1960).
[214] Frisman, Yanovskaya, and Budtov, Vysokomolekulyarnye soedineniya 4, 560 (1962); Engl. Abstract, Polymer Sci. USSR 3, 753 (1962).
[215] V. N. Tsvetkov and A. E Grishchenko, ibid. 5, (1963).
[216] O. B. Ptitsyn, ibid. 3, 390 (1961).
[217] G. Meyerhoff, J. Polym. Sci. 29, 399 (1958).
[218] A. Münster and H. Diener, Symposium Makromol., Wiesbaden, A11, 2 (1959).
[219] R. Signer, Z. phys. Chem. A50, 257 (1930).
[220] R. Signer, Trans. Faraday Soc. 32, 296 (1936).
[221] E. V. Frisman and V. N. Tsvetkov, DAN SSSR 108, 42 (1956).
[222] E. V. Frisman, ibid. 118, 72 (1958); Soviet Phys.-Doklady 3, 81 (1958).
[223] M. V. Vol'kenshteĭn, Konfiguratsionnaya statistika polimernykh tsepeĭ (Configurational Statistics of Polymeric Chains), Izd. AN SSSR, L. (1959); Engl. Transl., Interscience, New York (1963).
[224] H. Eyring, Phys. Rev. 39, 746 (1932).
[225] W. J. Taylor, J. Chem. Phys. 15, 412 (1947).
[226] R. Kubo, J. Phys. Soc. Japan 2, 84 (1947).
[227] R. S. Stein and A. V. Tobolsky, J. Polym. Sci. 11, 285 (1953).
[228] D. Saunders, Trans. Faraday Soc. 52, 1425 (1956); 53, 37 (1957).
[229] Gotlib, Vol'kenshteĭn, and Byutner, DAN SSSR 99, 935 (1954).
[230] T. M. Birshteĭn and O. B. Ptitsyn, Zhur. Fiz. Khim. 28, 213 (1954).
[231] Yu. A. Gotlib, ZhTF 27, 707 (1957); 28, 801 (1958); Soviet Phys. Tech. Phys. 2, 637 (1958); 3, 749 (1958).
[232] T. M. Birshteĭn, Vysokomolekulyarnye Soedineniya 1, 748 (1959); Engl. Abstract, Polymer Sci. USSR 1, 276 (1960).
[233] Birshteĭn, Vol'kenshteĭn, Gotlib, and Ptitsyn, ibid. 4, 670 (1962); Engl. Abstract, Polymer Sci. USSR 3, 973 (1962).
[234] V. N. Tsvetkov and S. Ya. Magarik, DAN SSSR 115, 911 (1957); Soviet Phys. Doklady 2, 403 (1958).
[235] Yu. V. Mitin and N. A. Glukhov, DAN SSSR 115, 1 (1957).
[236] Tsvetkov, Vitovskaya, and Lyubina, Vysokomolekulyarnye soedineniya 4, 577 (1962), Engl. Abstract, Polymer Sci. USSR 3, 754 (1962).
[237] K. G. Denbigh, Trans. Faraday Soc. 36, 936 (1940).
[238] V. N. Tsvetkov and S. Ya. Magarik, DAN SSSR 127, 840 (1959).
[239] Frisman, Martsynovskiĭ, and Domnicheva, Vysokomolekulyarnye soedineniya 2, 1148 (1960).
[240] V. N. Tsvetkov and L. N. Verkhotina, ZhTF 28, 97 (1956); Soviet Phys. Tech. Phys. 3, 87 (1958).

[241] Mitsengendler, Andreeva, Sokolova, and Korotkov, Vysokomolekulyarnye soedineniya 4, 1366 (1962).
[242] Tsvetkov, Magarik, Klenin, and Eskin, ibid. 5, 3 (1963).
[243] Tsvetkov, Magarik, Boĭtsova, and Okuneva, J. Polym. Sci. 54, 635 (1961).
[244] V. N. Tsvetkov, J. Polym. Sci. 57, 727 (1962).
[245] F. Danusso and G. Moraglio, J. Polym. Sci. 24, 161 (1957).
[246] F. Danusso and G. Moraglio, Macromol. Chem. 28, 250 (1958).
[247] Tsvetkov, Skazka, and Krivoruchko, Vysokomolekulyarnye soedineniya 2, 1045 (1960).
[248] V. N. Tsvetkov and M. G. Vitovskaya, ibid. 3, 1600 (1961).
[249] Stein, Holmes, and Tobolsky, J. Polym. Sci. 14, 443 (1954).
[250] Bazhenov, Vol'kenshteĭn, Gotlib, and Rozenshteĭn, ZhTF 26, 1430 (1956); Soviet Phys. Tech. Phys. 1, 1677 (1956).
[251] W. Kuhn and R. Pasternak, Helv. Chim. Acta 30, 1705 (1947); 31, 340 (1948).
[252] E. V. Frisman and V. Andreĭchenko, Vysokomolekulyarnye soedineniya 4, 1559 (1962).
[253] Kuhn, Künzle, and Katchalsky, Helv. Chim. Acta. 31, 1994 (1948).
[254] R. M. Fuoss and R. Signer, J. Am. Chem. Soc. 73, 5872 (1951).
[256] Jordan, Mathieson, and Porter, J. Polym. Sci. 21, 463, 473 (1956); A. R. Mathieson and M. R. Porter, ibid. 483.
[257] Tsvetkov, Lyubina, and Barskaya, Vysokomolekulyarnye Soedineniya 5, (1963).
[258] Ch. Sadron, J. chim. phys. 58, 877 (1961).
[259] D. T. F. Pals and J. J. Hermans, J. Polym. Sci. 5, 733 (1950).
[260] Boeckel, Gensling, Well, and Benoit, J. chim. phys. 59, 999 (1962).
[261] Mukohata, Ikeda, and Isemura, J. Mol. Biol. 5, 570 (1962).
[262] V. N. Tsvetkov and S. Ya. Lyubina, Vysokomolekulyarnye Soedineniya 2, 75 (1960).
[263] Tsvetkov, Lyubina, and Bolevskiĭ, ibid. 5, (1963).

Translated by M. V. King